Model fluids versus *real* fluids

How can we compare experimental and modelling results on complex fluids?

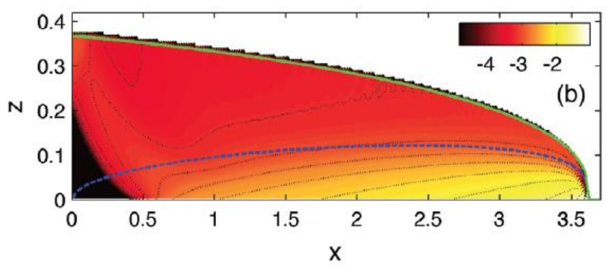

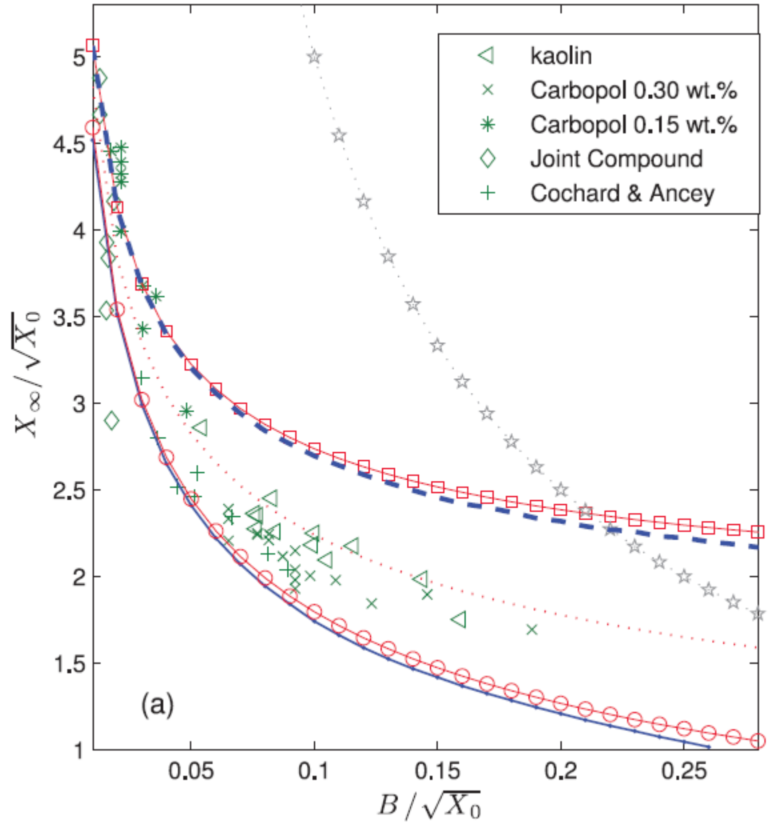

Liu et al., JNNFM, 2016

Guillaume Chambon

Viscoplastic fluids

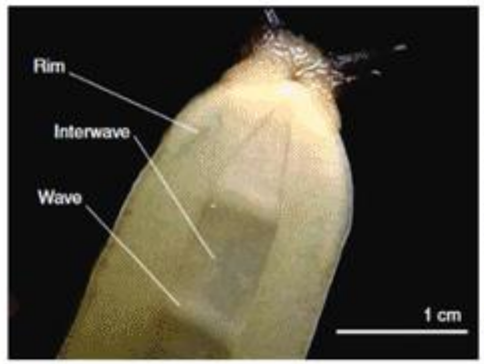

- Yield stress (solid-fluid transition)

Formation of deposits

Models: depth-averaged…

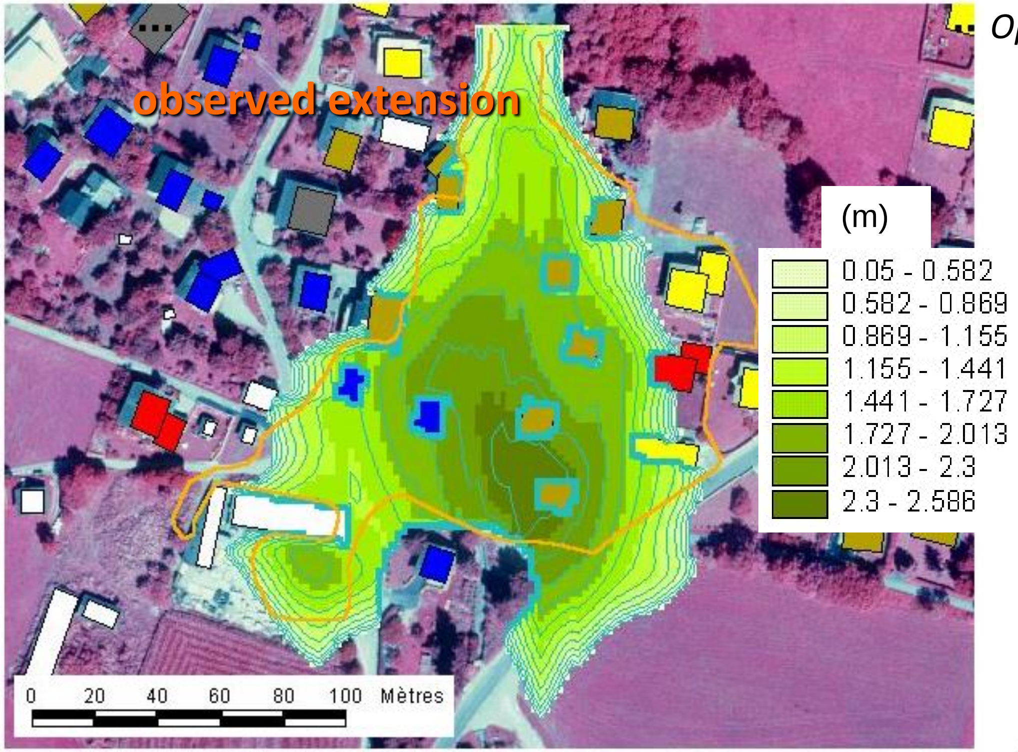

Operational model (LAVE2D, Irstea)

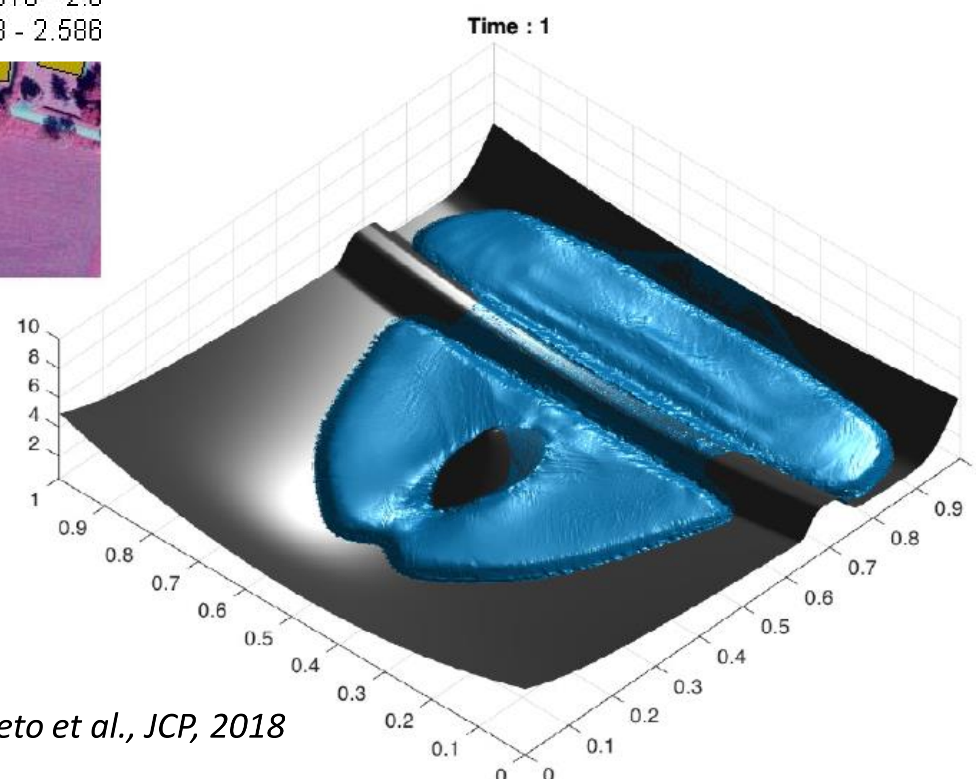

Fernandez-Nieto et al., JCP, 2018

Models: … vs DNS

Fouling layers

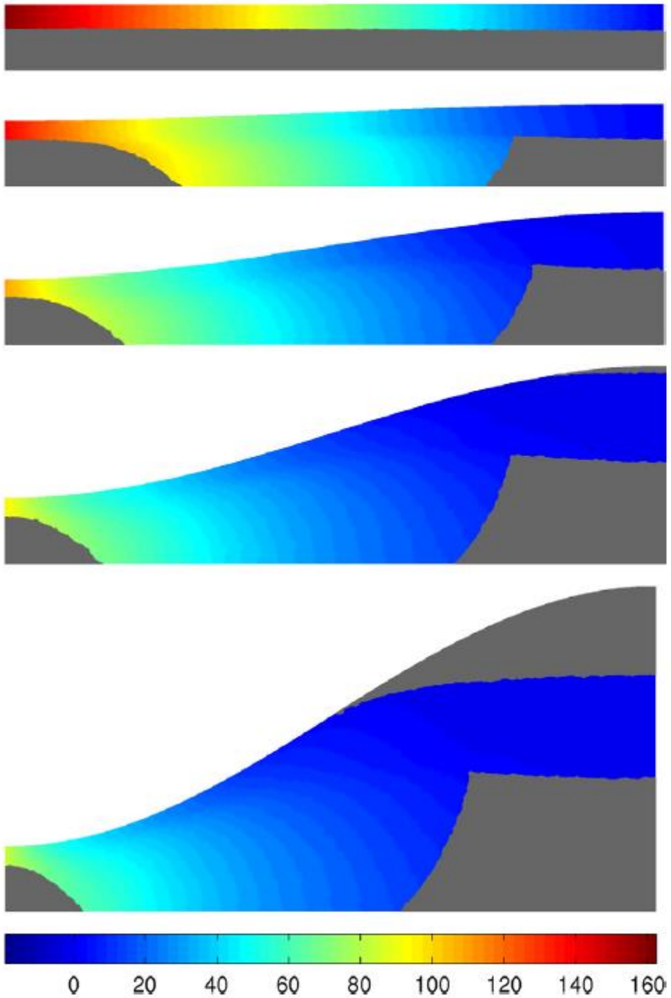

Roustaei & Frigaard, JNNFM,, 2013

Drop encapsulation

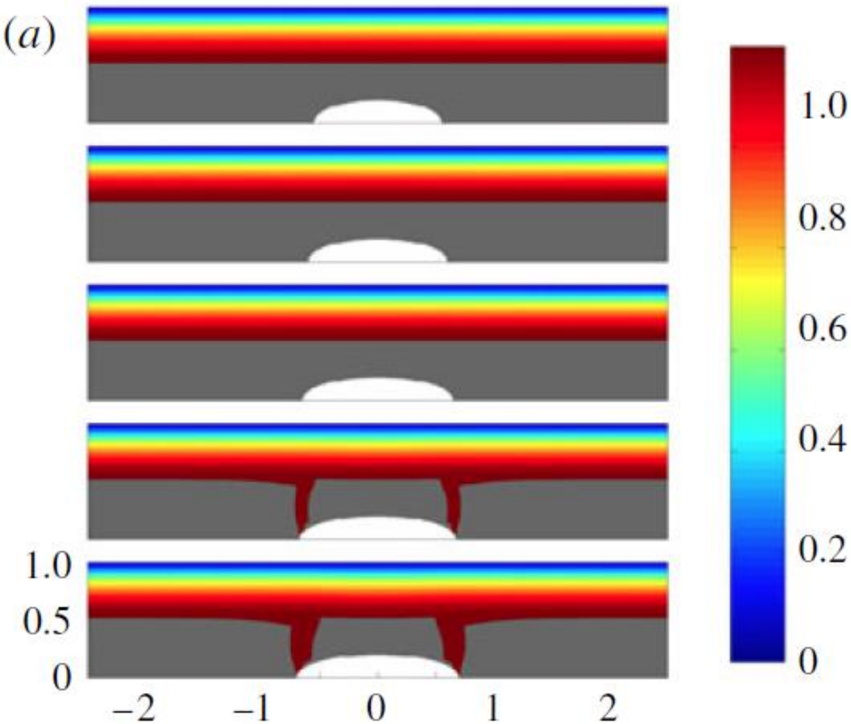

Maleki et al., JFM,, 2015

A first case study

Dam break experiments

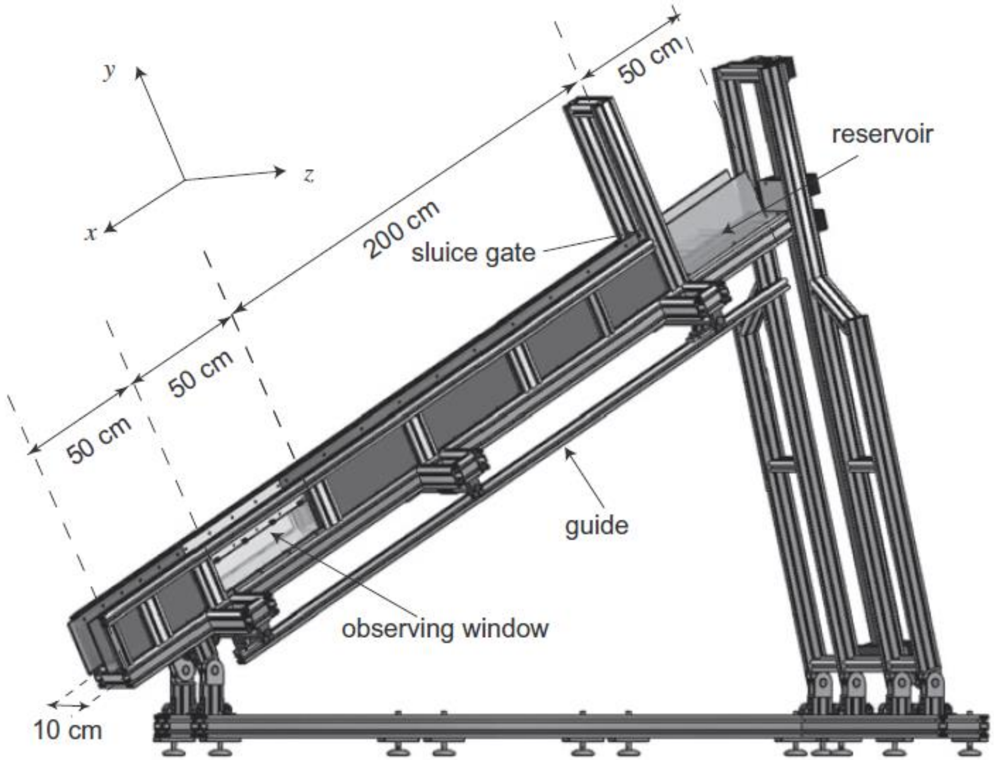

Ancey et al., Adv. Wat. Res., 2012

advanced measuring techniques

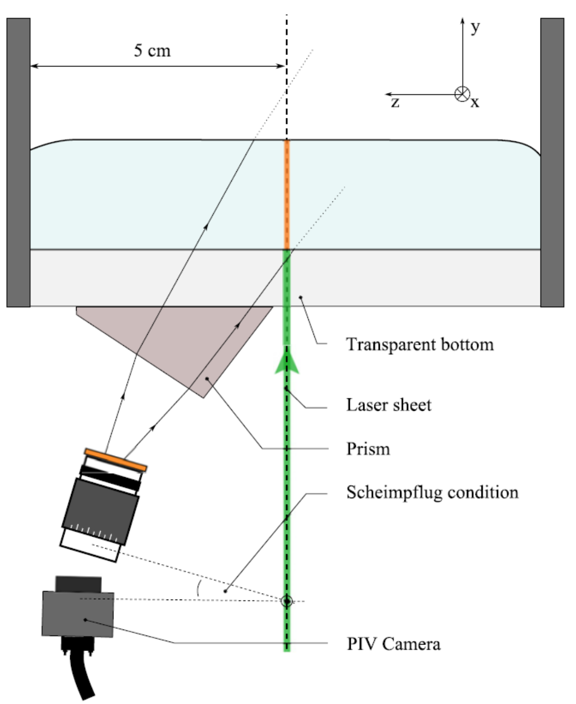

A model viscoplastic fluid: Carbopol

[redacted]

LHE, EPFL

Independent measurements of rheological parameters

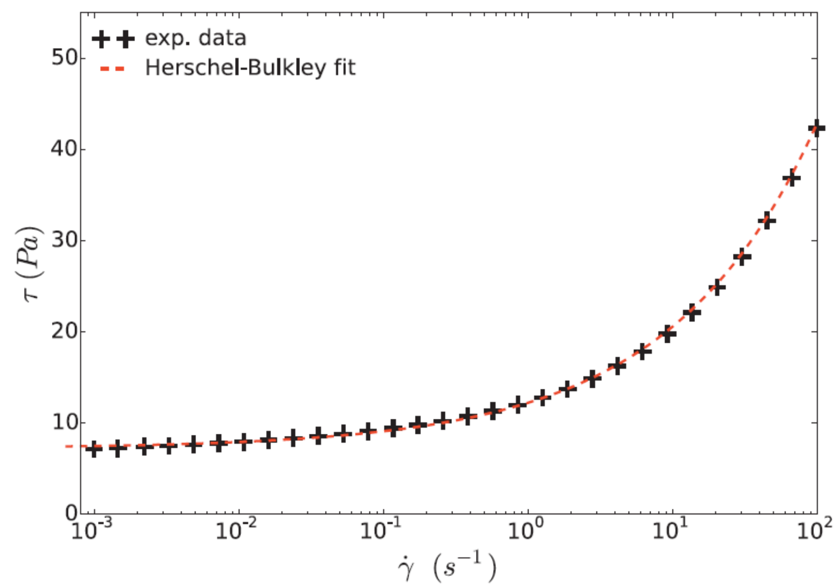

Herschel-Bulkley law

$$\begin{cases} \dot{\gamma} = 0 & \text{si } \tau < \tau_c \\ \tau = \tau_c + K\dot{\gamma}^n & \text{si } \tau \geq \tau_c \end{cases}$$

Comparison with 3 flow models of increasing complexity:

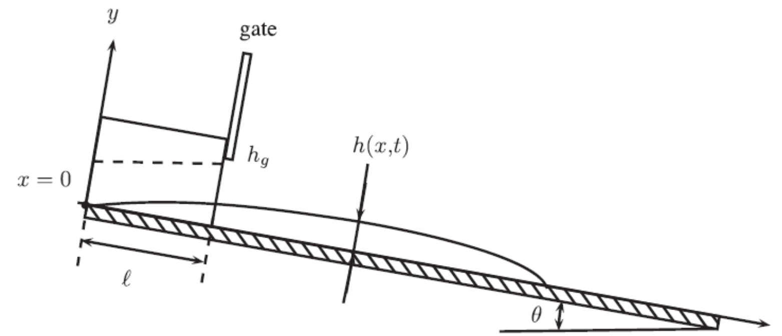

- Kinematic-wave model
  (assumption of locally uniform flow)

$$\frac{\partial h}{\partial t} + f'(h)\frac{\partial h}{\partial x} = 0,$$

with

$$f'(h) = Ah(h - h_c)^{1/n} \text{ and } A = \left(\frac{\varrho g \sin\theta}{\mu}\right)^{1/n}.$$

- Advection-diffusion model
  (account for longitudinal pressure gradient in frame of lubrication approximation)

$$\frac{\partial h}{\partial t} + nK\frac{\partial}{\partial x}\left[\left(\tan\theta - \frac{\partial h}{\partial x}\right)^{1/n}\frac{h(1+n)+nh_c}{(n+1)(2n+1)}Y_0^{1+1/n}\right] = 0,$$

$$\text{with } Y_0 = \max\left(0, h - h_c\left|1 - \cos\theta\frac{\partial h}{\partial x}\right|^{-1}\right).$$

- 2-equation shallow-water model
  (empirical rheological closure of Coussot)

$$\frac{\partial h}{\partial t} + \frac{\partial h\bar{u}}{\partial x} = 0,$$

$$\frac{\partial h\bar{u}}{\partial t} + \frac{\partial h\bar{u}^2}{\partial x} + gh\cos\theta\frac{\partial h}{\partial x} = gh\sin\theta - \frac{\tau_b}{\rho}$$

$$\tau_b = \tau_c(1 + 1.93G^{3/10}) \quad \text{with } G = \left(\frac{\mu}{\tau_c}\right)^3\frac{\bar{u}}{h}$$

Kinematic-wave model:

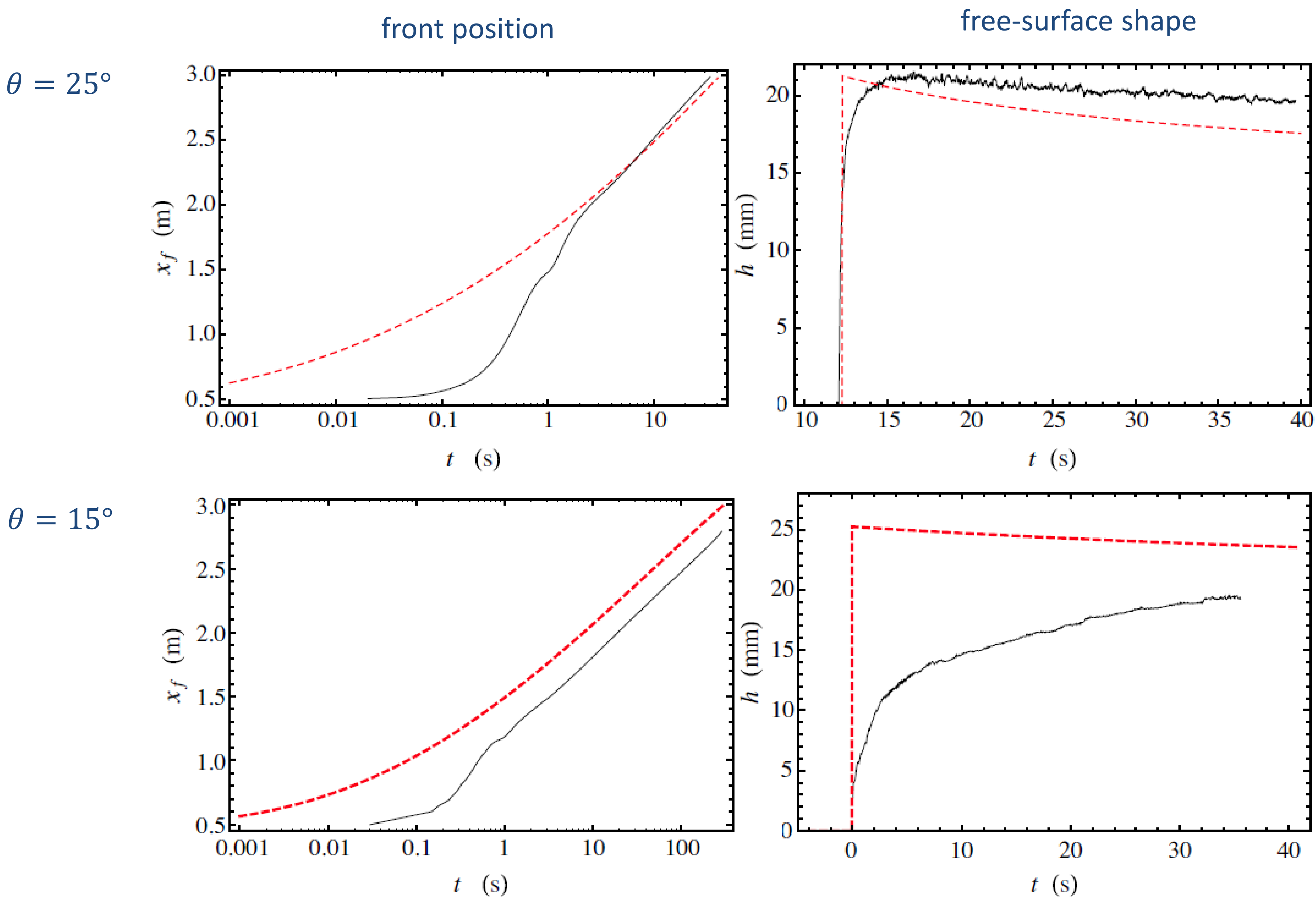

Advection-diffusion model:

front position | free-surface shape

$\theta = 25°$

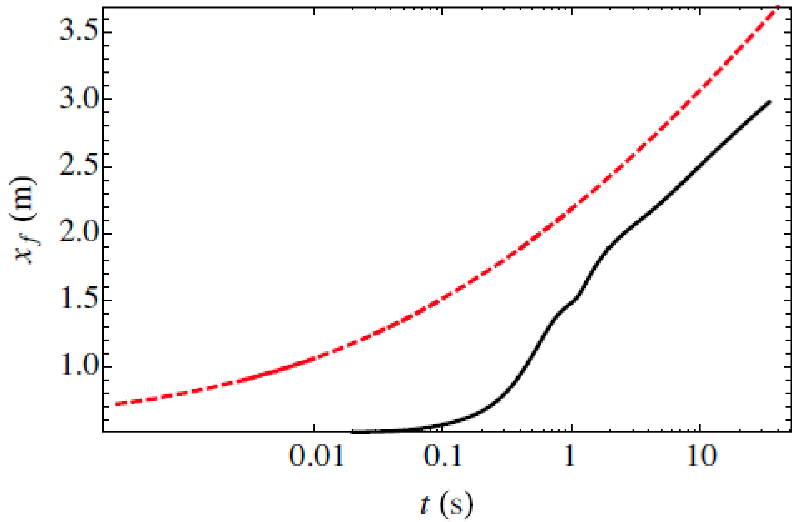

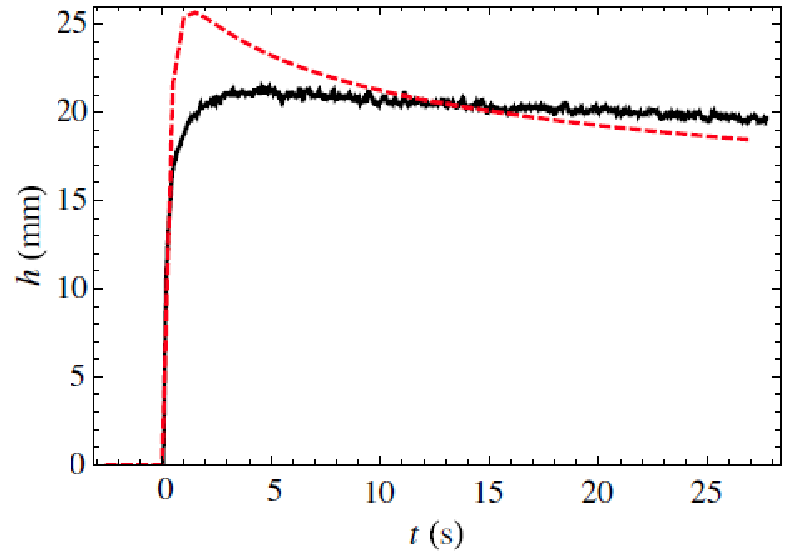

$\theta = 15°$

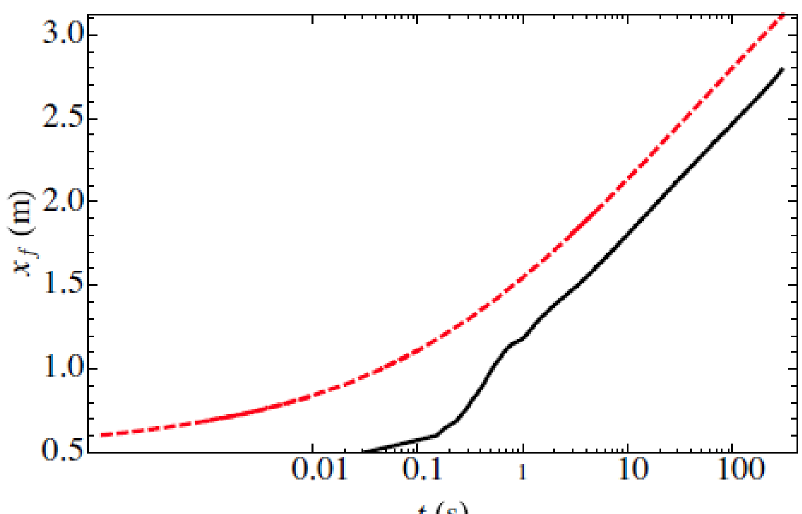

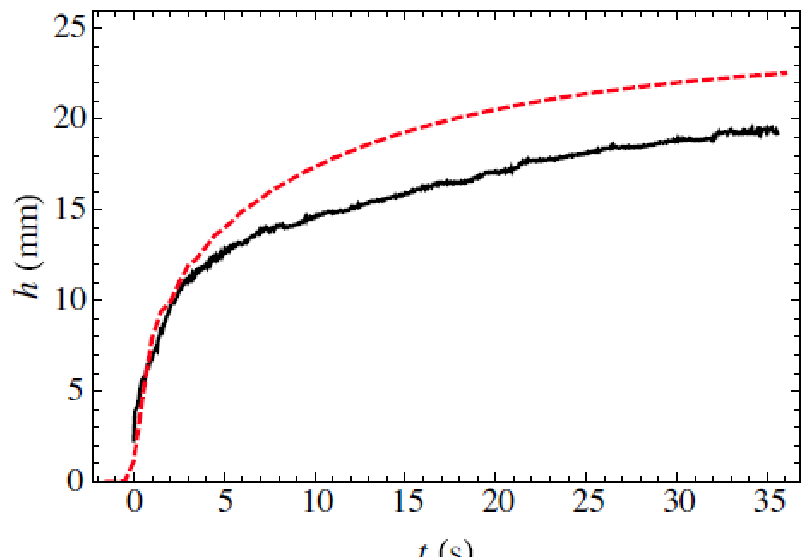

Kinematic-wave model:

front position

free-surface shape

$\theta = 25°$

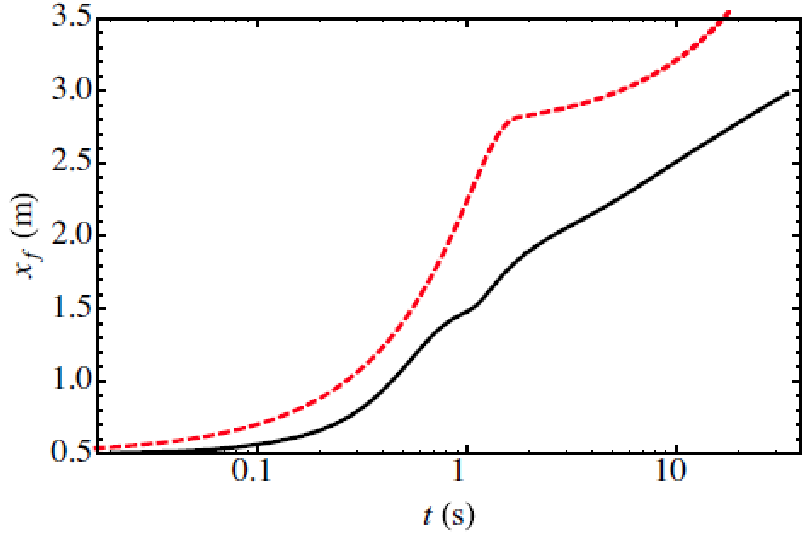

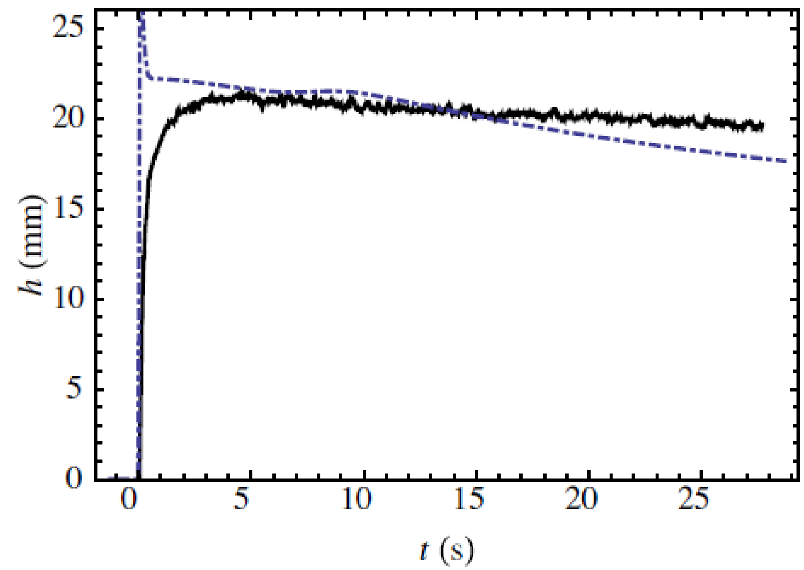

$\theta = 15°$

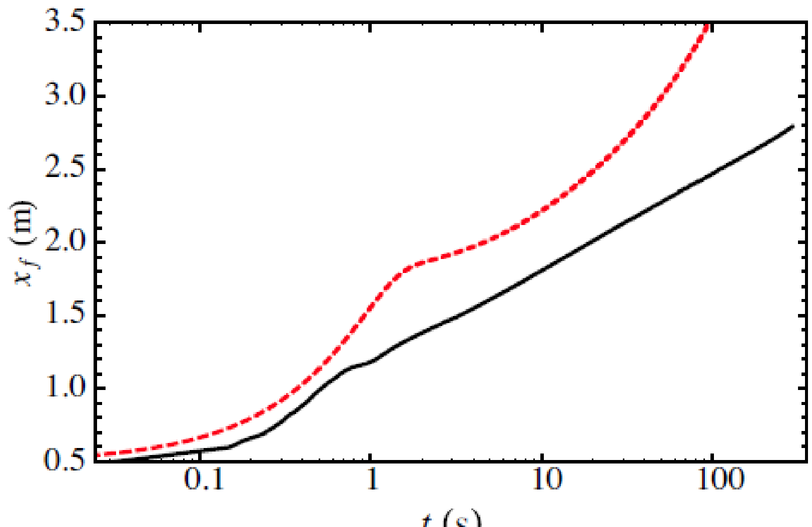

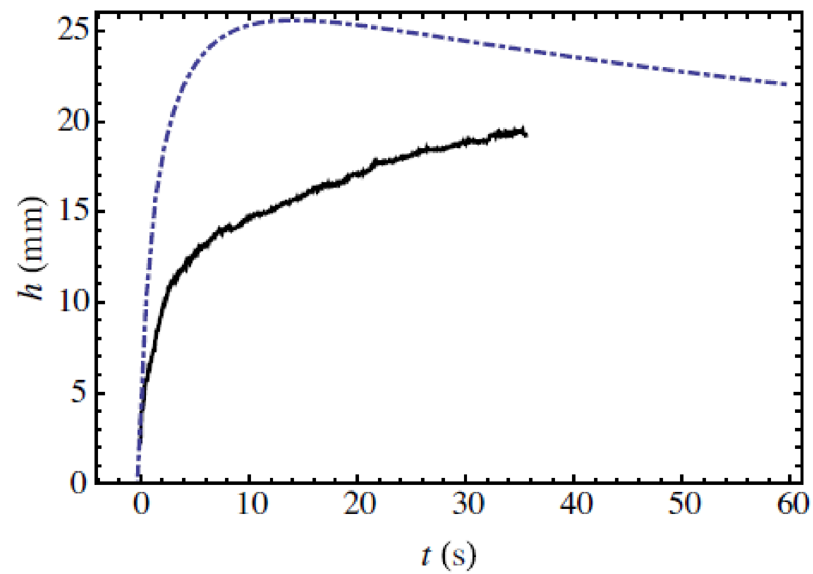

Conclusions of the authors:

- Simple models are not outperformed by more sophisticated models
- Best agreement with data is obtained with the simple kinematic-wave model, in particular for front position at large times
- Predictions of shallow-water model are particularly poor, notably at large times

Avalanche models are "cloudy"

Sciences

SCIENCES | Vidéos | Archéologie | Affaire de logique | Astronomie | Biologie | Cerveau | Géophysiqu

ÉDITION ABONNÉS

Des modèles d'avalanches brumeux

La simulation des coulées neigeuses reste un exercice incertain. Un spécialiste met en garde contre son utilisation inconsidérée dans la définition des zones à risque en montagne.

LE MONDE SCIENCE ET TECHNO | 24.02.2014 à 16h48 • Mis à jour le 25.02.2014 à 14h01 |

Par Viviane Thivent

Abonnez vous à partir de 1 € | Réagir | Ajouter | Partager | Tweeter

Velocity profiles:

(based on measured values of $\partial_x h$)

$\theta = 25°$

$\theta = 15°$

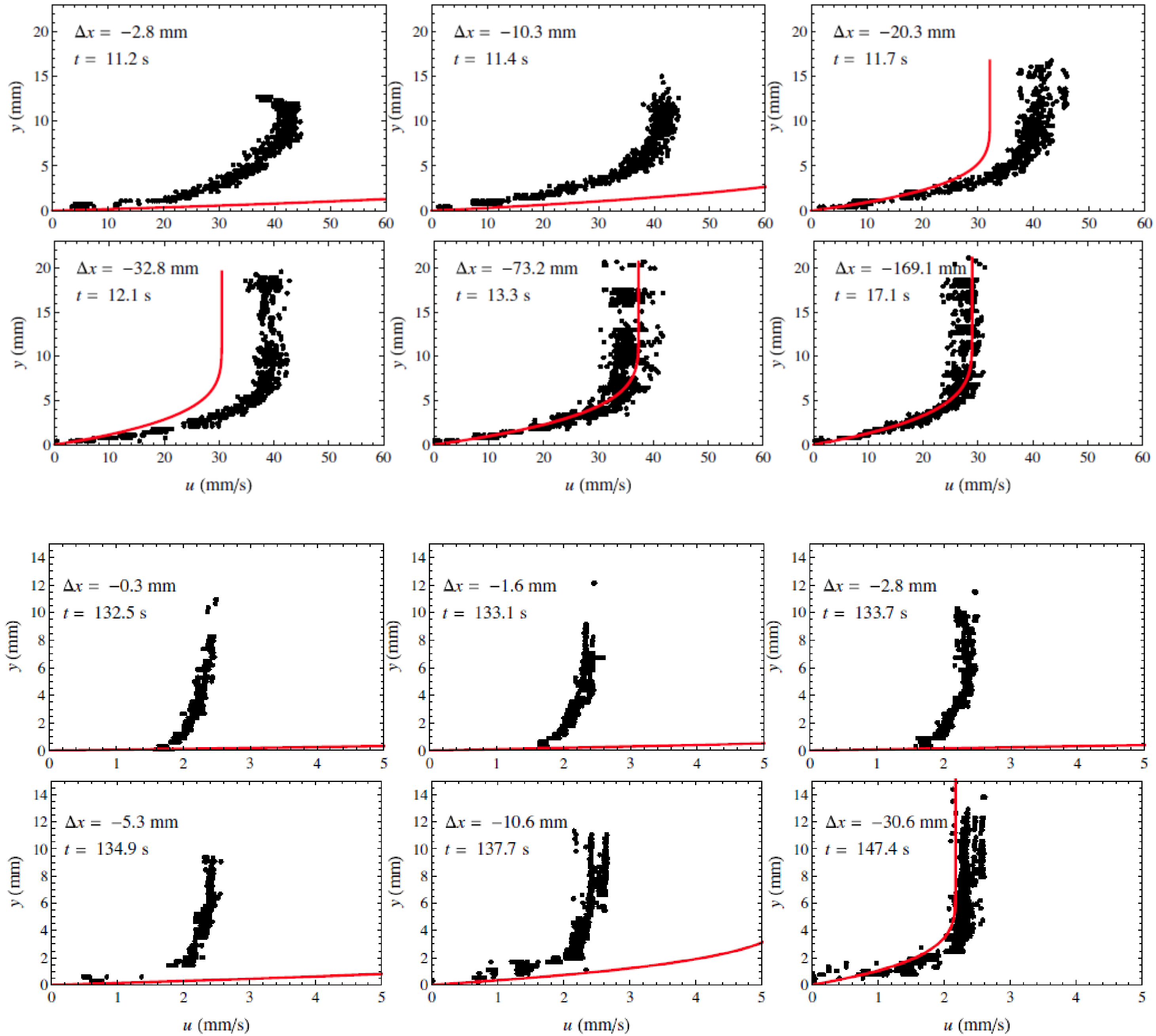

➢ Flow conditions within the head significantly depart from lubrication conditions

Comparisons with a Newtonian fluid:

velocity profiles

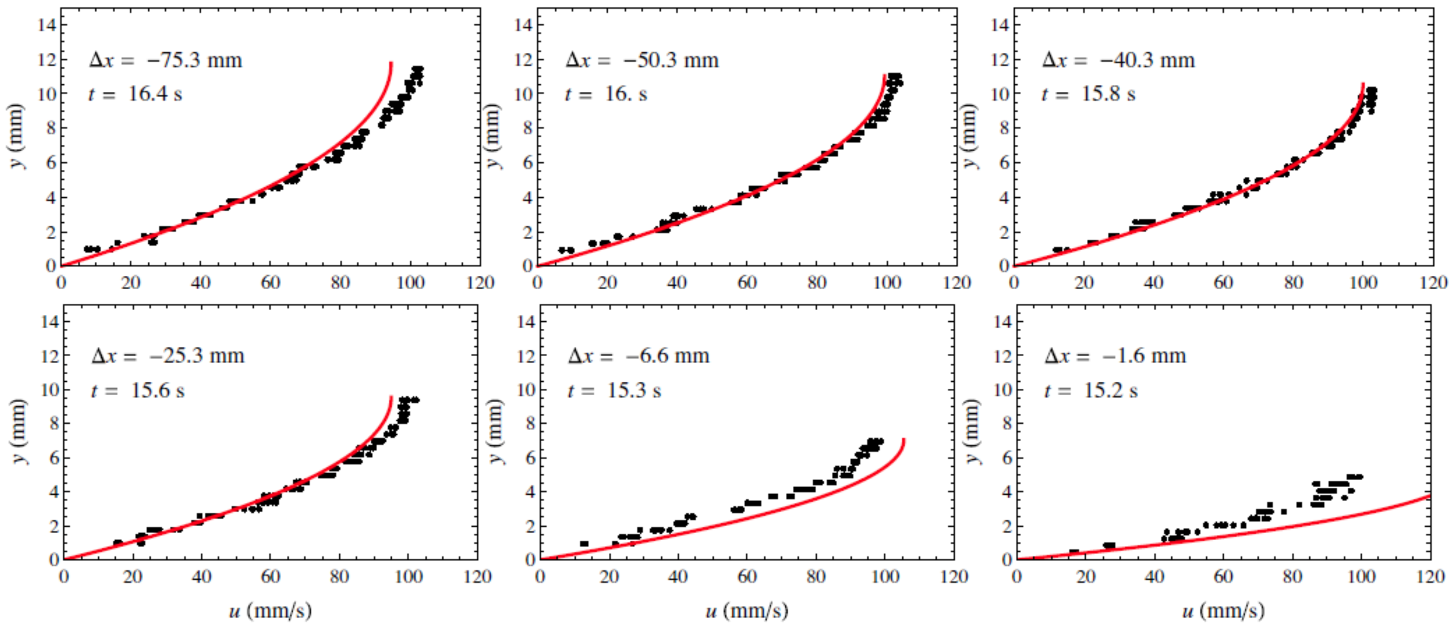

front position

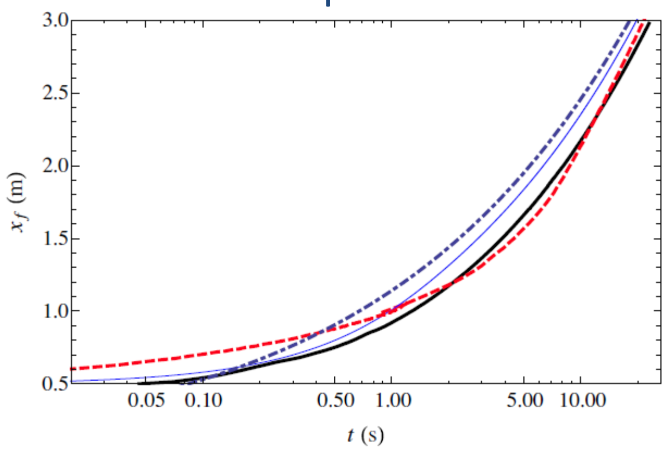

free-surface shape

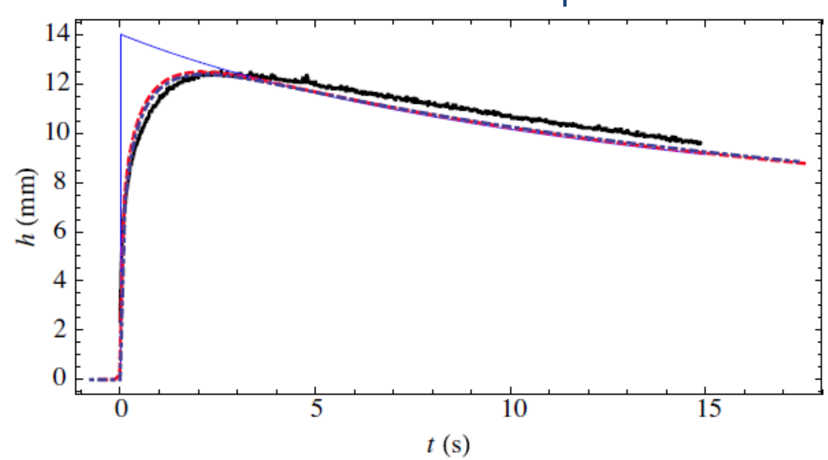

A second example

Flow in an expansion-contraction (cavity)

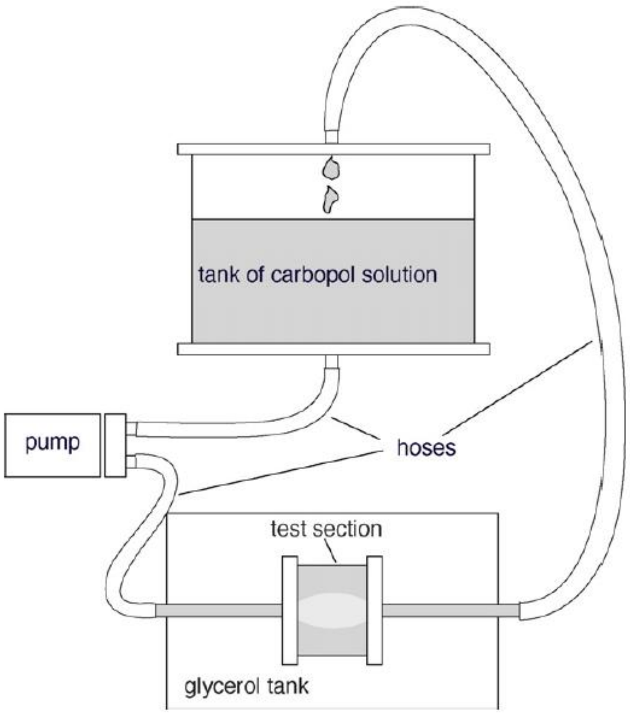

numerical solution based on a regularized viscoplastic model

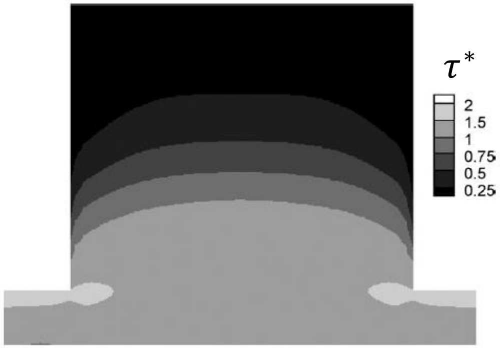

$$\tau = \left[1 - \exp\left(-\frac{\eta_0 \dot{\gamma}}{\tau_c}\right)\right] (\tau_c + K\dot{\gamma}^n)$$

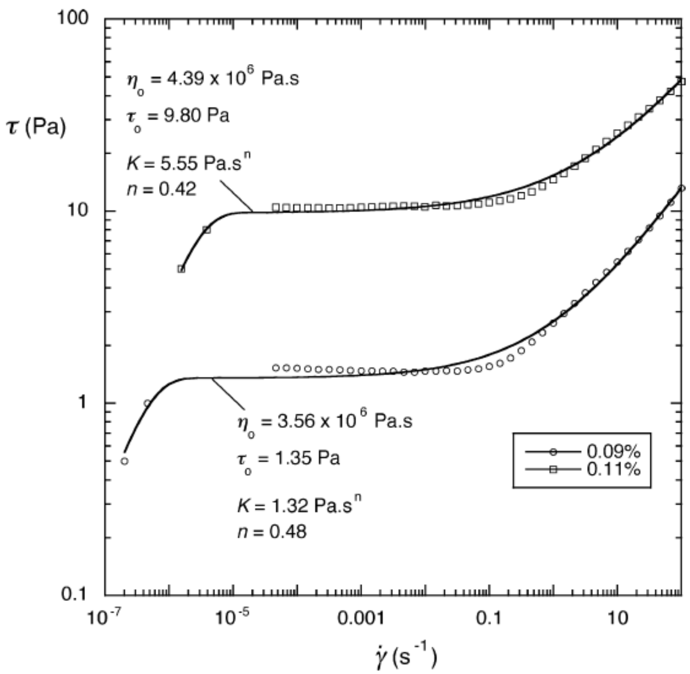

de Souza Mendes et al., JNNFM, 2007

Experimental flow patterns

Decreasing values of τ_c

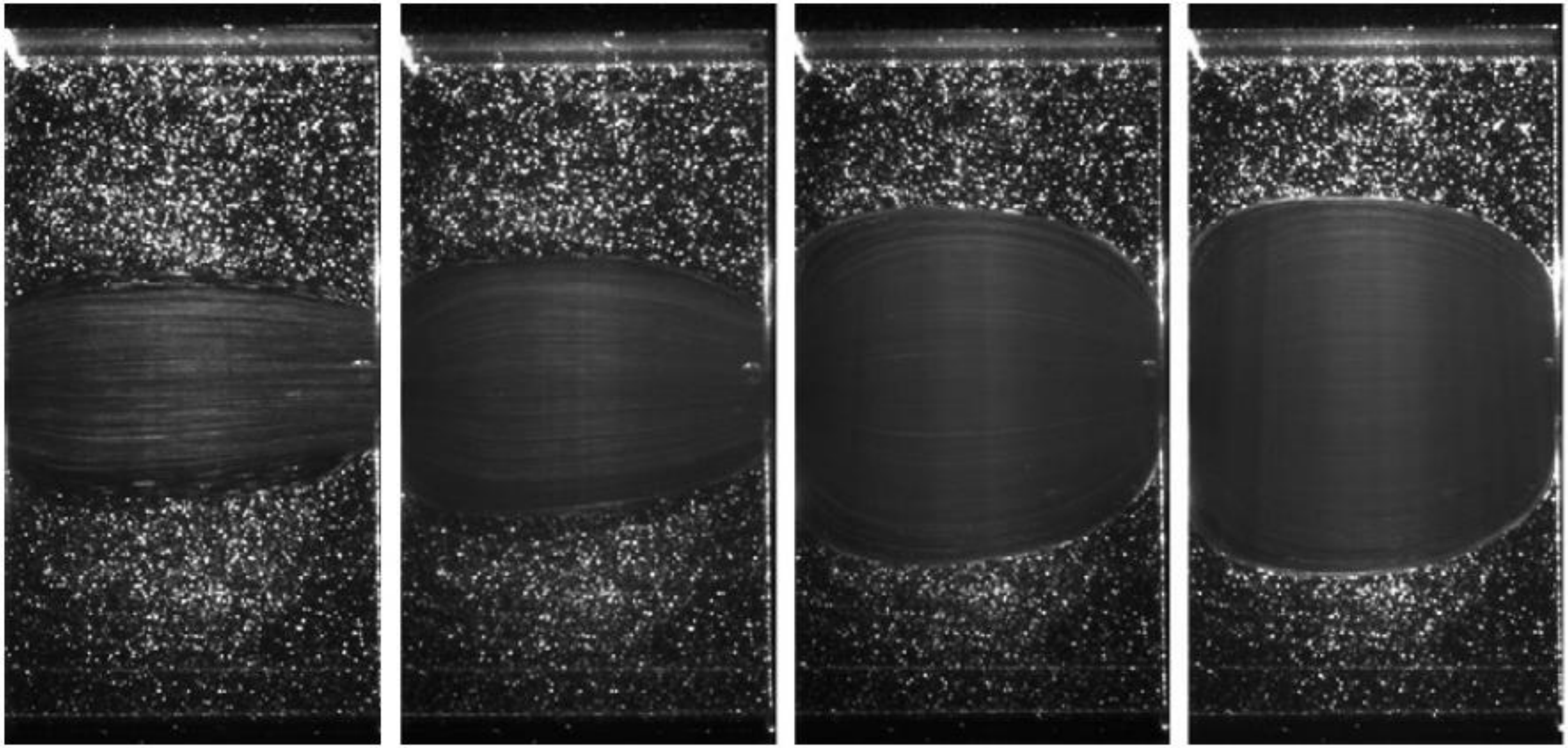

Model comparison

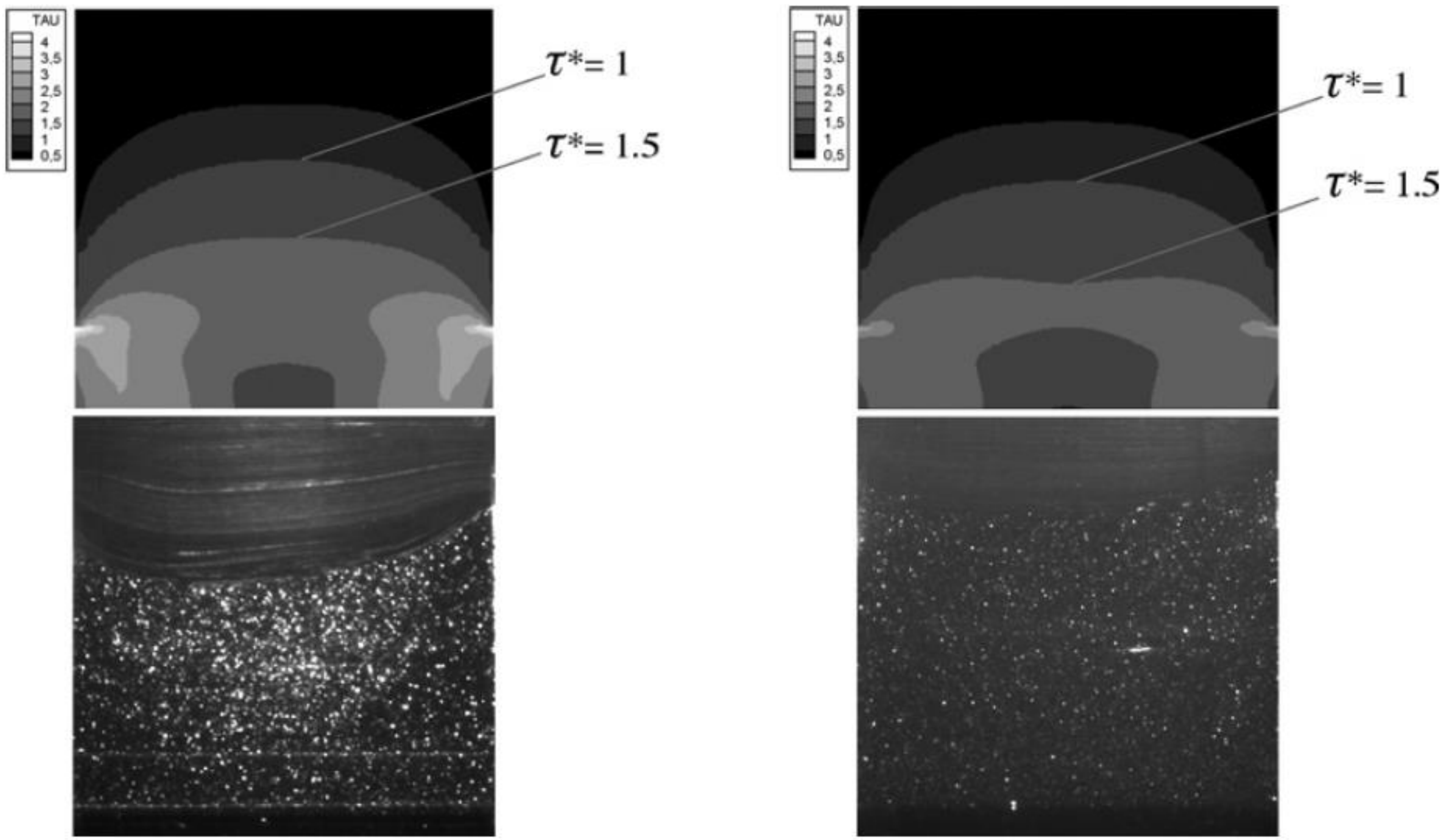

- Significant overestimation of the size of the yielded zone
- Prediction of symmetric yield surfaces

Shortcomings and open questions:

- Origin of the discrepancies for viscoplastic fluids?
  - model assumptions
    - thin-layer assumptions
    - rheological closures
  - numerical methods
    - numerical schemes
    - regularization
  - comparison methods
    - yield surfaces
    - “cumulative” discrepancies (case of velocity profiles)

- What about experimental uncertainties?
  - dynamical measurements (PIV, fronts, etc.)
  - 3D effects (front)
  - rheological characterization
    - repeatability
    - more complex rheological trends of the fluids

- How to circumvent these difficulties?
  - How credible are rheometrical measurements?
  - Are “real” yield-stress materials really viscoplastic?
  - How to account for experimental uncertainties in the comparisons with models?
  - Possible to “measure” plug zones?

Rheometrical measurements

Laboratory rheometers

Simple-shear (viscosimetric) flow

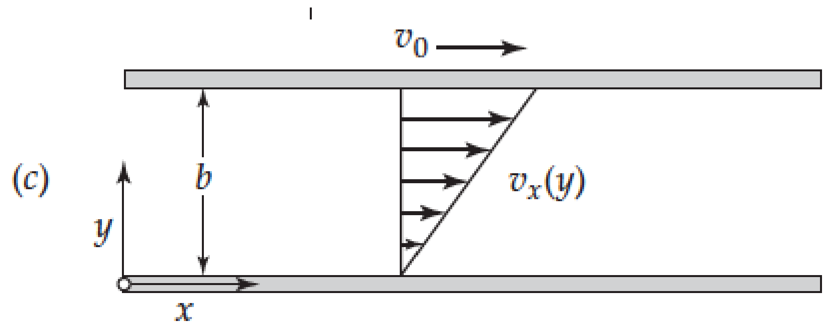

$$D(\boldsymbol{v}) = \frac{1}{2}\begin{pmatrix} 0 & \dot{\gamma} & 0 \\ \dot{\gamma} & 0 & 0 \\ 0 & 0 & 0 \end{pmatrix} \Rightarrow \boldsymbol{\Sigma} = \begin{pmatrix} \sigma_{xx} & \sigma_{xy} & 0 \\ \sigma_{xy} & \sigma_{yy} & 0 \\ 0 & 0 & \sigma_{zz} \end{pmatrix}$$

$$\tau = \sigma_{xy} = f(\dot{\gamma})$$
$$N_1 = \sigma_{xx} - \sigma_{yy} = g_1(\dot{\gamma})$$
$$N_2 = \sigma_{yy} - \sigma_{zz} = g_1(\dot{\gamma})$$

- stress-imposed or strain-rate imposed
- in the former case: $\dot{\gamma}_{min} \approx 10^{-3} - 10^{-2}$ s^{-1}

Cone and plate device

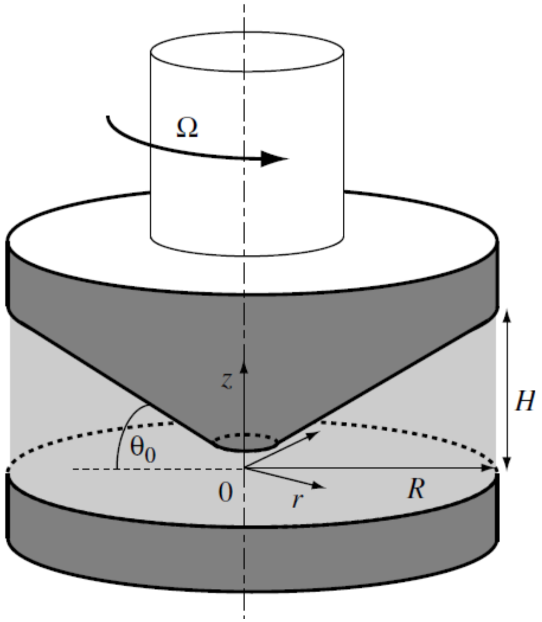

Raw measurements:

- Ω: rotation velocity
- Γ: torque
- (F_N: normal force)

$$\dot{\gamma} \approx \frac{\Omega r}{\theta_0 r} = \frac{\Omega}{\theta_0} \;\Rightarrow \text{constant}$$

$$\Gamma \approx \int_0^R 2\pi r^2\,\tau\,dr \;\Rightarrow \tau = \frac{3\Gamma}{2\pi R^3}$$

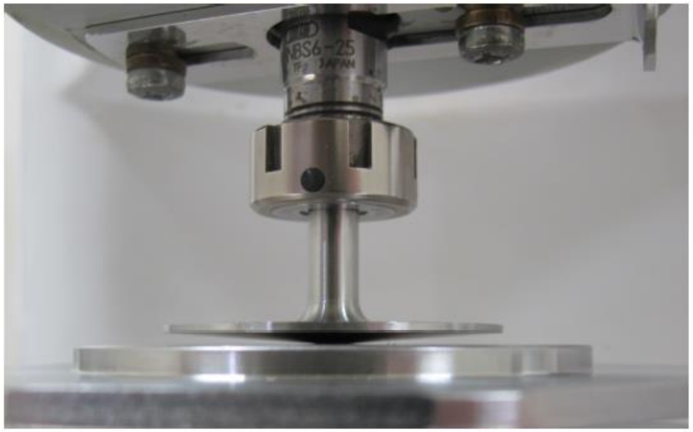

Parallel-plates device

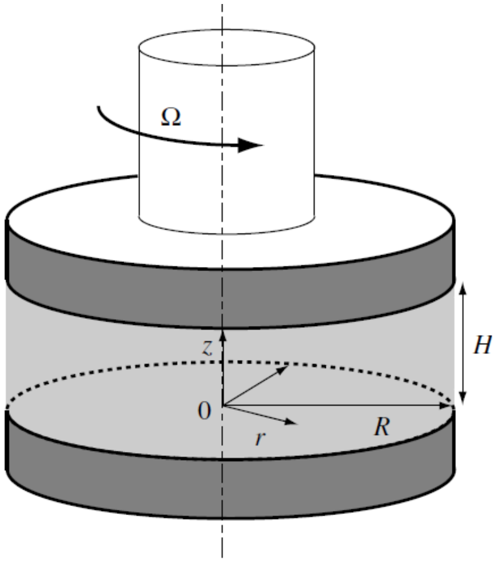

$$\dot{\gamma}(r) \approx \frac{\Omega r}{H} \Rightarrow \text{heterogeneous}$$

$$\Gamma = \int_0^R 2\pi r^2\, \tau(r) dr \;\Rightarrow \tau \approx \frac{3\Gamma}{2\pi R^3}$$

$$\Rightarrow \tau(R) = \frac{\Gamma}{2\pi R^3}\left(3 + \frac{\dot{\gamma}(R)}{\Gamma}\frac{\partial \Gamma}{\partial \dot{\gamma}(R)}\right)$$

numerical differentiation
is required

Couette (concentric cylinder) device

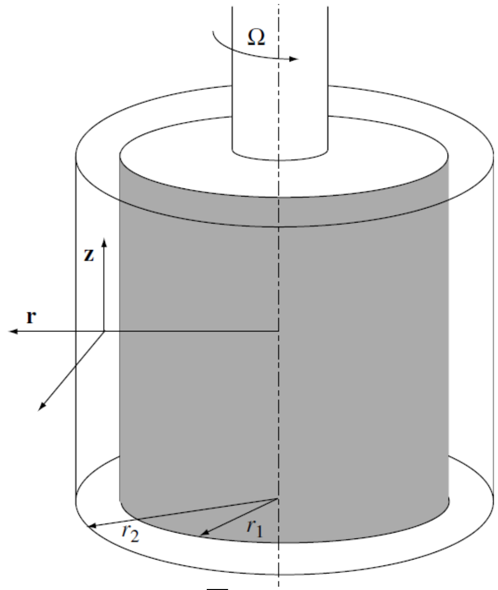

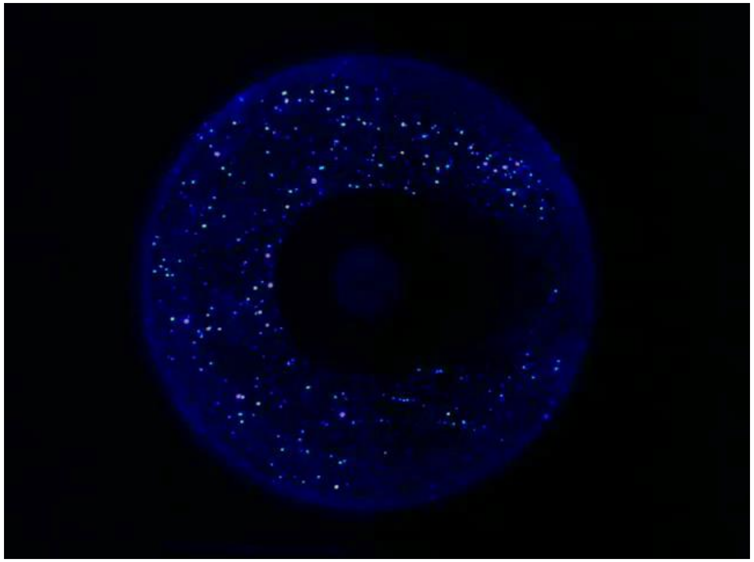

LHE, EPFL

$$\tau(r) = \frac{\Gamma}{2\pi H r^2}$$

$$\Omega = \int_{r_1}^{r_2} \frac{\dot{\gamma}(r)}{r}\, dr \;\Rightarrow \text{inverse problem}$$

- small gap approximation ($r_2 - r_1 \ll r_1$): $\Omega \approx \dot{\gamma}\, \dfrac{r_2 - r_1}{r_1}$
- in general:
  - series expansion
  - Tikhonov regularization
  - Wavelet-vaguelette decomposition
  - …

shear-rate heterogeneity

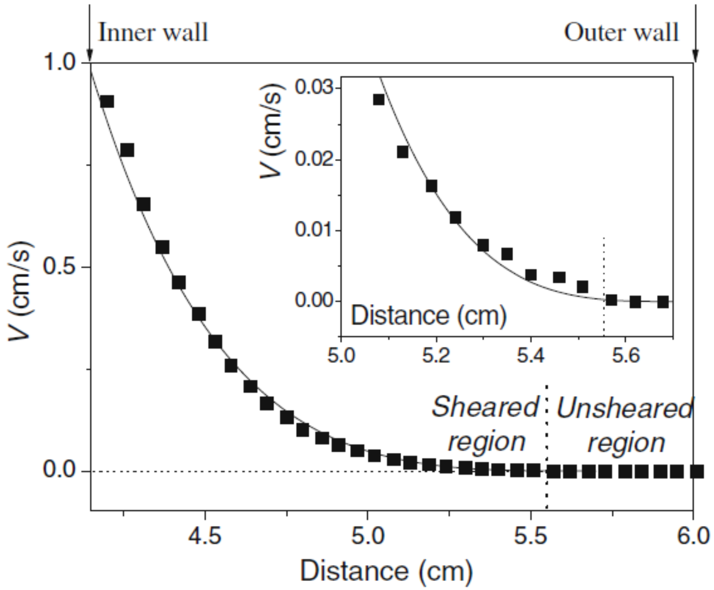

Ovarlez et al., 2009

Experimental procedures

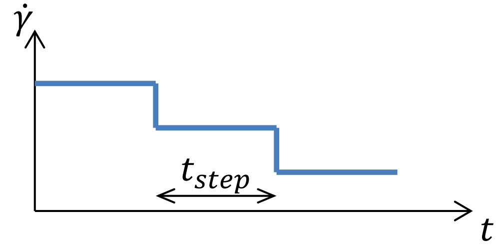

Strain-rate (or stress) "ramps": flow curve

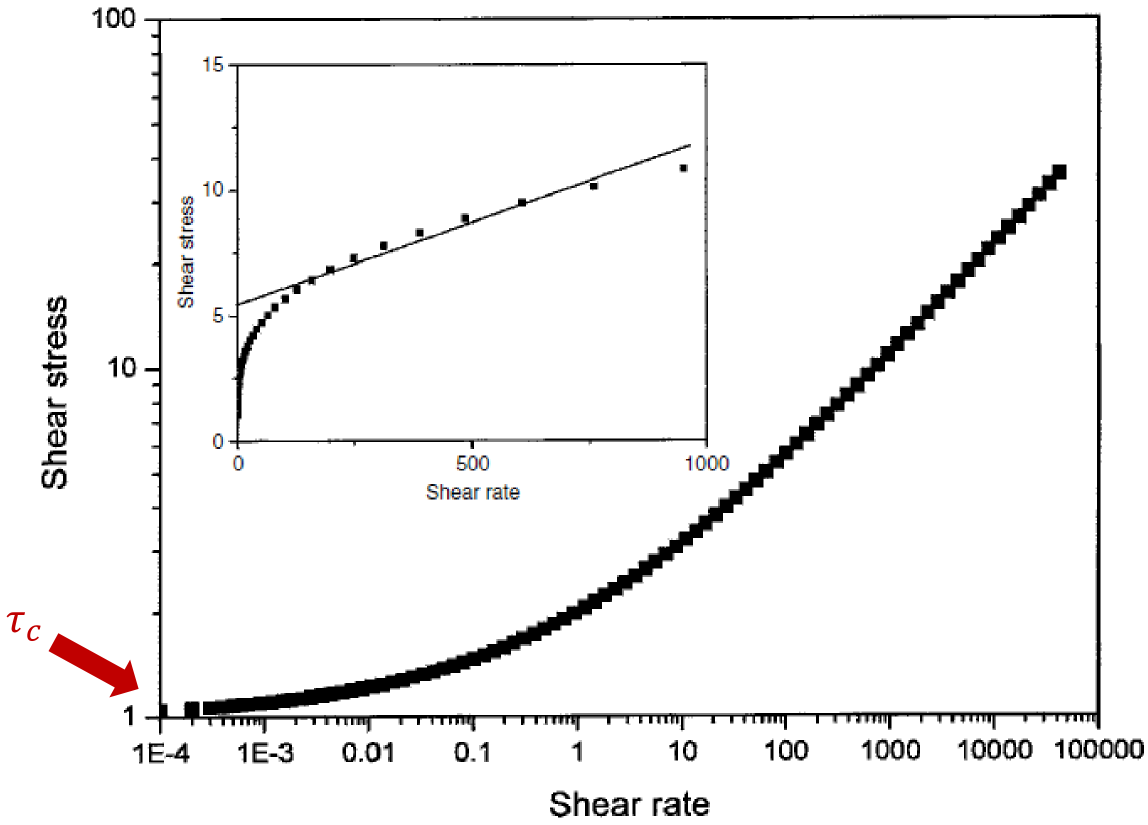

- Flow curve
- Yield stress (extrapolation: fitting)
- Influence of t_{step} (steady-state)?

Experimental procedures

Constant strain rate: flow startup

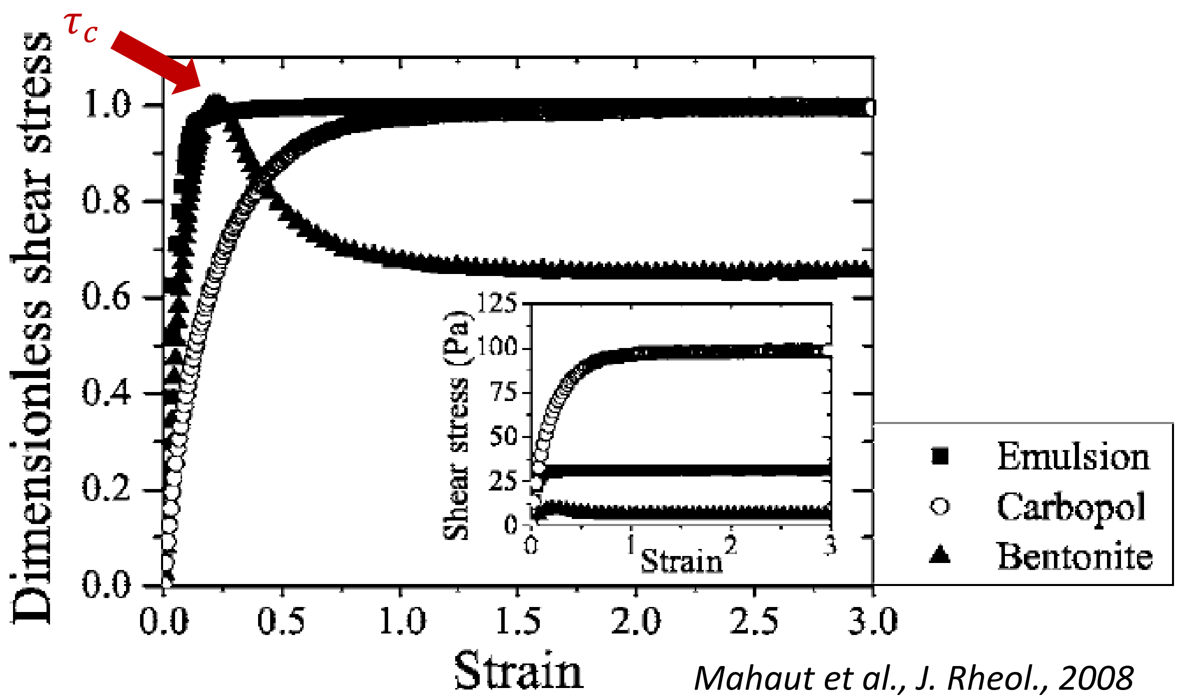

Mahaut et al., J. Rheol., 2008

- Yield stress
- Pre-yielding behavior

Experimental procedures

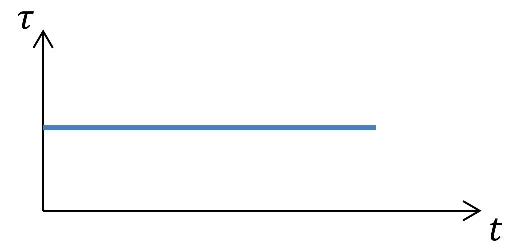

Constant stress: creep test

Clay

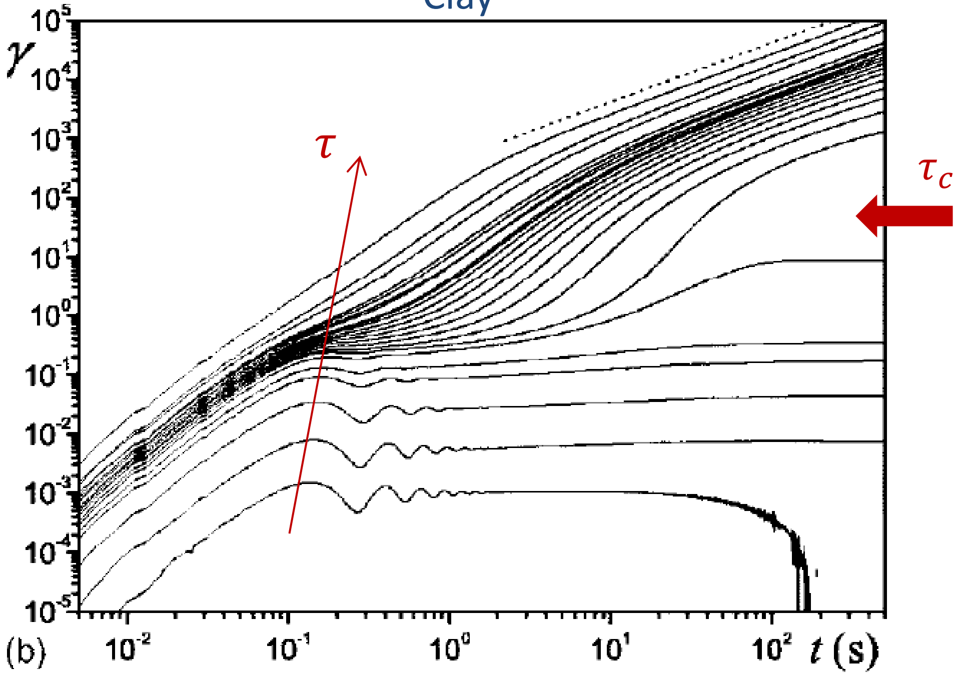

Gel

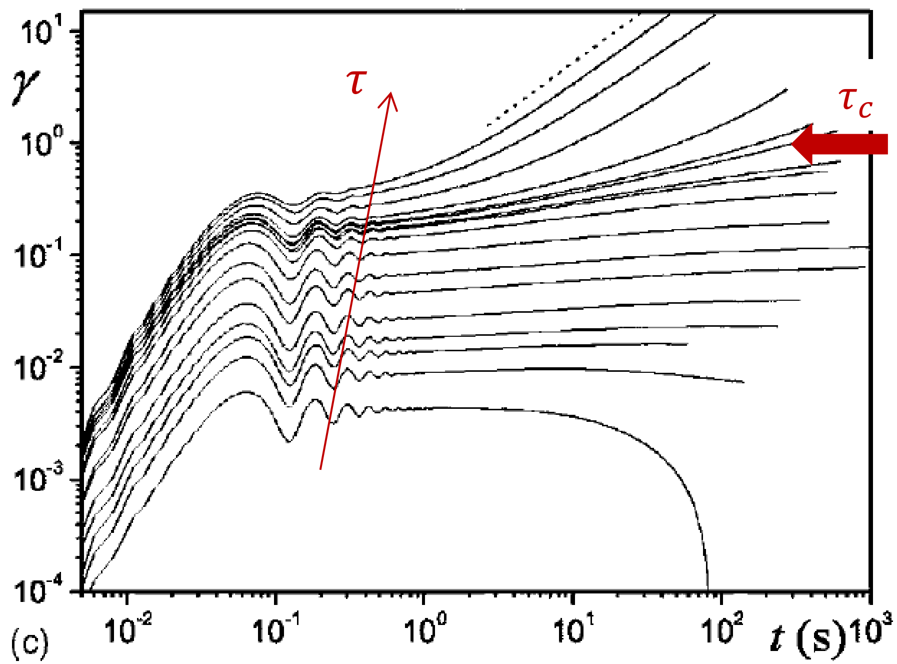

Coussot et al., J. Rheol., 2006

- Yield stress

Perturbative factors in rheometry

Free-surface perturbations

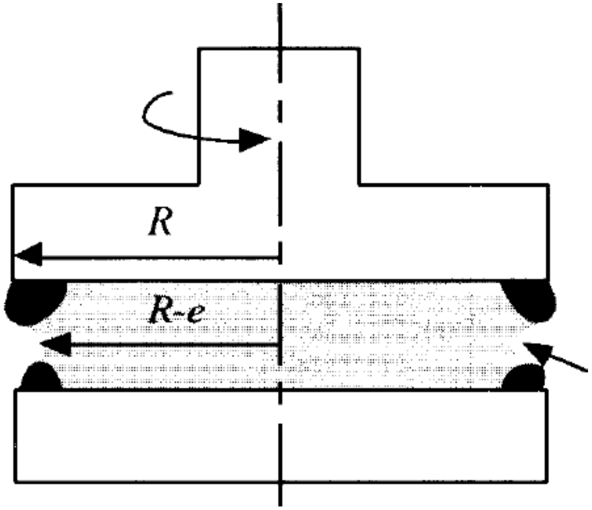

$$\tau \approx \frac{3\Gamma}{2\pi R^3}$$

strong influence of geometry errors

Wall-slip

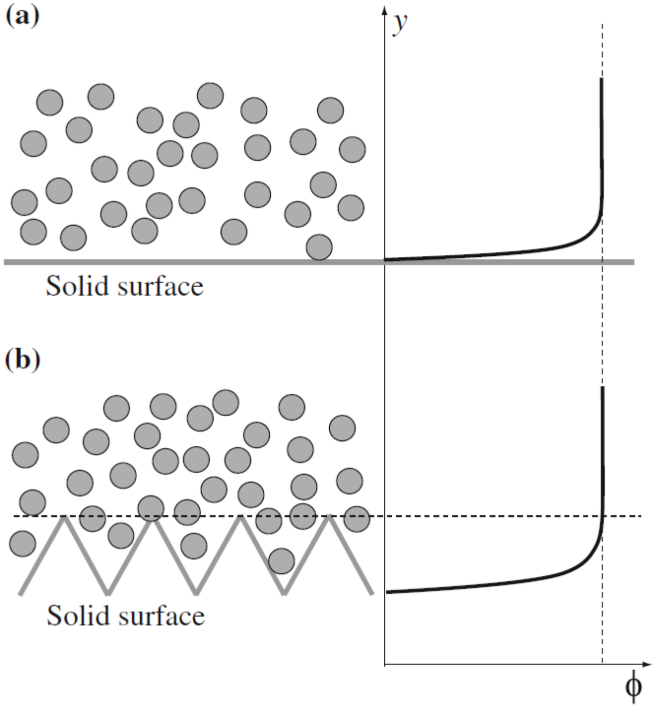

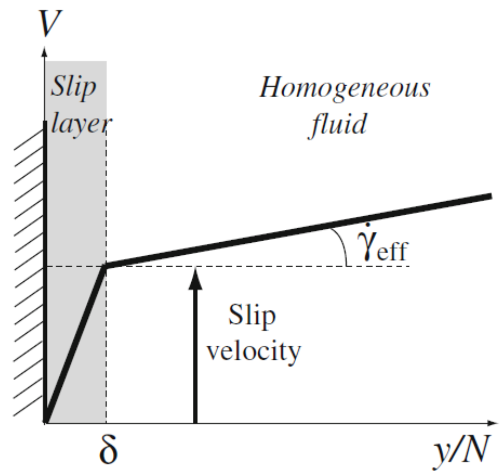

use of rough tools

influence on flow curve (Carbopol)

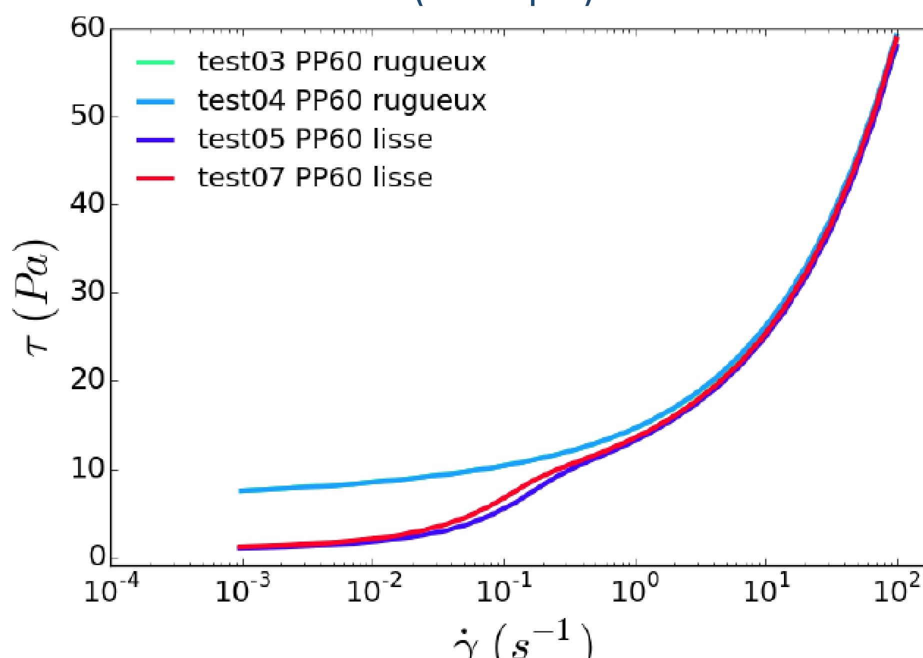

Shear-banding, cracking

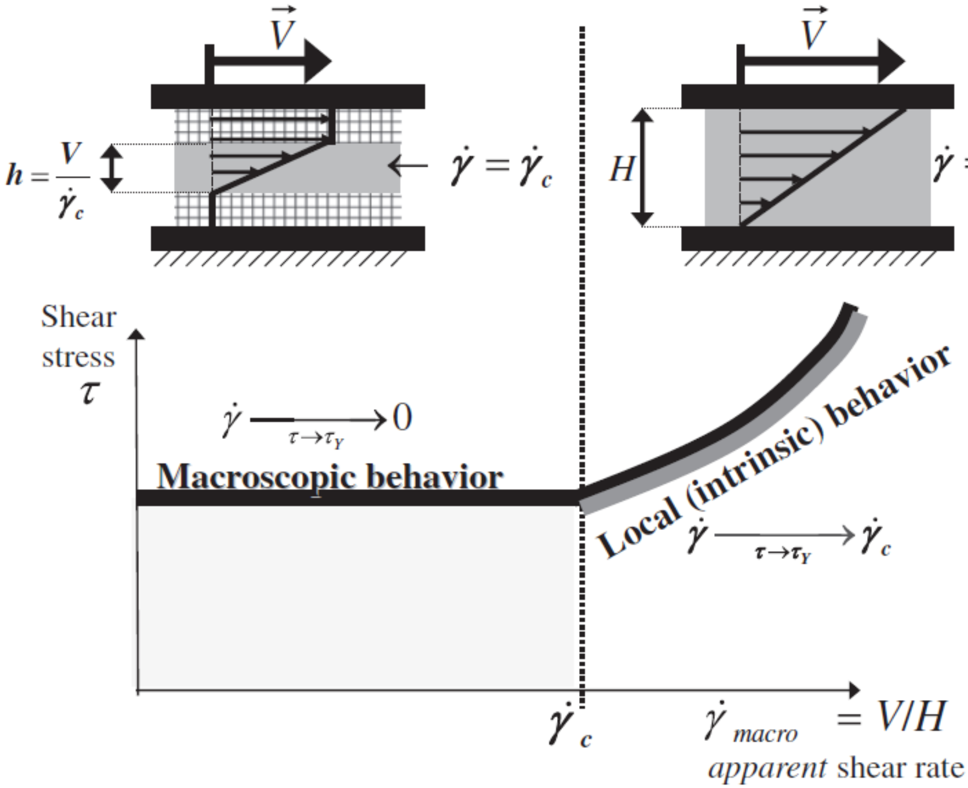

Ovarlez et al., JNNFM, 2012

critical shear rate below which flow becomes **heterogeneous**

⇒ related to thixotropic behavior of the material

apparent plateau in flow curves (bentonite)

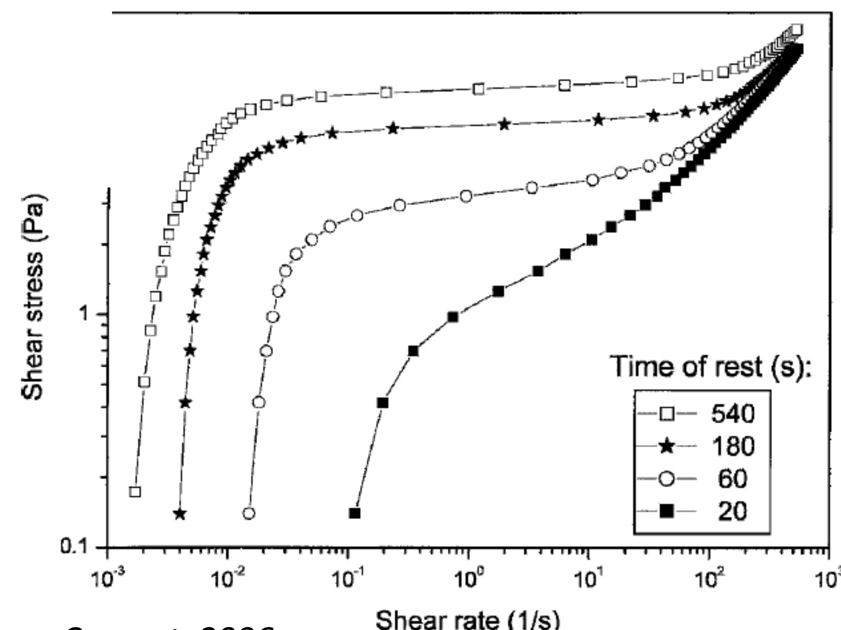

Coussot, 2006

Steady-state

Kaolin

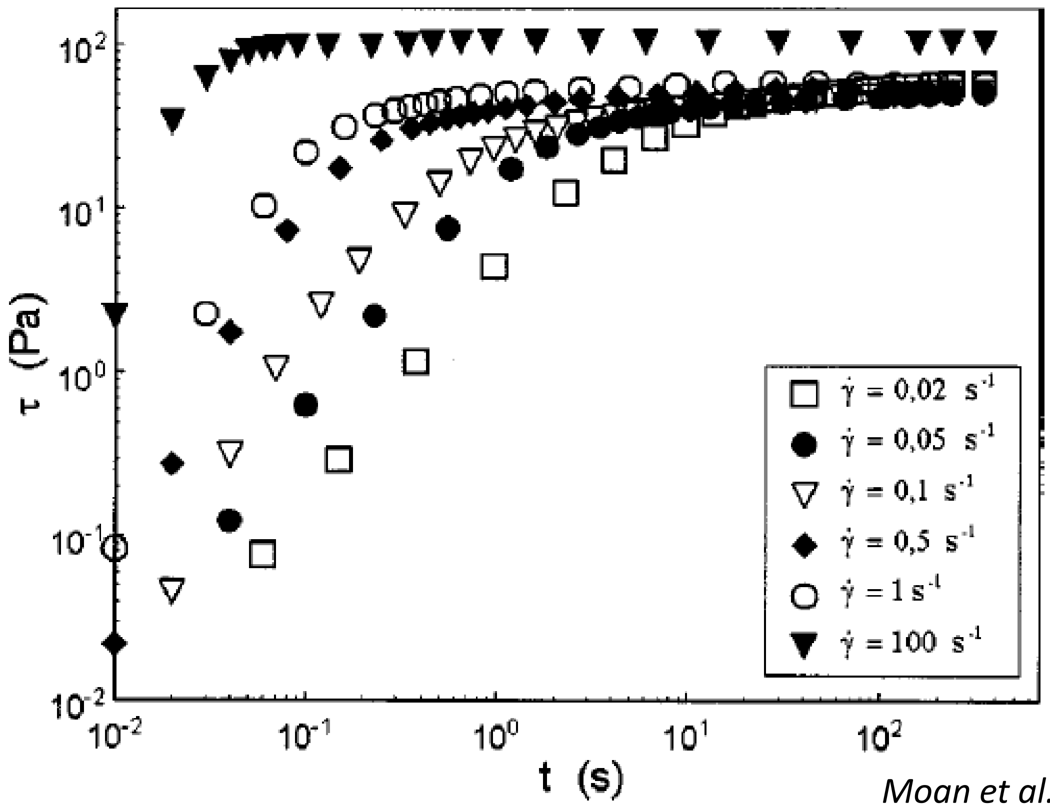

Moan et al., J. Rheol., 2003

- Time to reach equilibrium increases when $\dot{\gamma}$ decreases
- Need to be accounted for when measuring the flow curve: $t_{step} > t_{eq}$

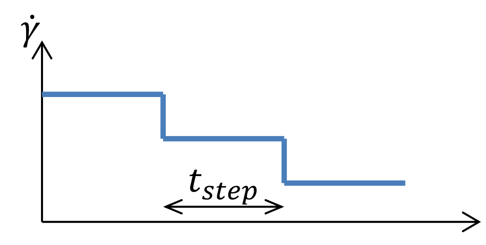

Steady-state

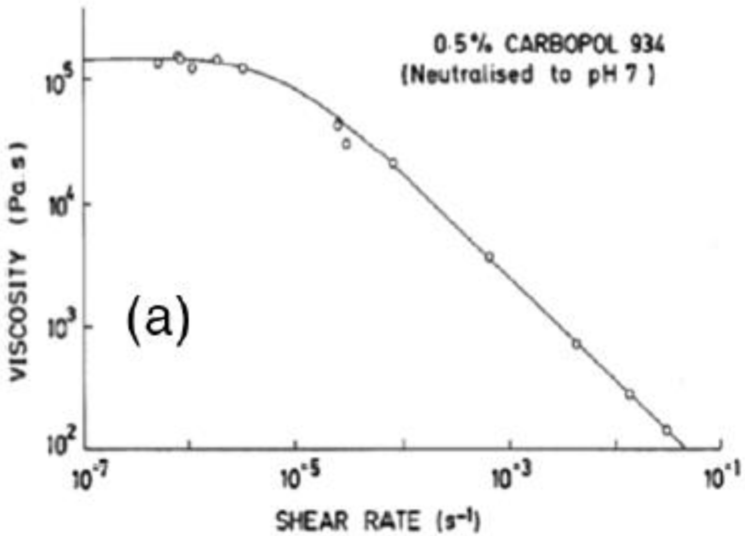

Barnes & Walters, Rheol. Act., 1995

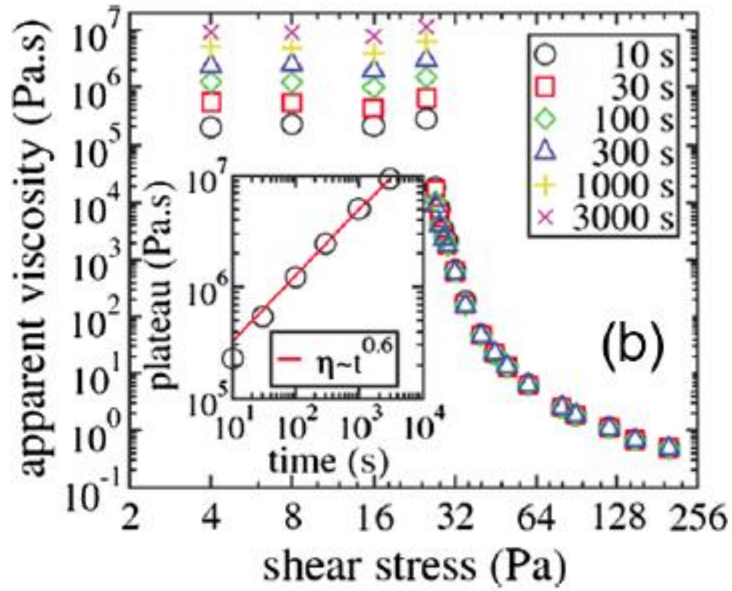

Moller et al., EPL, 2009

ELSEVIER

J. Non-Newtonian Fluid Mech., 81 (1999) 133–178

Journal of Non-Newtonian Fluid Mechanics

The yield stress—a review or ‘παντα ρει’—everything flows?

Howard A. Barnes

Unilever Research Port Sunlight, Bebington, Wirral, L63 3JW Merseyside, UK

Received 30 March 1998; received in revised form 4 May 1998

Confinement effects

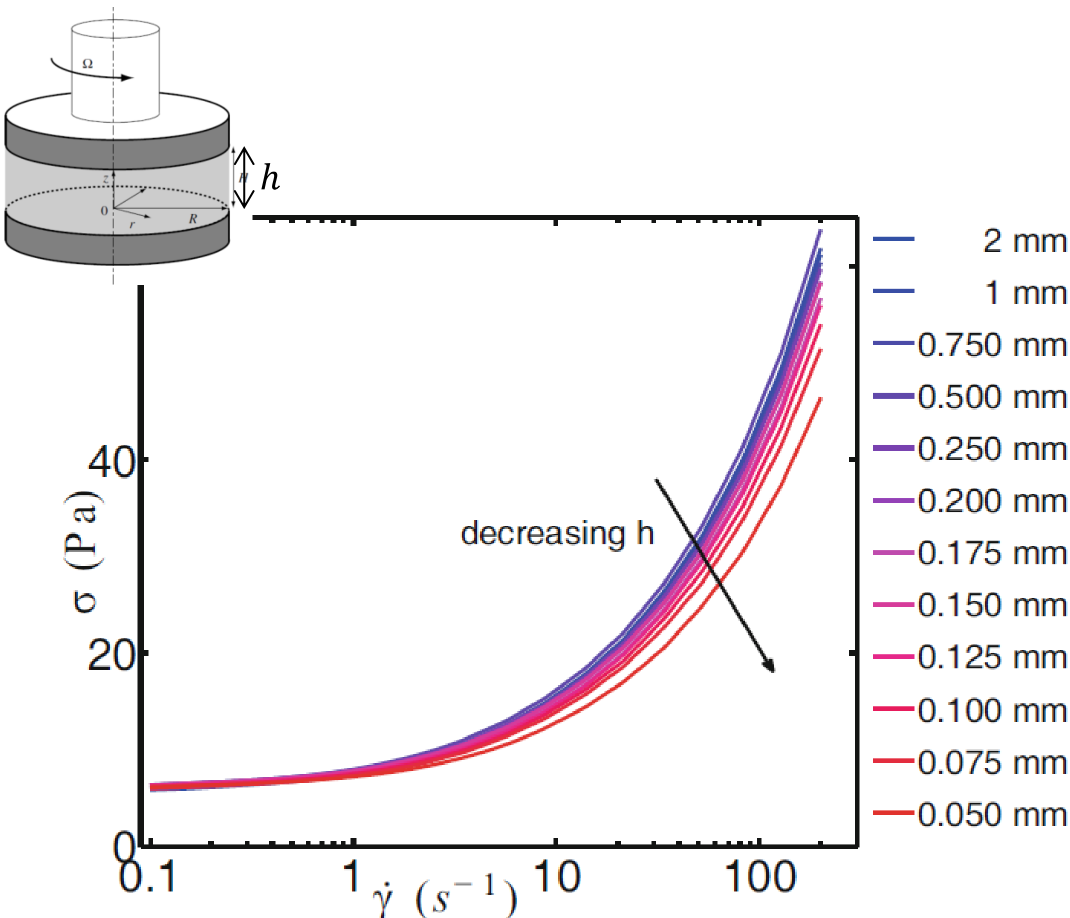

Géraud et al., EPJE, 2013

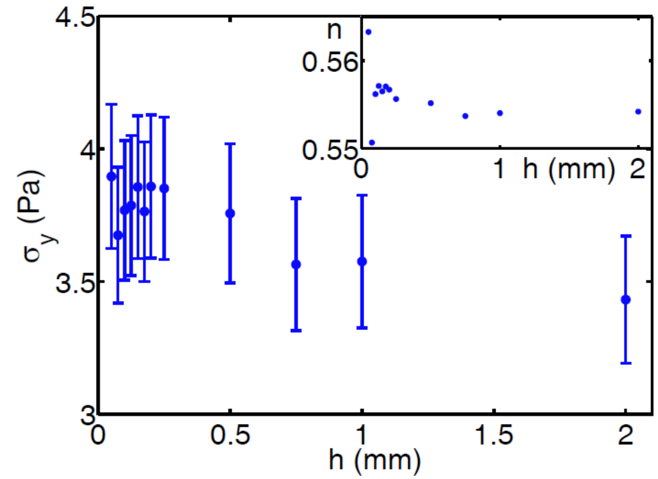

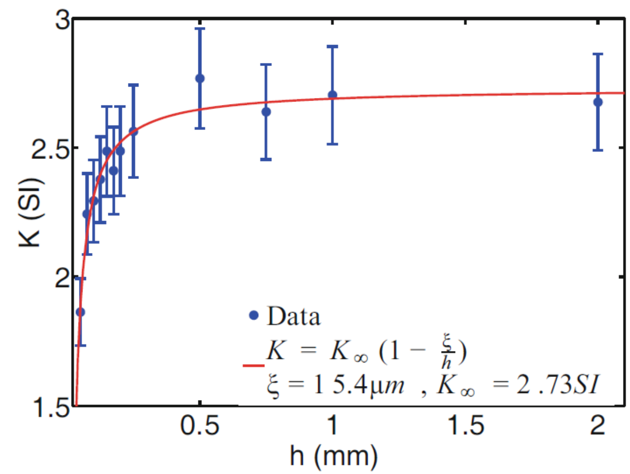

Effects relative to microstructure size (cooperativity length ξ)

Conclusion: measurement repeatability

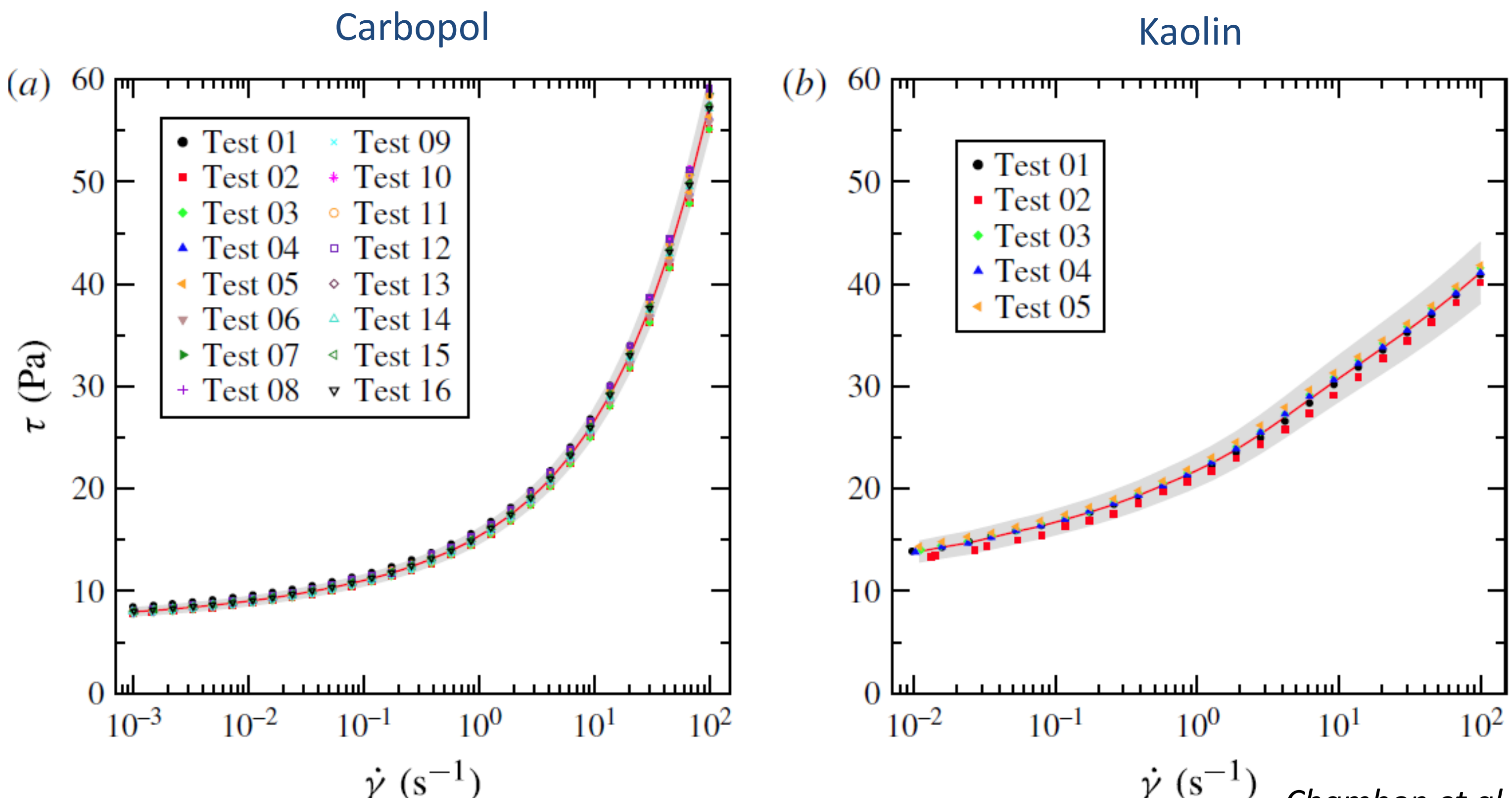

Chambon et al., JFM, 2014

- ➢ Rheometry of viscoplastic fluids is an art!
- ➢ Typical uncertainty levels on HB parameters (for a given protocol!):
  - τ_c and K: $\pm 5 \ - 10\%$
  - n: $\pm 1\%$

Complex rheological trends of yield-stress materials

Thixotropy: dependence on flow/deformation history

thixotropic yield-stress fluids

Up and down ramps

"simple" yield-stress fluid

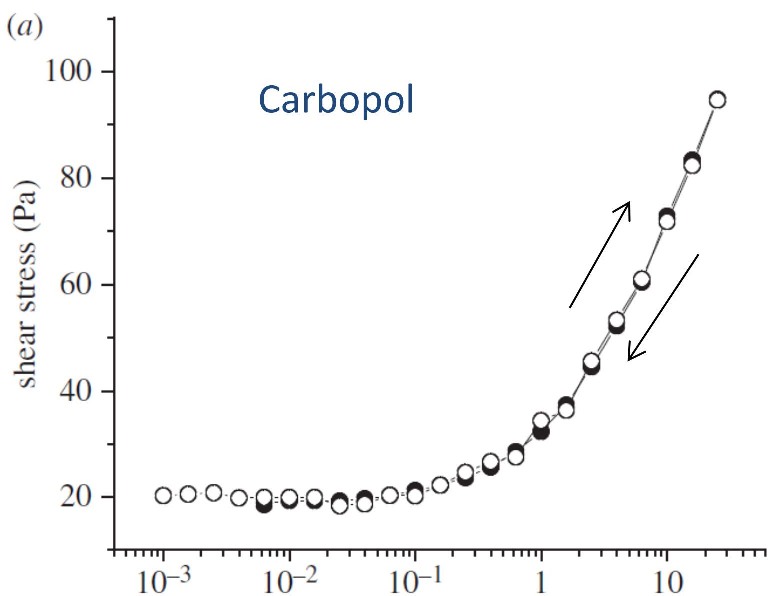

Moller et al., Phil. Trans. Roy. Soc. A, 2009

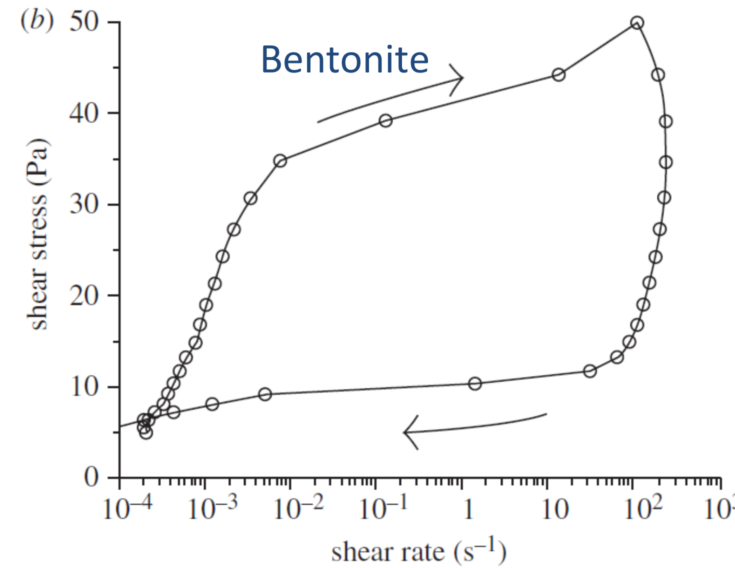

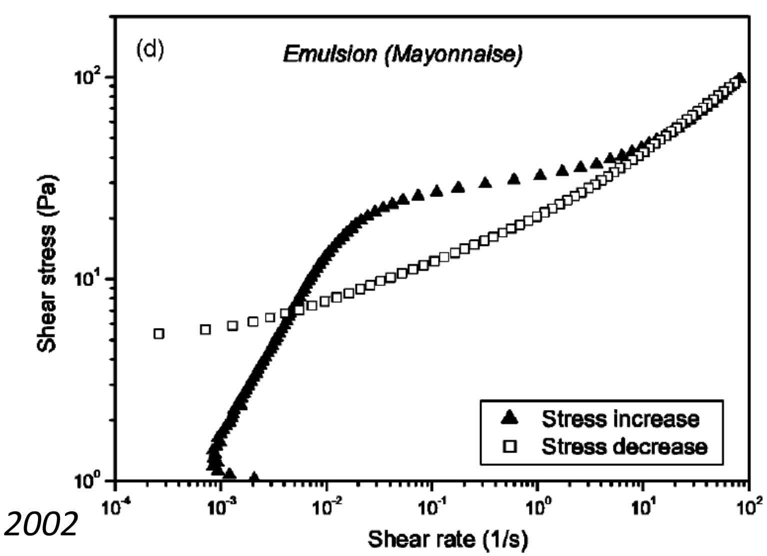

Da Cruz et al., PRE, 2002

Complex rheological trends of yield-stress materials

<u>Thixotropy</u>: ageing

Bentonite suspension:
dam break with increasing rest times

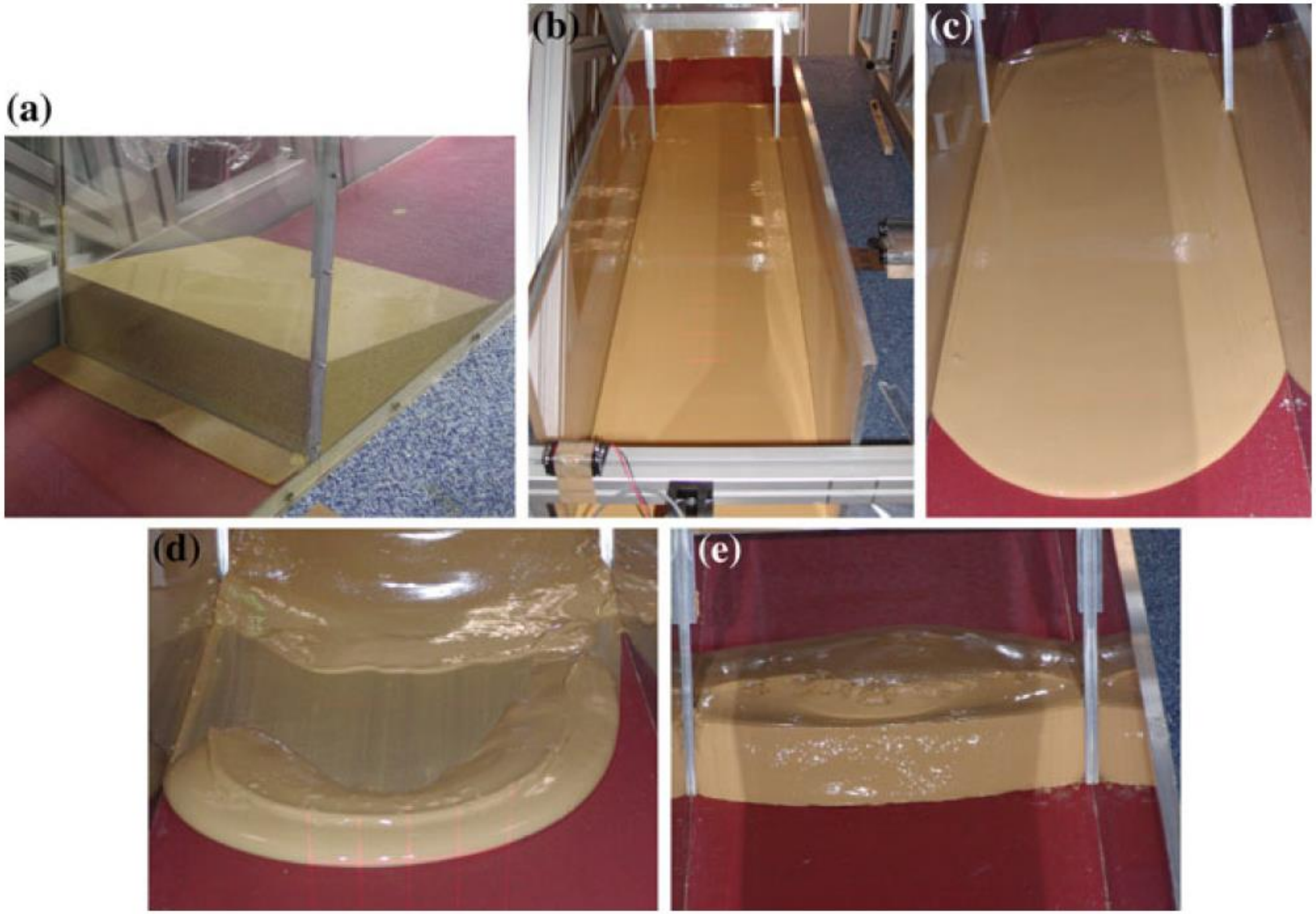

Coussot et al., Phys. Fluids, 2005

Viscosity bifurcation

Creep tests:

landslide clay

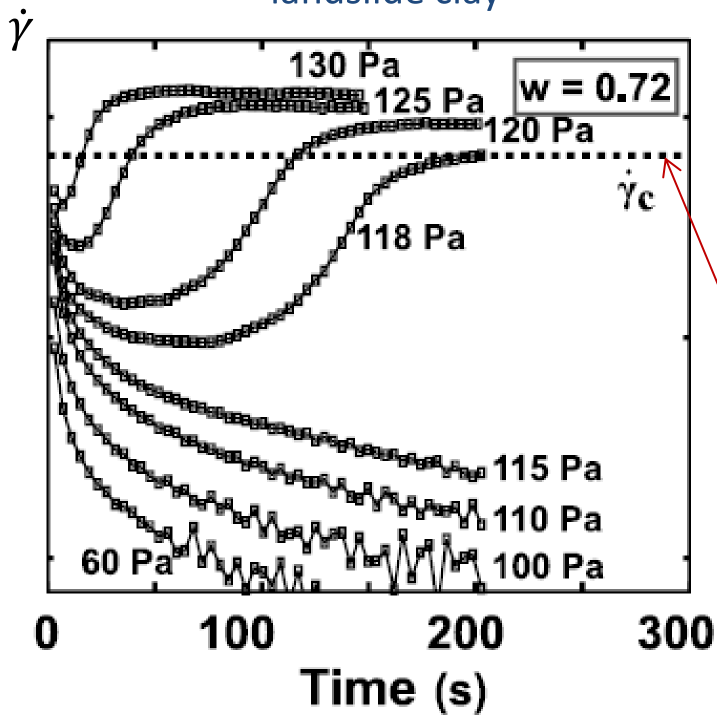

Mainsant et al., Geophys. Res. Lett., 2012

drilling mud

$$\eta = \frac{\tau}{\dot{\gamma}}$$

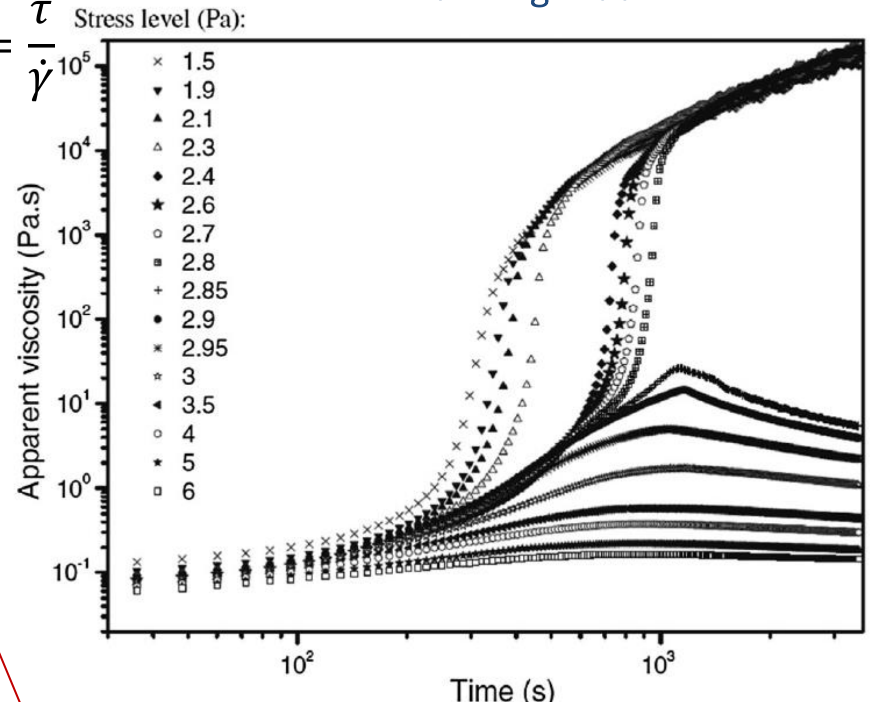

Ragouilliaux et al., Rheol. Act., 2006

existence of a critical shear rate below which no steady flows are possible

Consequences on flow behavior

Shear localization:

Couette cell:

cement paste

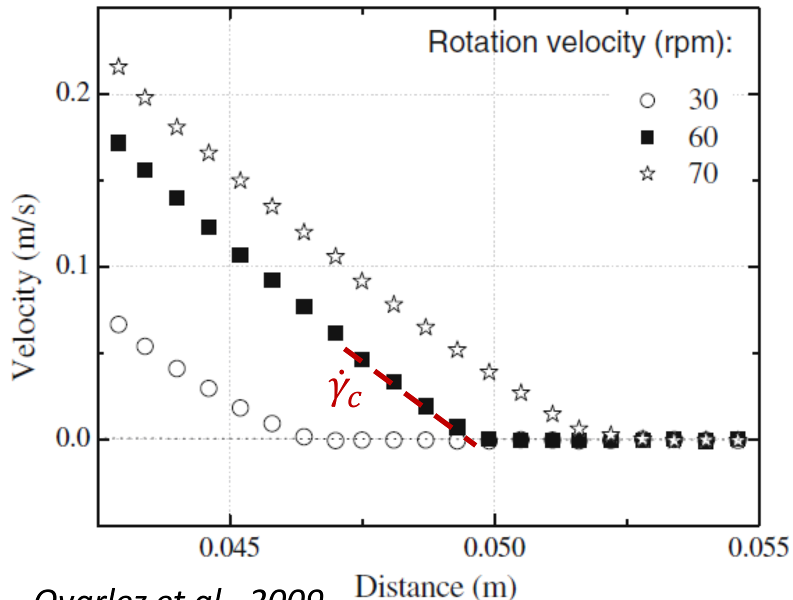

Ovarlez et al., 2009

gel

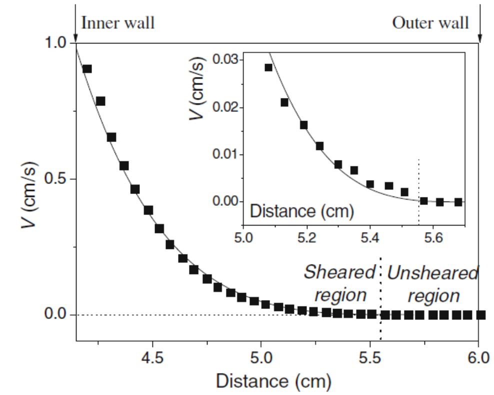

Cone and plate:

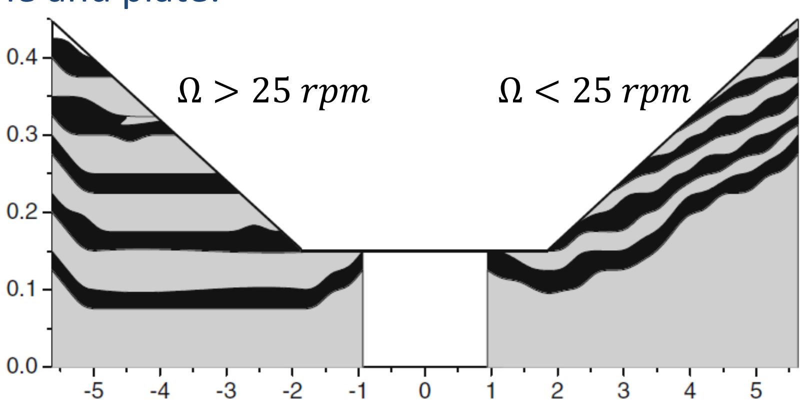

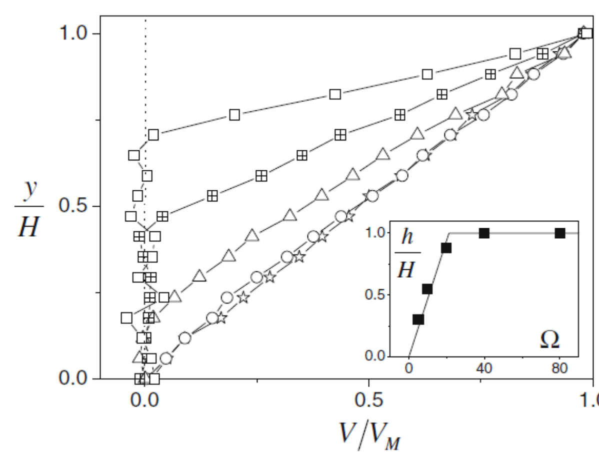

Ovarlez et al., Rheol. Act., 2009

Consequences on flow behavior

"Catastrophic" fluidization:

(a)

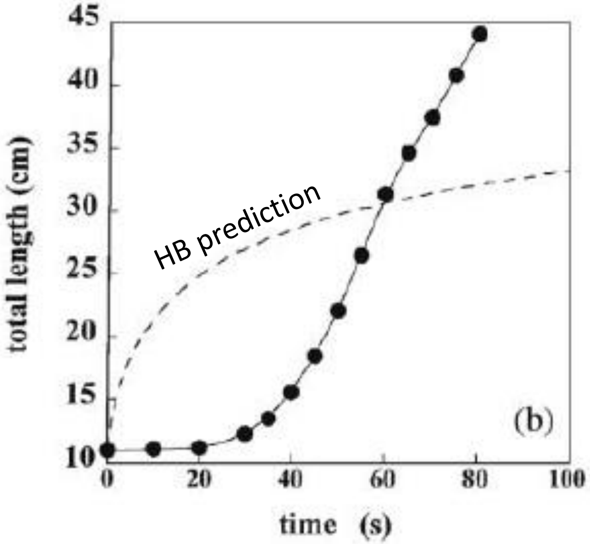

Coussot et al., Phys. Rev. Lett., 2002

A rather generic behavior

Creep tests on clay materials sampled in different landslides

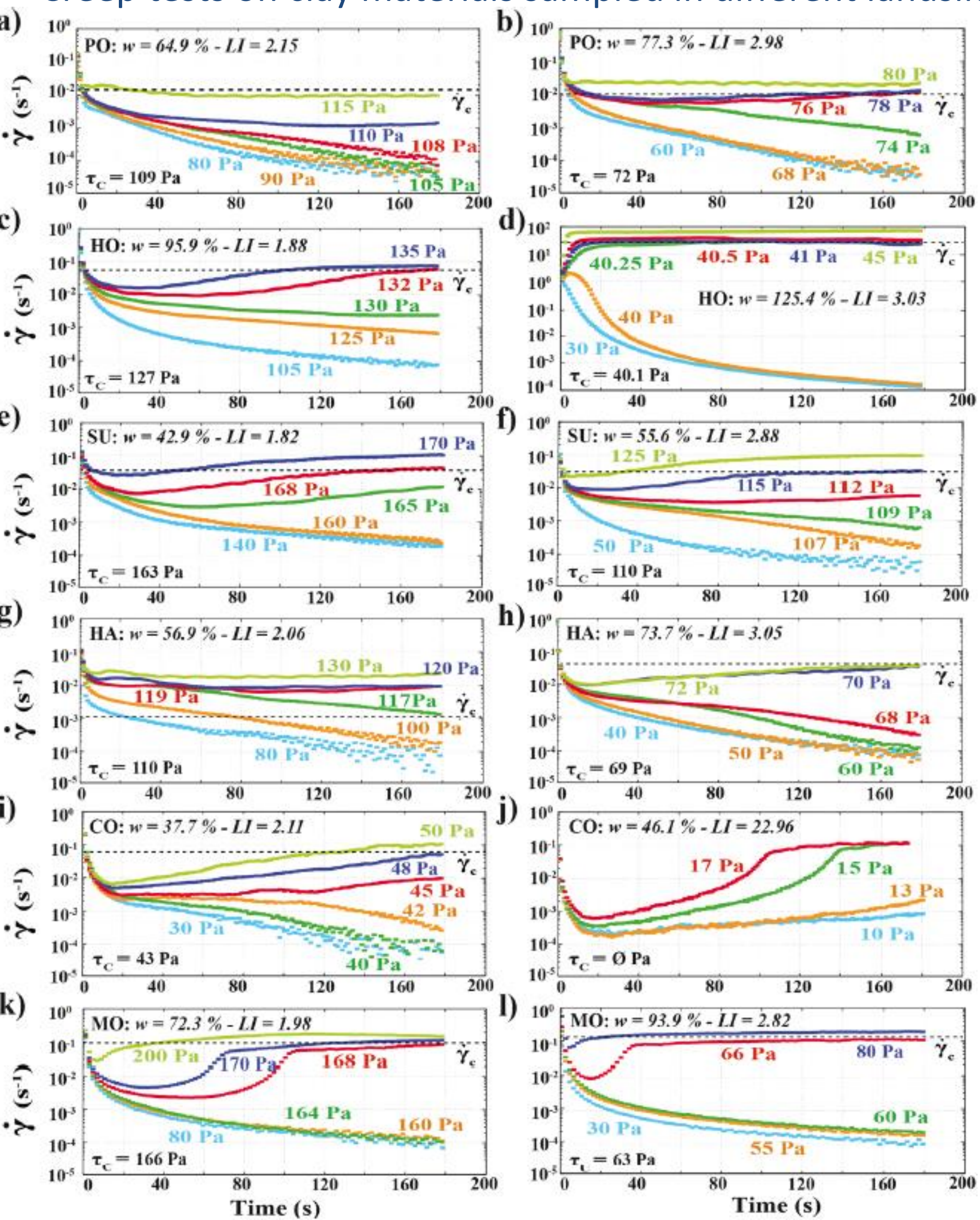

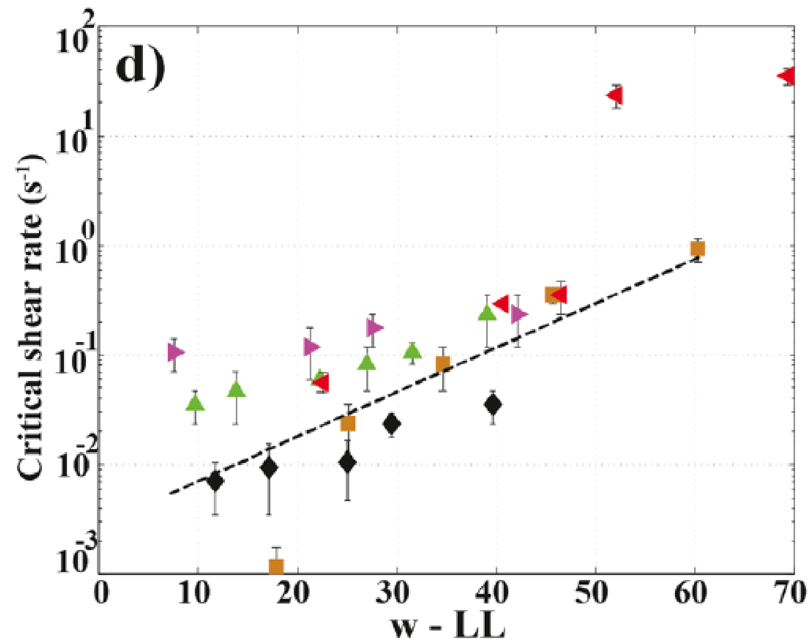

Carrière et al., Landslides, 2018

thixotropy observed as soon as Brownian effects and/or attractive interactions between constituents exist

A simple toy model

competition between ageing and shear rejuvenation

$$\begin{cases} \dfrac{d\lambda}{dt} = \dfrac{1}{T} - \alpha\lambda\,\dot{\gamma} \\ \eta = \eta_0(1+\lambda^n) \end{cases}$$

$$\dot{\gamma}_c = \frac{(n-1)^{1/n}}{\alpha T}$$

$$\tau_c = \frac{\eta_0}{\alpha T}{\lambda_0}^{n-1}$$

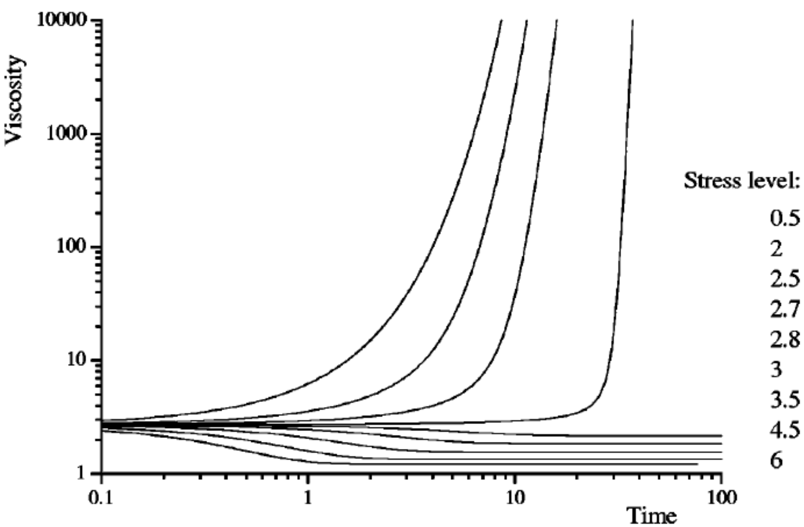

Coussot et al., J. Rheol., 2002

Different rest times

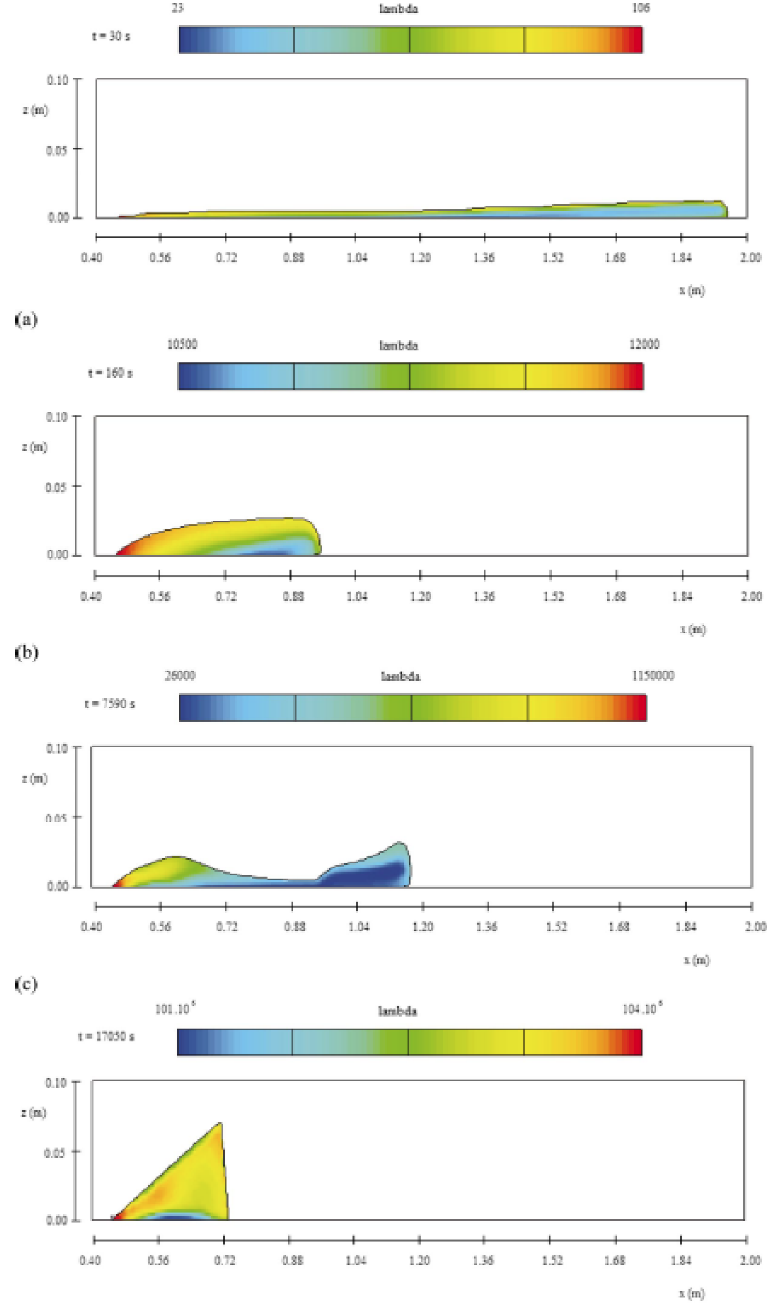

Coussot et al., Phys. Fluids, 2005

Transition from simple to thixotropic yield-stress behaviour

Carbopol samples

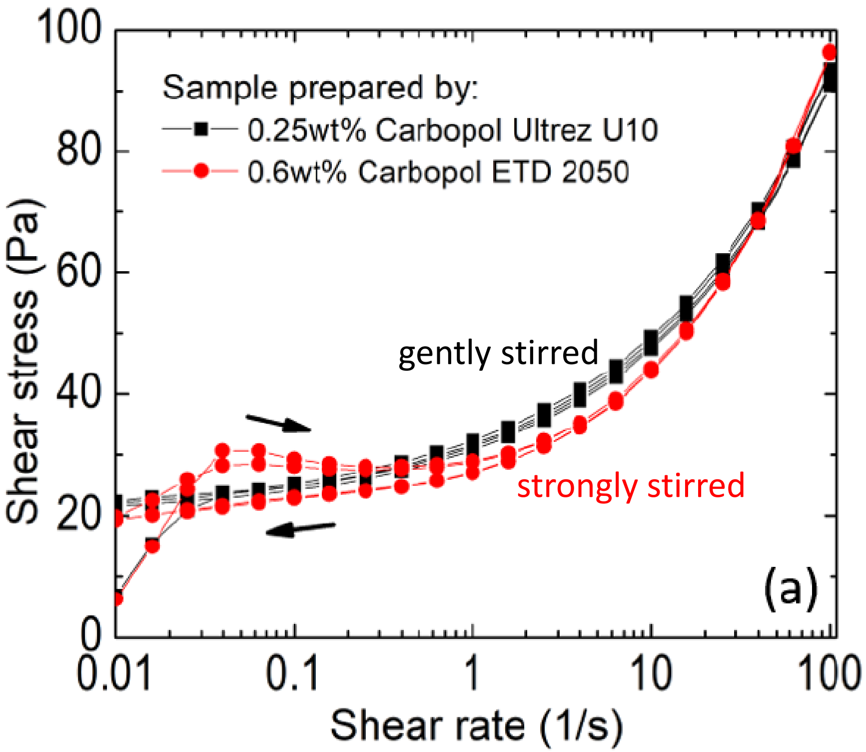

M. Dinkgreve, PhD, 2018

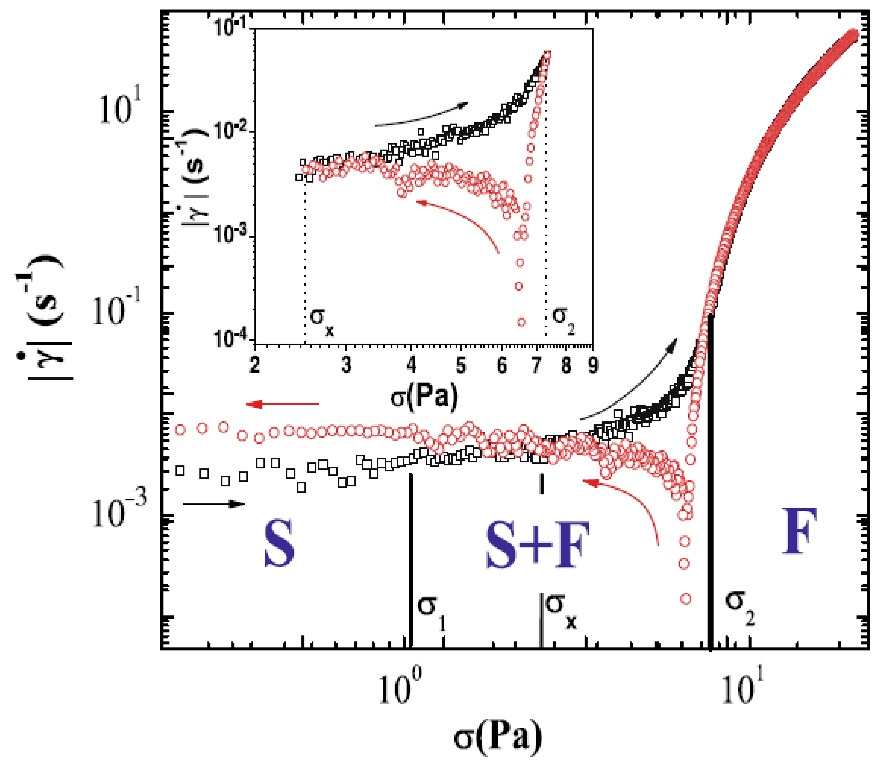

Putz & Burghelea, Rheol. Acto, 2009

Carbopol microgel microstructure

gently stirred

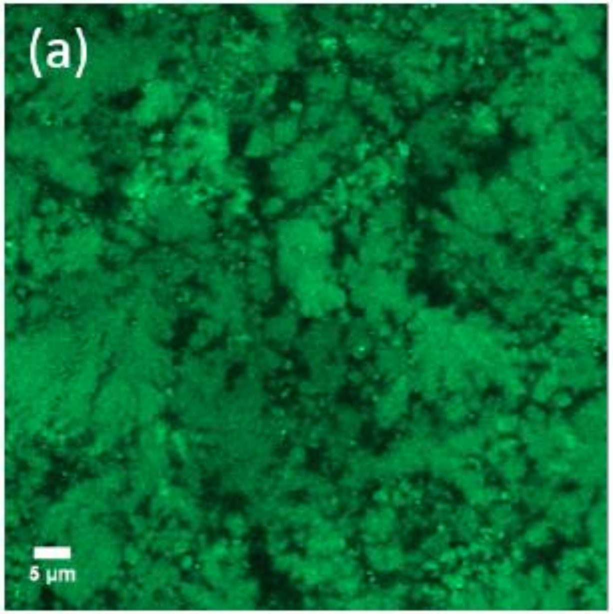

Large cross-linked sponges

strongly stirred

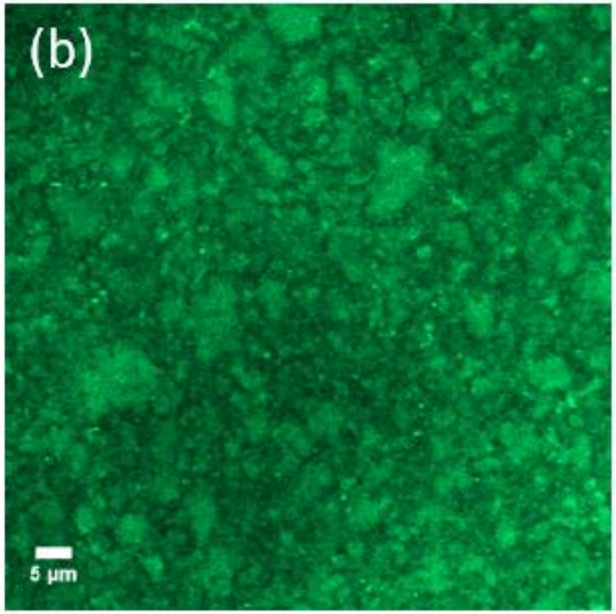

Smaller structures: Brownian effects

M. Dinkgreve, PhD, 2018

➢ Strong influence of preparation protocol!

Complex rheological trends of yield-stress materials

<u>Elasticity</u>

Carbopol samples

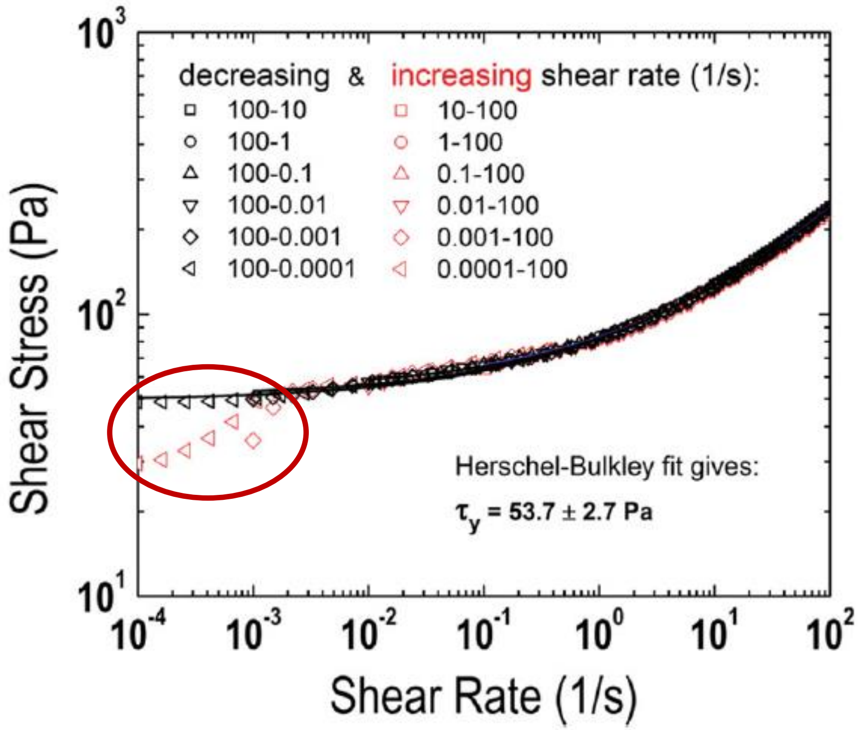

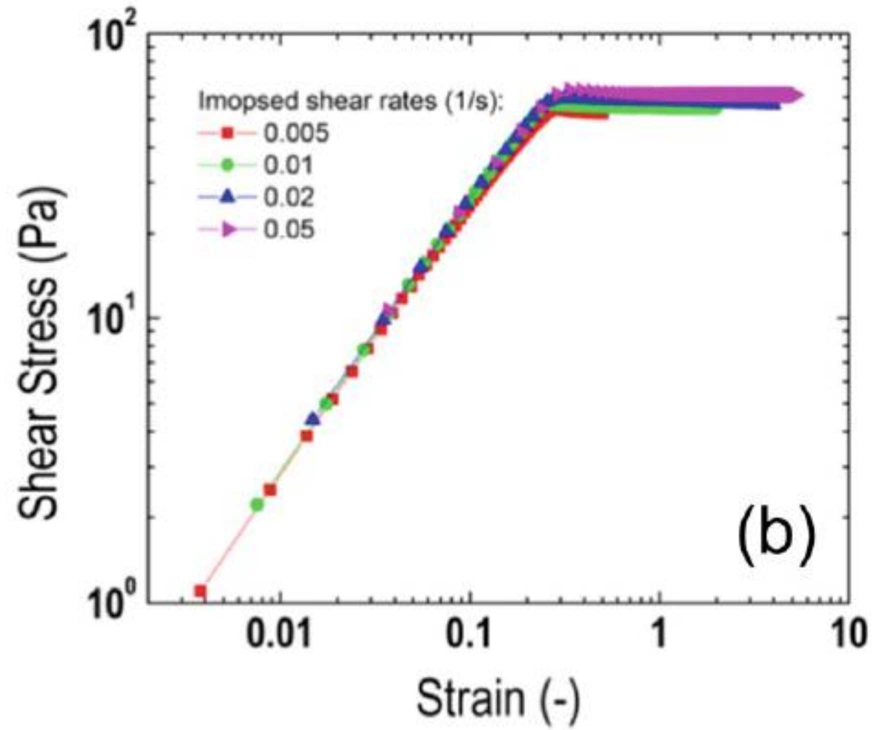

Dinkgreve et al., Rheol. Acto, 2017

Elastic pre-yielding deformation

Elasticity

Stress relaxation experiments (Carbopol)

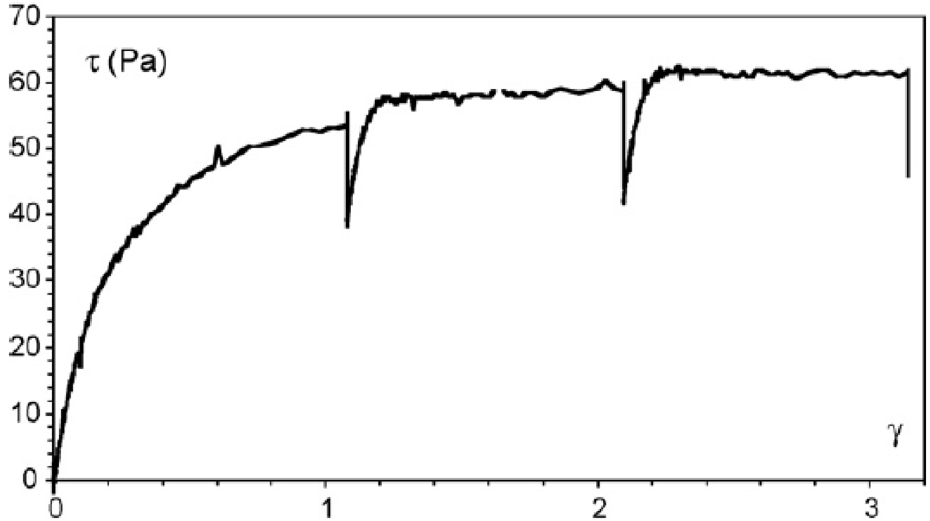

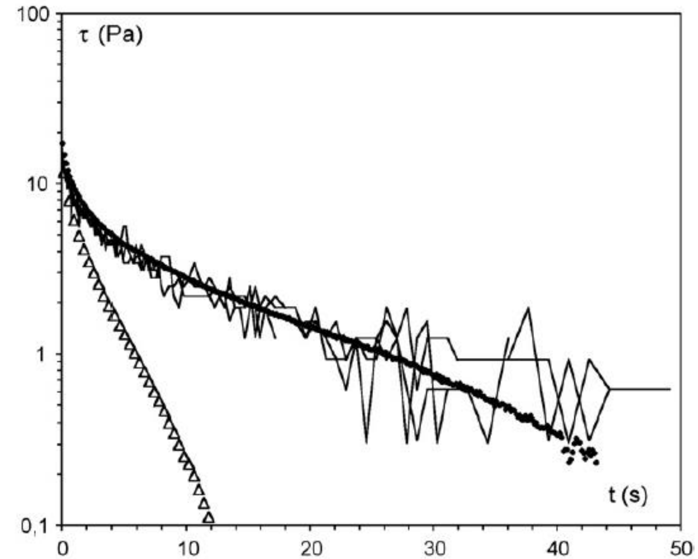

Piau, JNNFM, 2007

Significant elastic strains even above the yield stress

Influence on the flow: unsteady flows

Impact of yield stress fluids on a hydrophobic surface

Kaolin clay

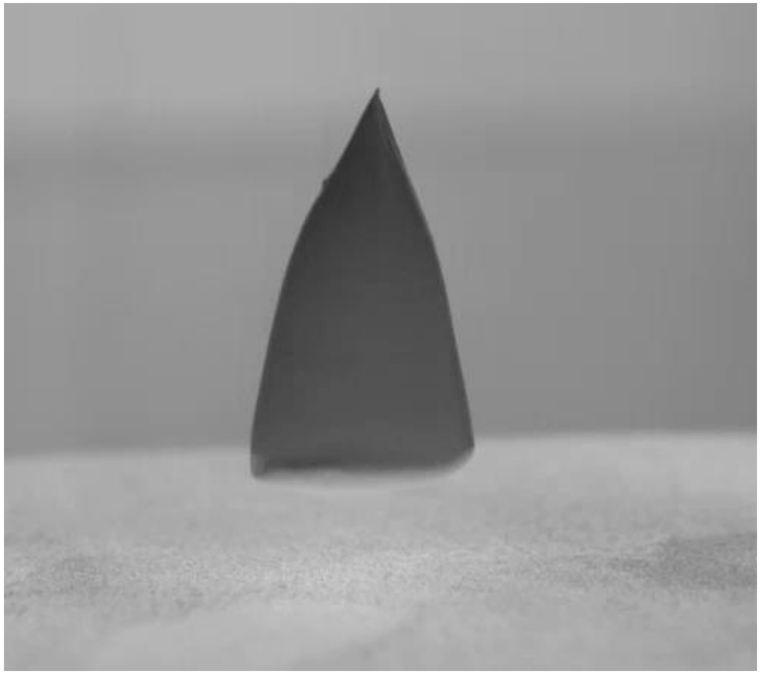

Carbopol

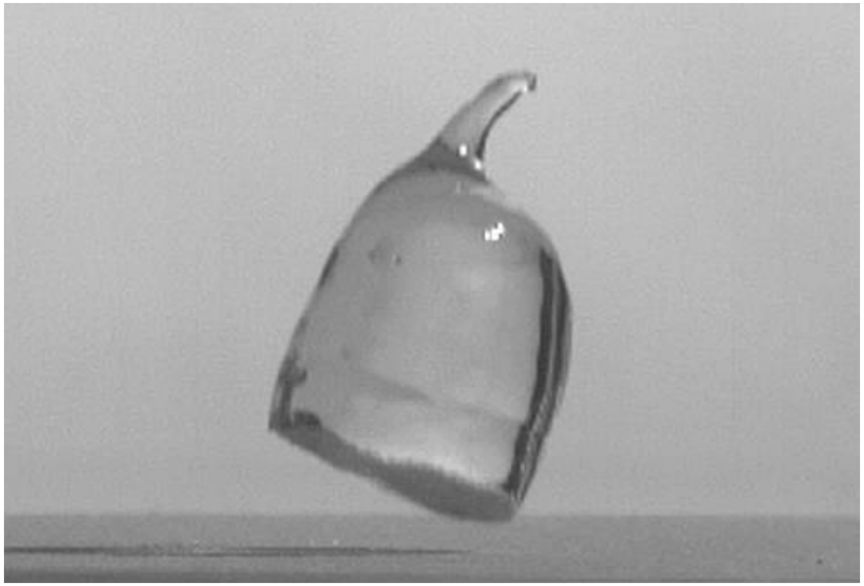

Luu & Forterre, JFM, 2009

Elasto-viscoplastic models

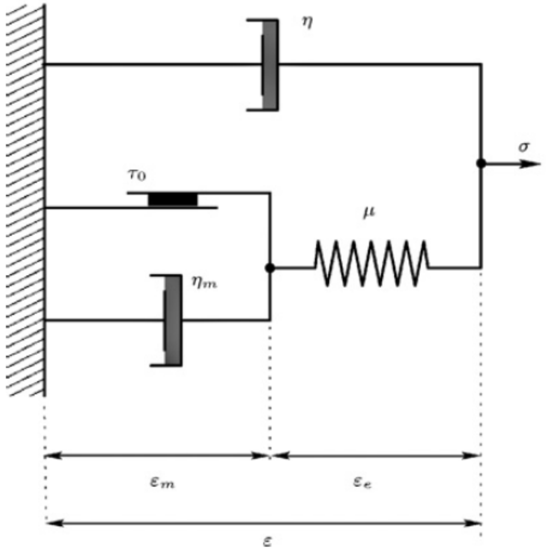

$$\lambda \dot{\tau} + \max\left(0, \frac{|\tau_d| - \tau_0}{|\tau_d|}\right)\tau - 2\eta_m D(\mathbf{v}) = 0,$$

Saramito, JNNFM, 2007

Large amplitude oscillations: model

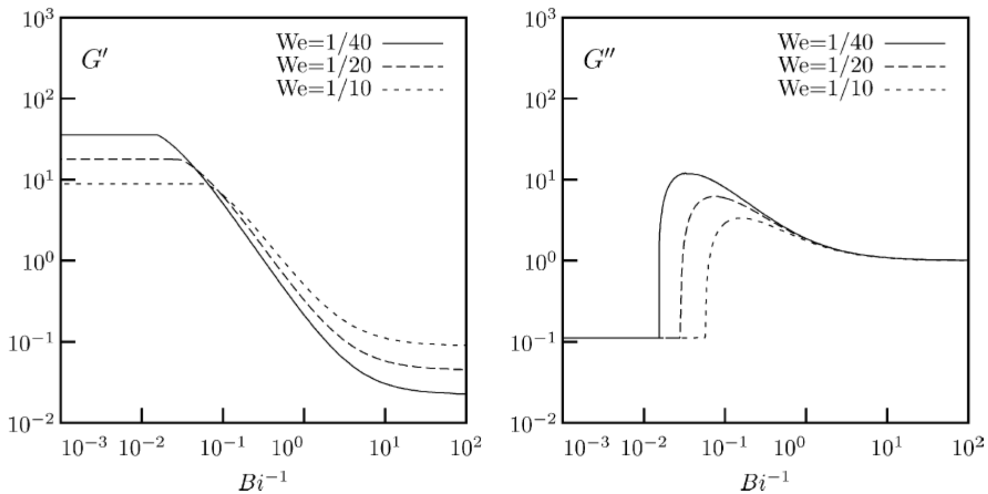

Experiments (Carbopol)

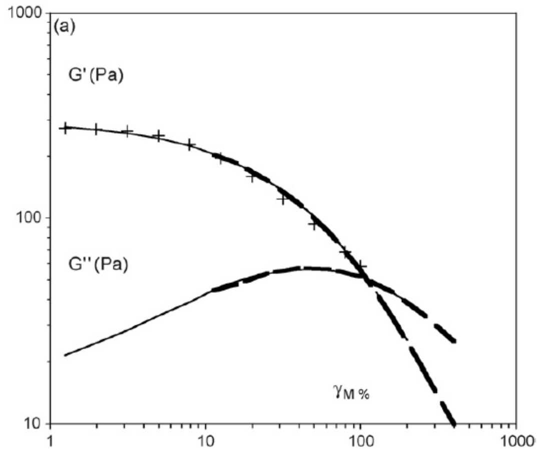

Drop rebound

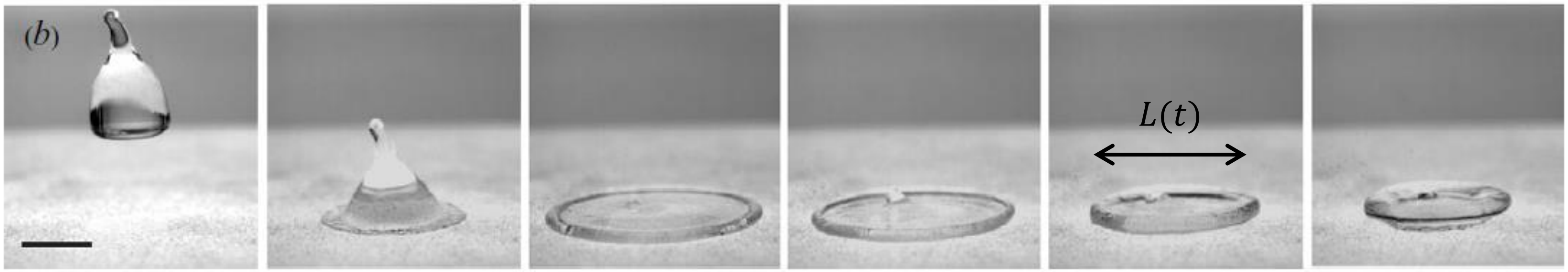

Luu & Forterre, JFM, 2009

Shows importance of elastic (reversible) deformations above yielding

model

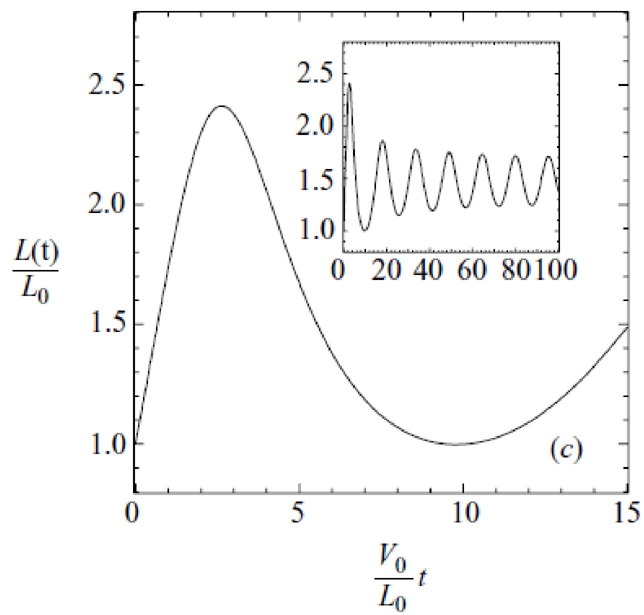

experiments

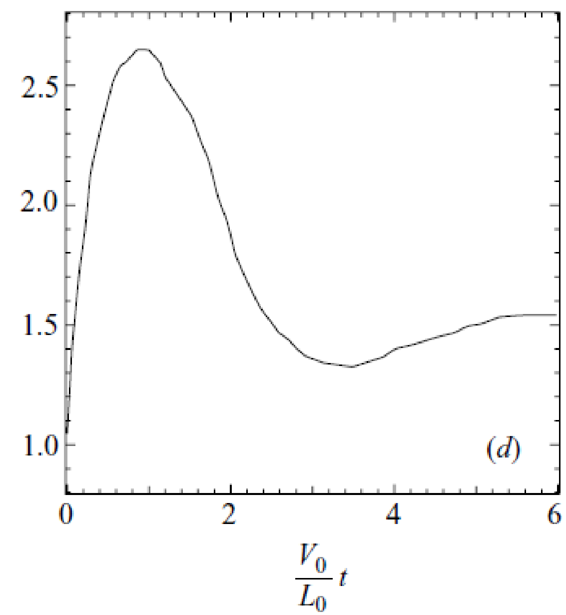

Influence on the flow: steady flows

Flow around a sphere (low Re)

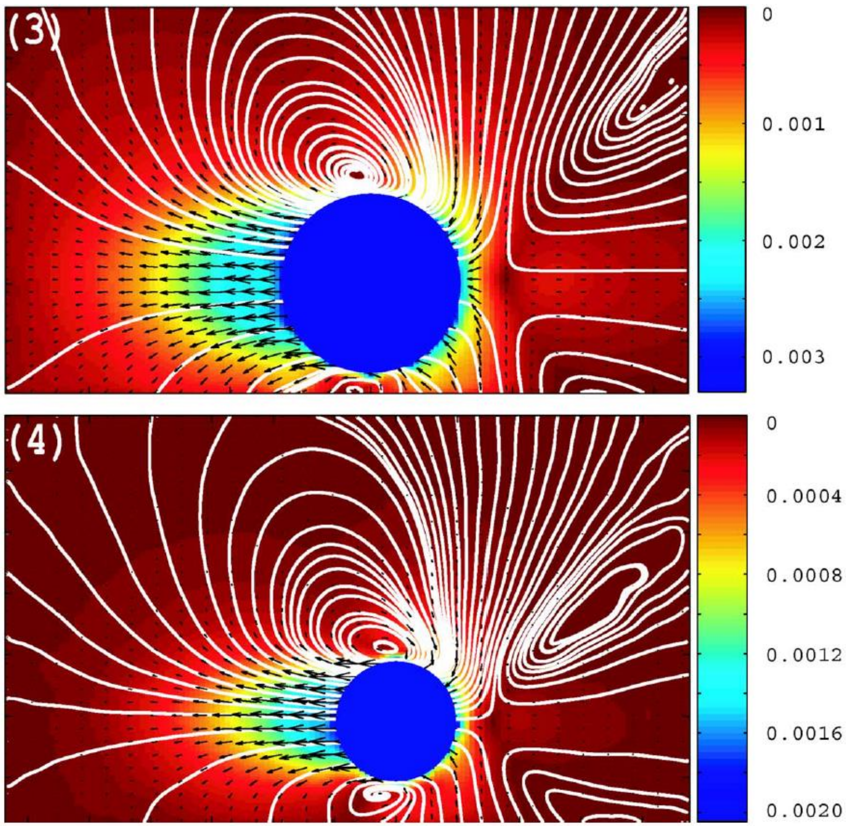

Putz et al., Phys. Fluids, 2008

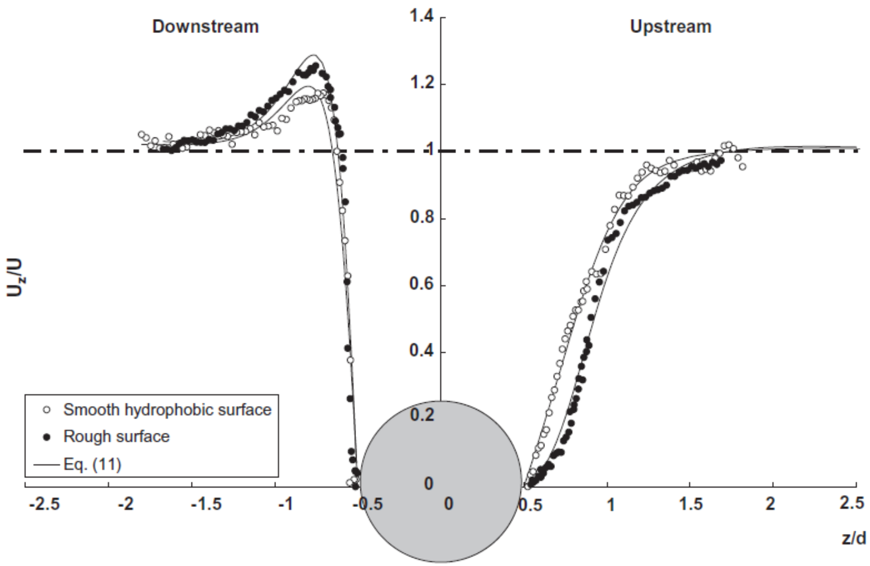

Ahonguio et al., JNNFM, 2014

strong fore-aft asymmetry of the velocity field

Influence on the flow: steady flows

Expansion-contraction geometry

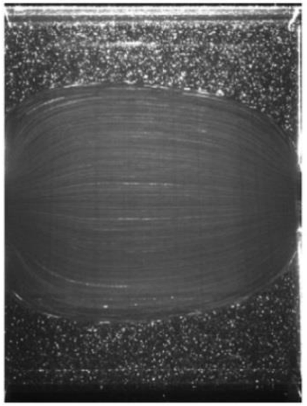

de Souza Mendes et al., JNNFM, 2007

Numerical simulations for increasing Deborah number

Nassar et al., JNNFM, 2011

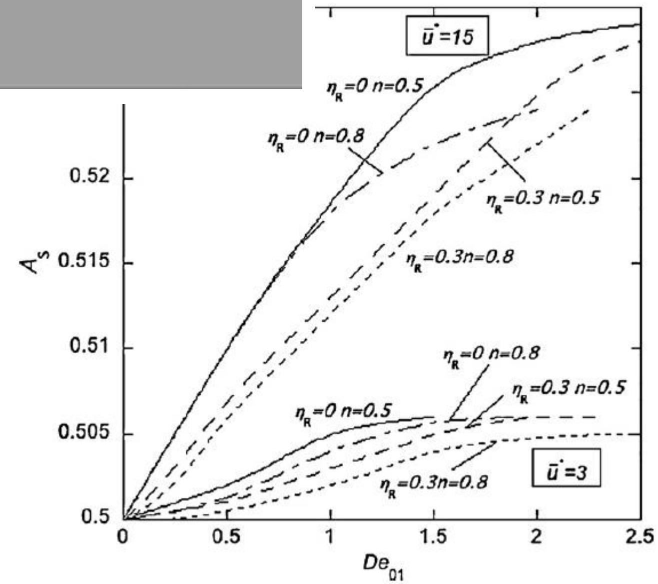

Asymmetry of the yield surface is explained by elasticity

Normal stresses

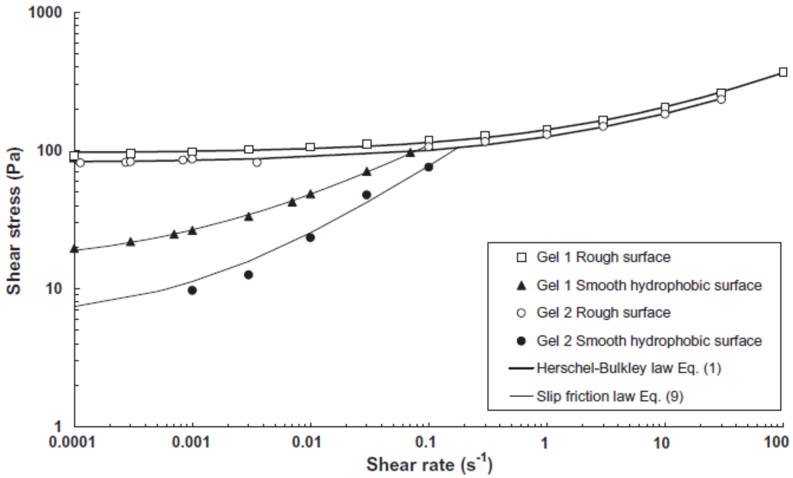

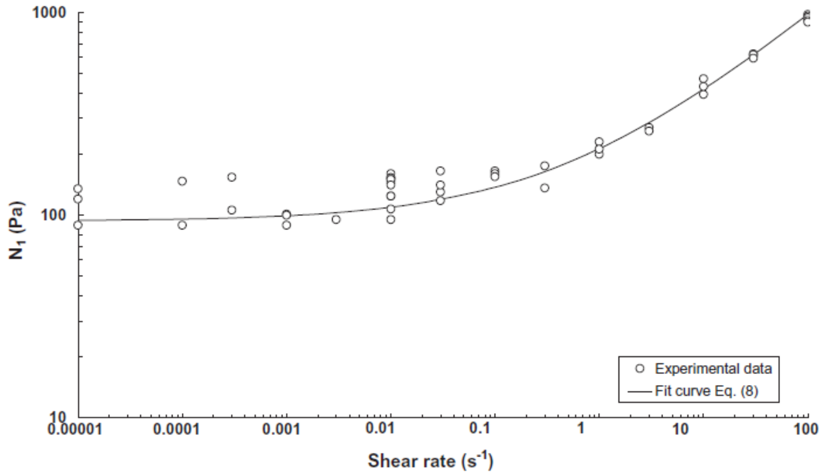

Ahonguio et al., JNNFM, 2014

Very few data on normal stresses in yield-stress materials

Complex rheological trends of yield-stress materials

More: towards thixotropic elasto-viscoplastic models?

Rheol Acta (2013) 52:673–694
DOI 10.1007/s00397-013-0699-1

ORIGINAL CONTRIBUTION

A unified approach to model elasto-viscoplastic thixotropic yield-stress materials and apparent yield-stress fluids

Paulo R. de Souza Mendes · Roney L. Thompson

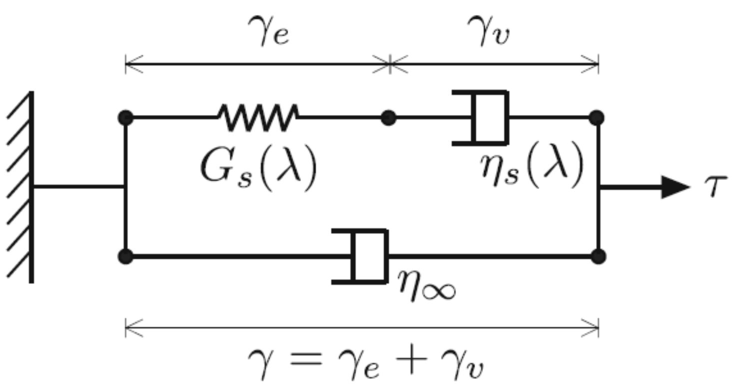

Complex rheological trends of yield-stress materials

<u>3D rheology</u>

Herschel-Bulkley law in simple shear:

$$\begin{cases} \dot{\gamma} = 0 & \text{si } \tau < \tau_c \\ \tau = \tau_c + K\dot{\gamma}^n & \text{si } \tau \geq \tau_c \end{cases}$$

3D extrapolation :

$$\begin{cases} \dot{\gamma}_{ij} = 0 & \text{if } |\tau| < \tau_c \\ \tau_{ij} = \tau_c \dfrac{\dot{\gamma}_{ij}}{|\dot{\gamma}|} + K{\dot{\gamma}_{ij}}^n & \text{if } |\tau| \geq \tau_c \end{cases}$$

$$|\tau| = \sqrt{\sum \frac{1}{2} {\tau_{ij}}^2} \qquad |\dot{\gamma}| = \sqrt{\sum \frac{1}{2} {\dot{\gamma}_{ij}}^2}$$

von-Mises criterion

Combination of shear and squeeze flow

Carbopol and emulsions

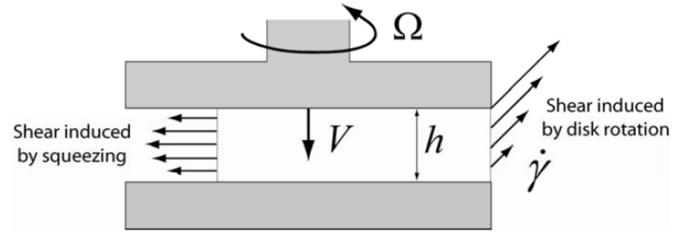

Ovarlez et al., Nature Mat., 2010

Yield criterion

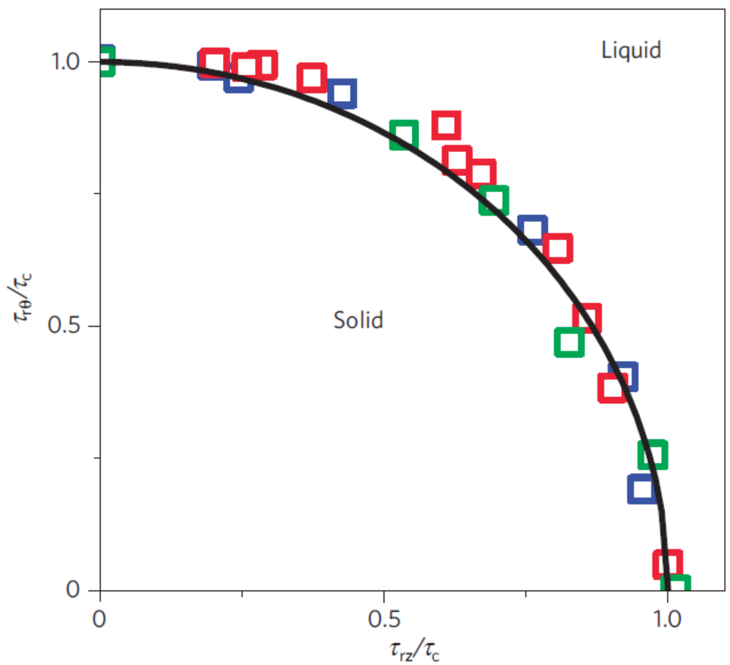

$$\sqrt{\tau_{r\theta}{}^2 + \tau_{rz}{}^2} = \tau_c$$

3D rheology

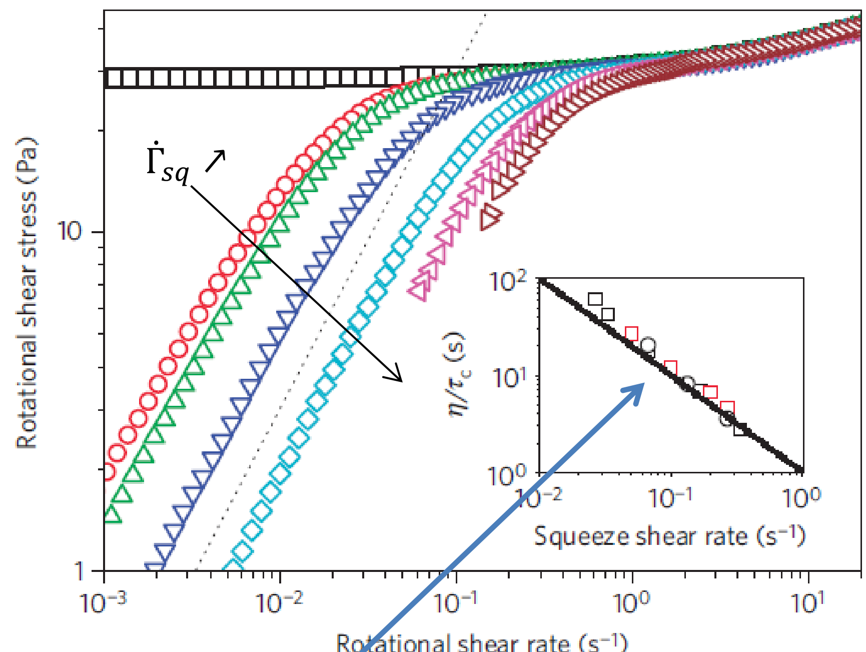

For $\dot{\gamma}_{r\theta} \ll \dot{\Gamma}_{sq}$: $\tau_{r\theta} \propto \eta(\dot{\Gamma}_{sq})\,\dot{\gamma}_{r\theta}$

Elongational behavior

Carbopol

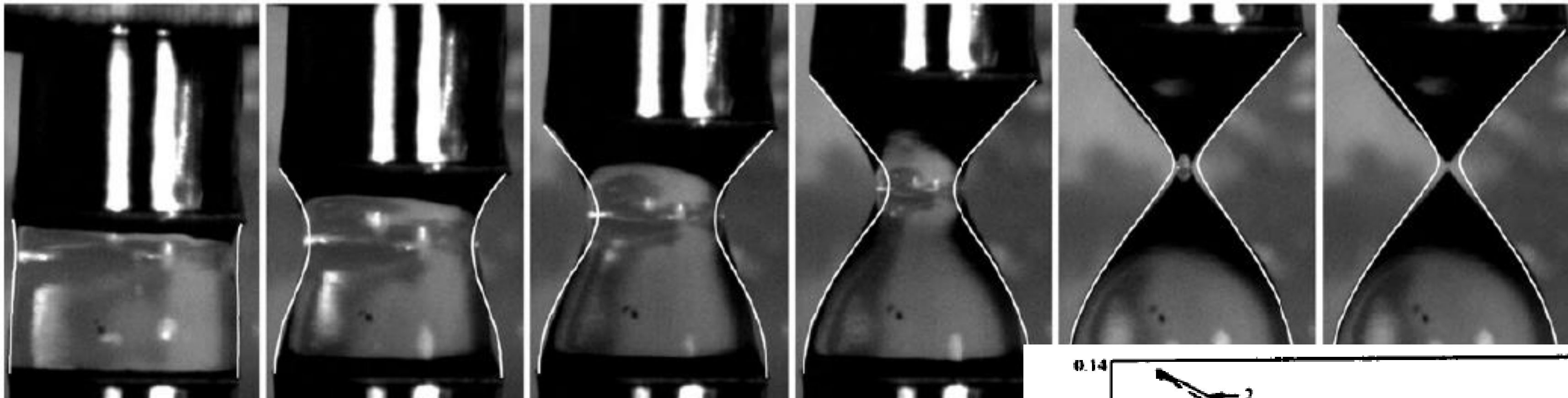

Balmforth et al., JNNFM, 2010

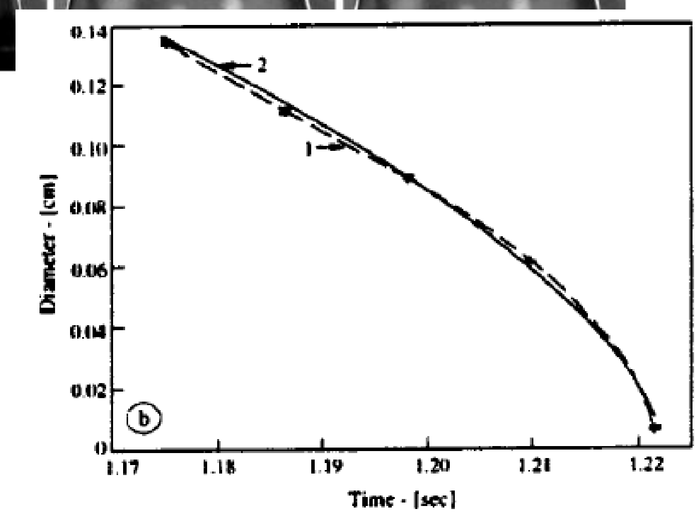

Yarin et al., J. Rheol,, 2004

Kaolin

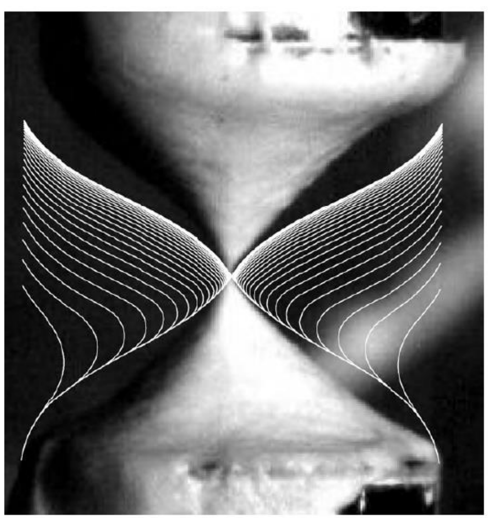

- Good validity of 3D rheology for Carbopol and simple yield-stress fluids
- What for more complex fluids?

Free surface flow in steady uniform regime

<u>Conveyor belt channel</u>

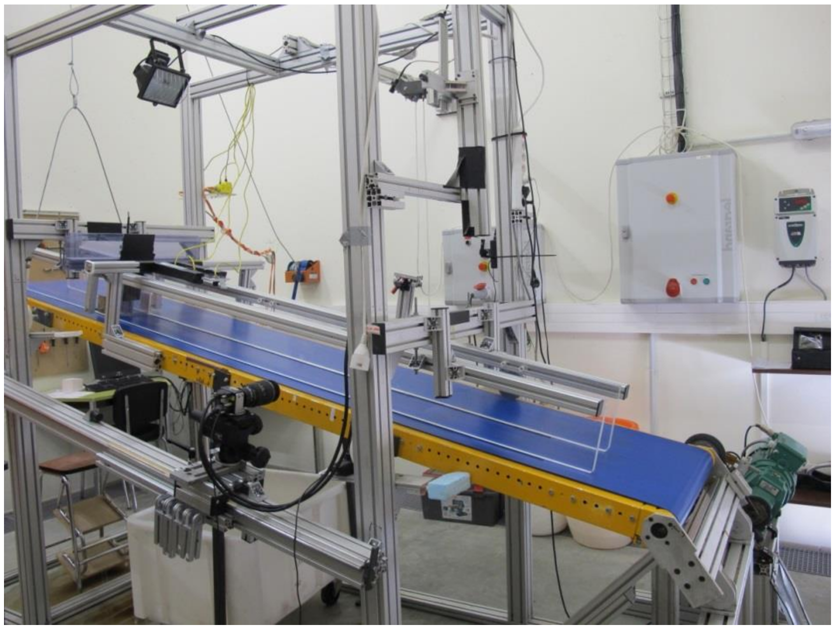

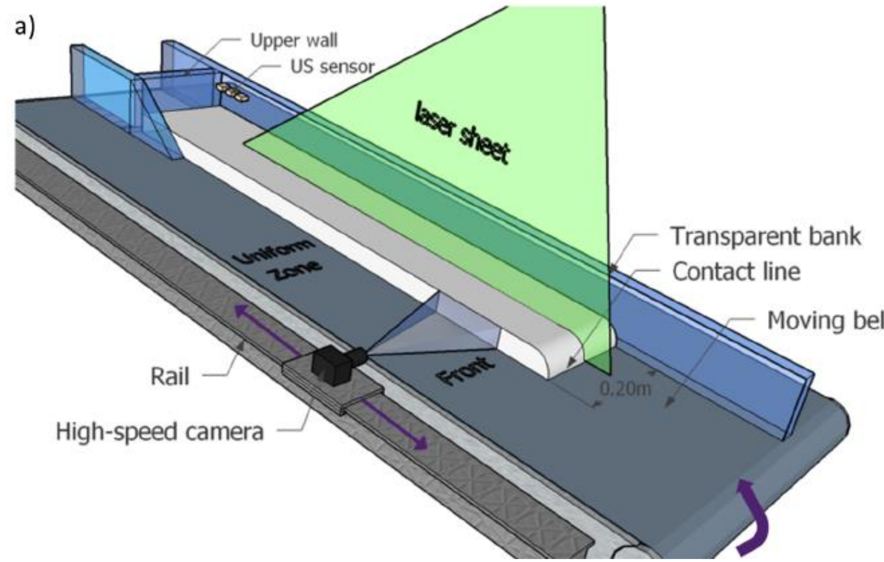

Chambon et al., JFM, 2014

Carbopol

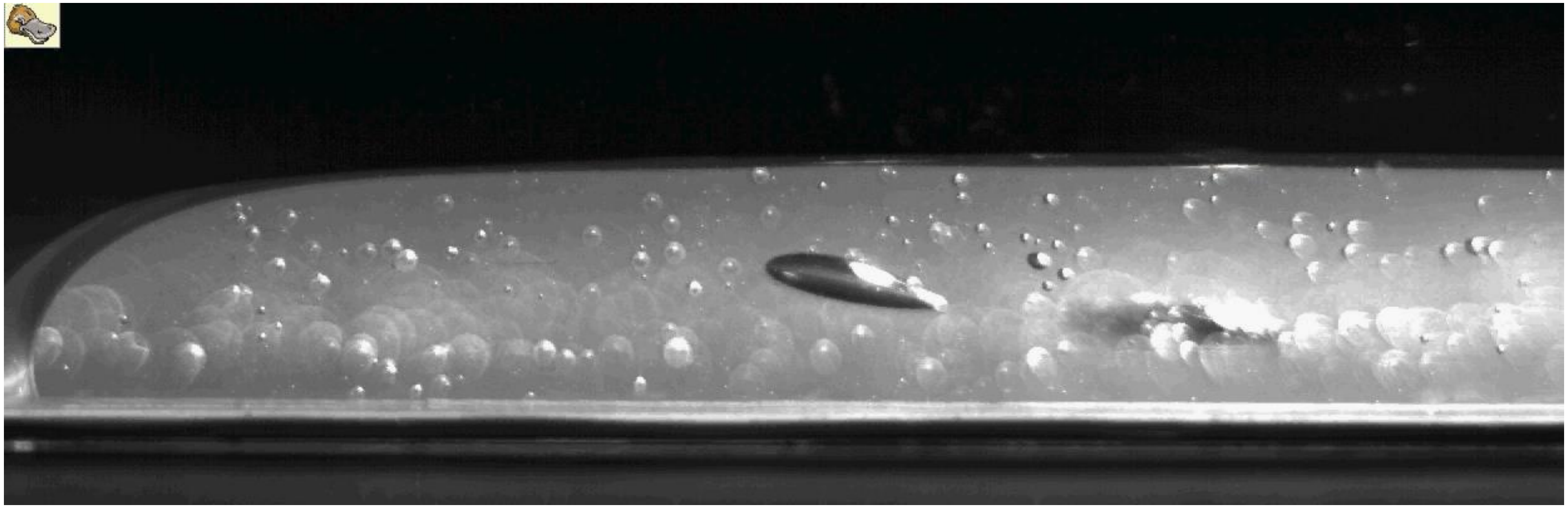

Assessing measurement accuracy

Flow height

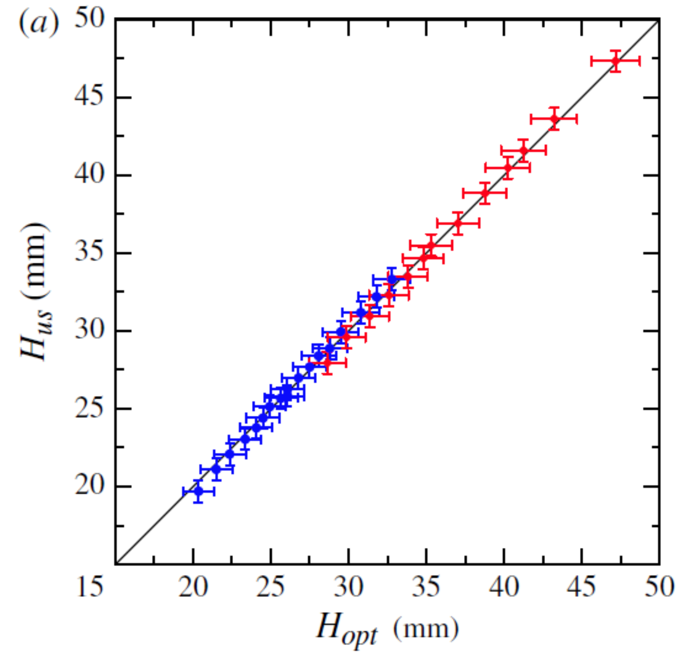

Velocity profiles (linear PIV)

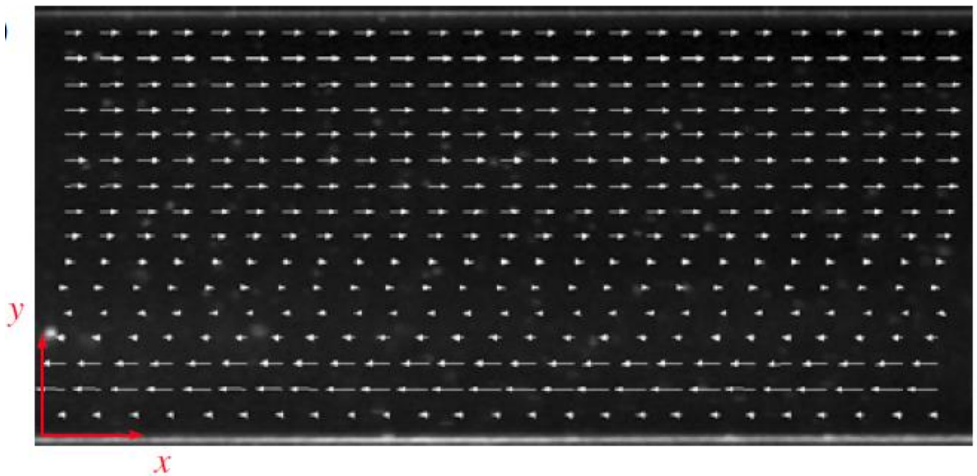

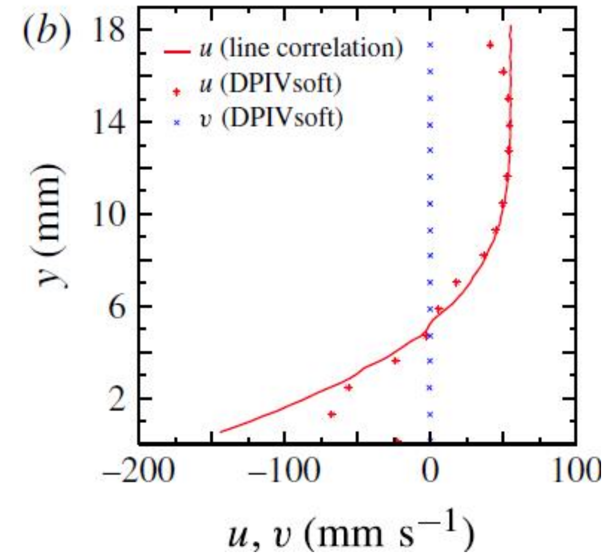

Theoretical predictions in steady uniform regime

$$u(y) = \begin{cases} u_0\left[1-\left(1-\dfrac{y}{h-h_c}\right)^{(n+1)/n}\right]-u_b, & y < h-h_c \\ u_0 - u_b, & y \geq h-h_c \end{cases}$$

$$u_0 = \frac{n}{n+1}\left(\frac{\rho g \sin\theta}{K}\right)^{1/n} \quad (h-h_c)^{(n+1)/n}$$

$$h_c = \frac{\tau_c}{\rho g \sin\theta}$$

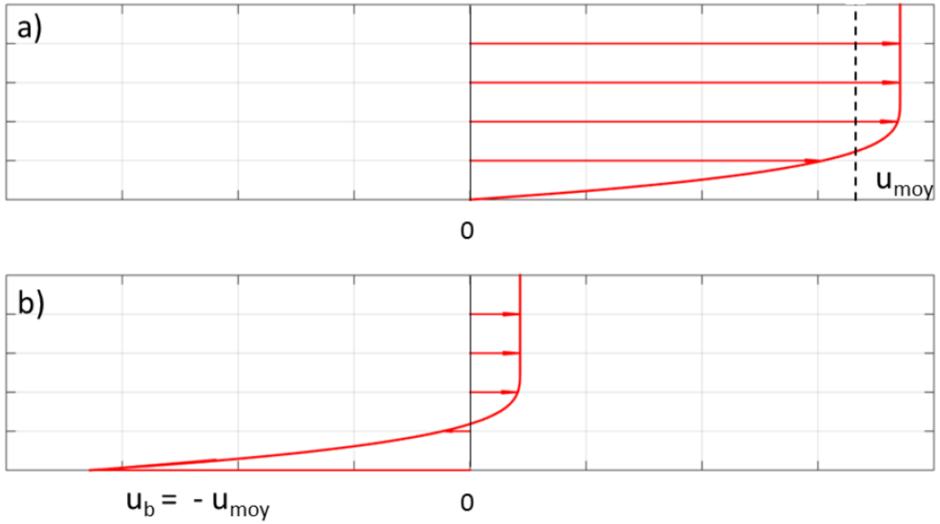

Relation between h and u_b: $u_b = u_0\left(1-\frac{n}{2n+1}\frac{h-h_c}{h}\right)$

Height-velocity relation

Kaolin

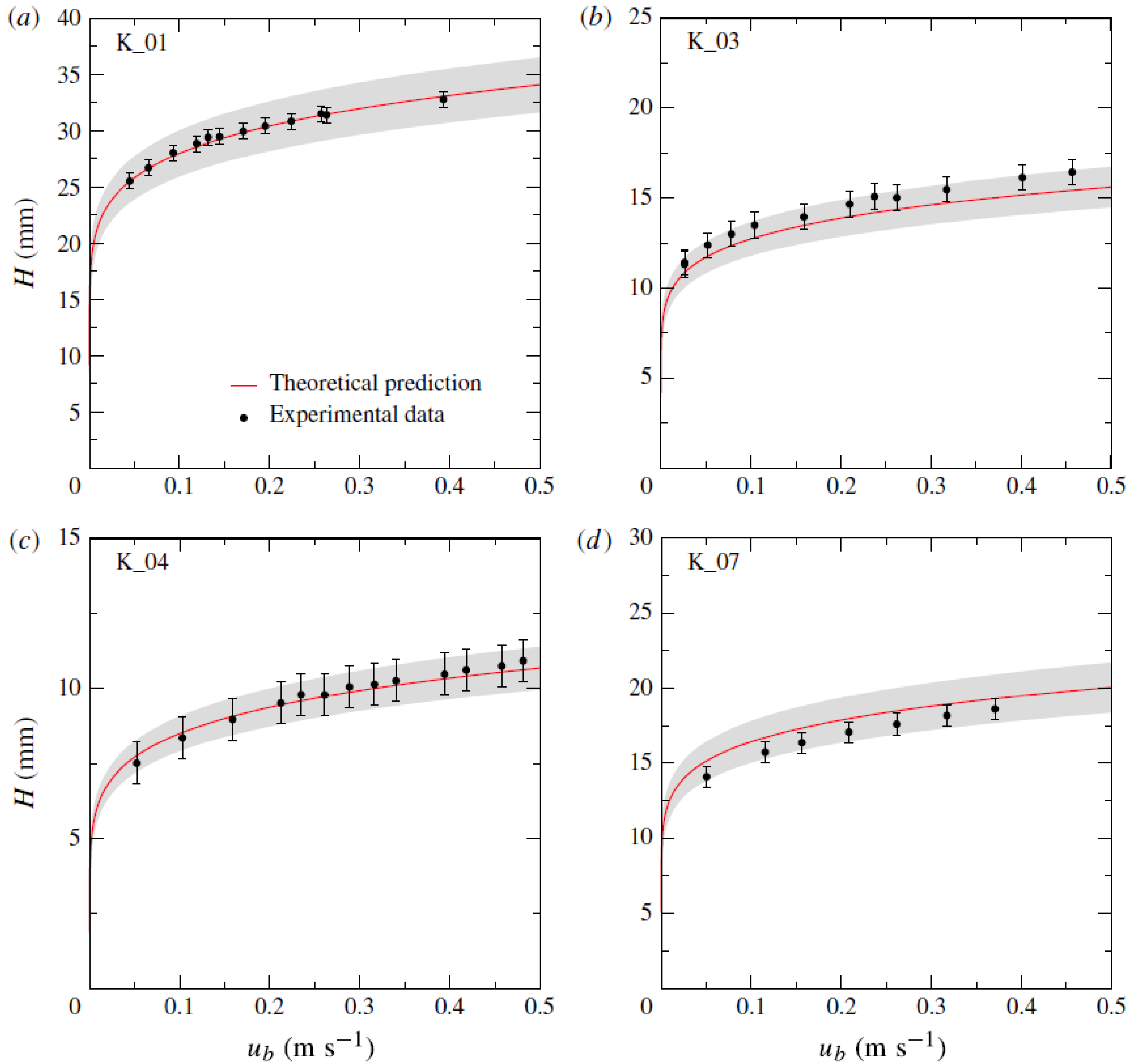

Height-velocity relation

Carbopol

- Systematic discrepancy

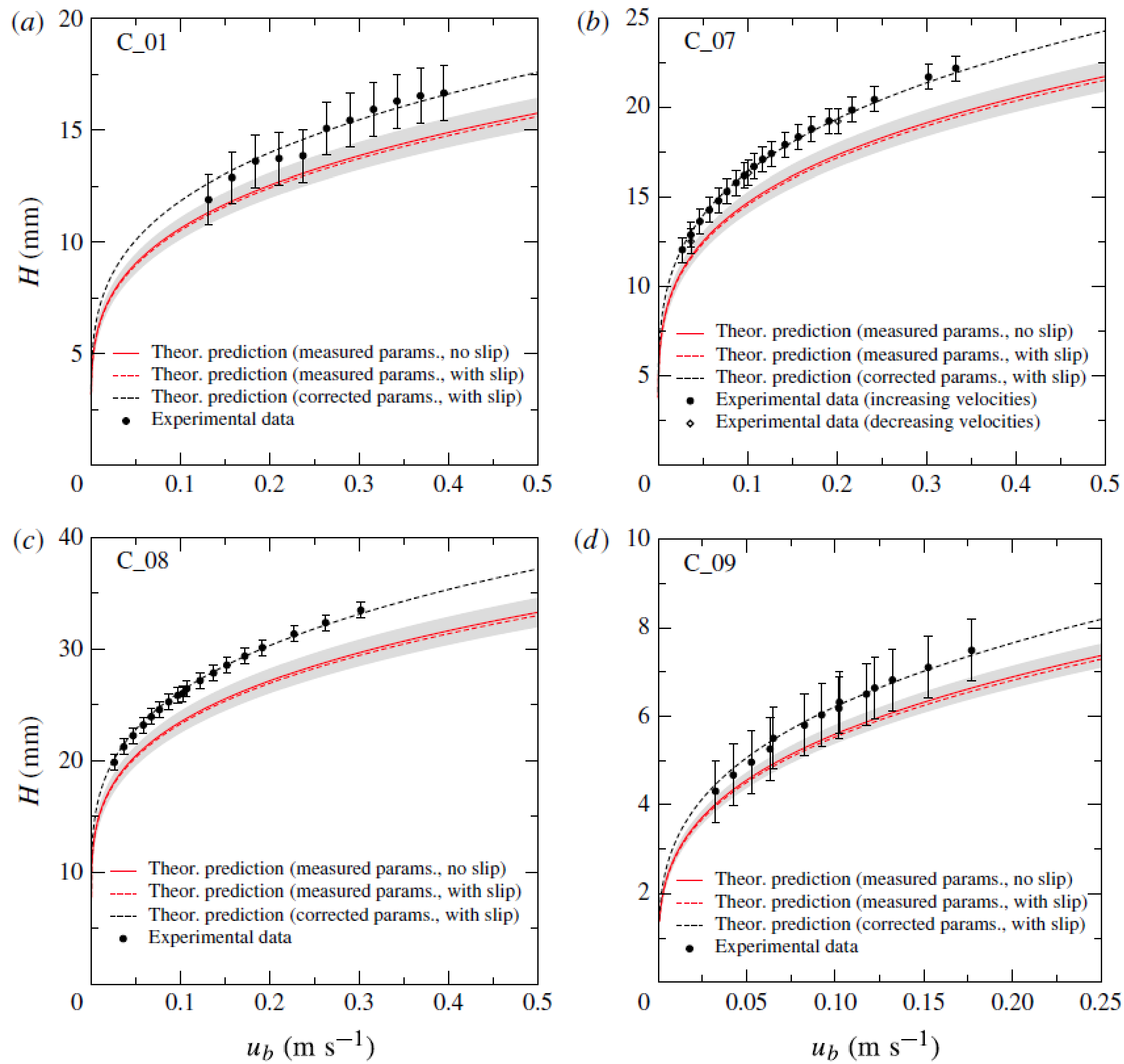

Velocity profiles

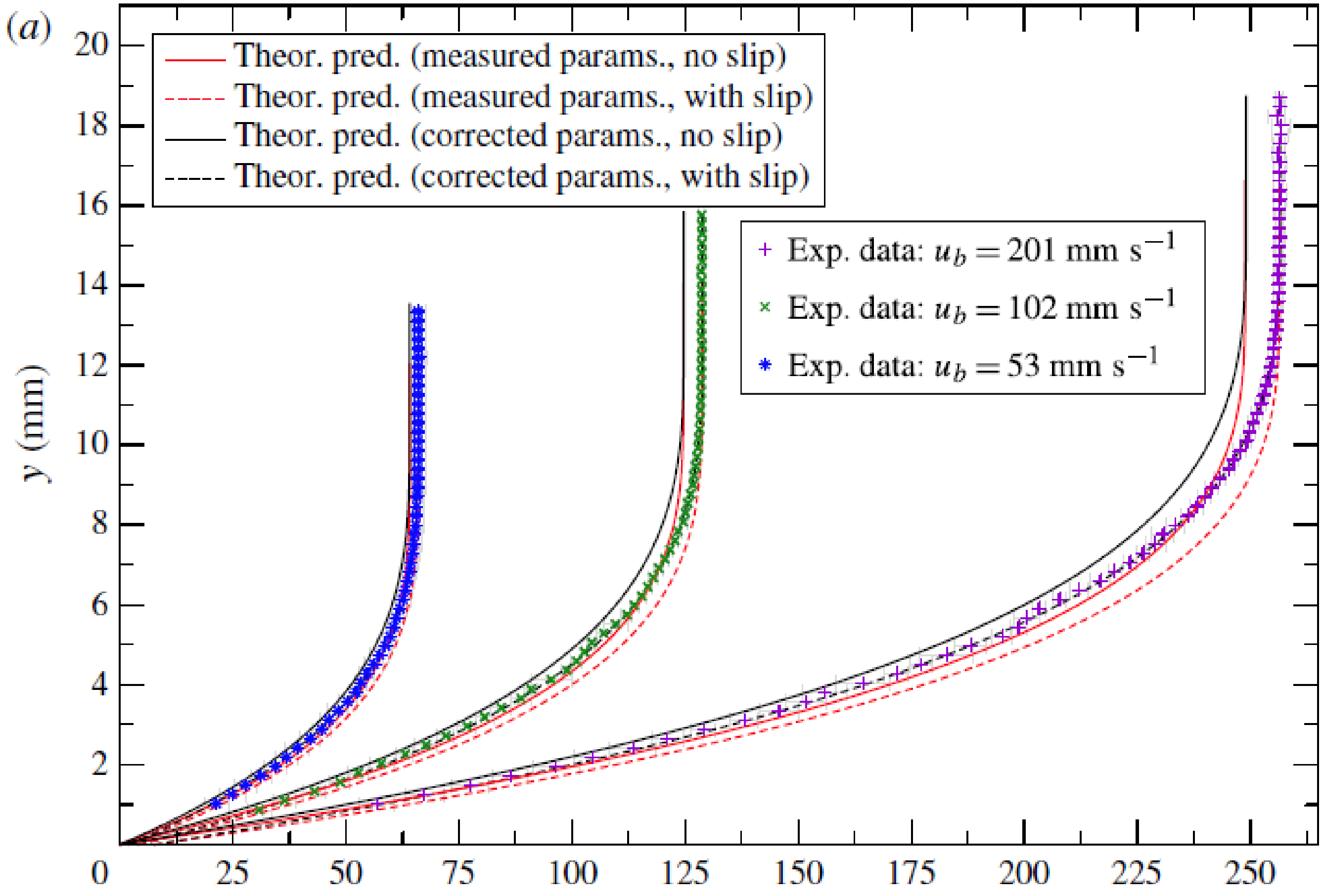

Apparent flow curve

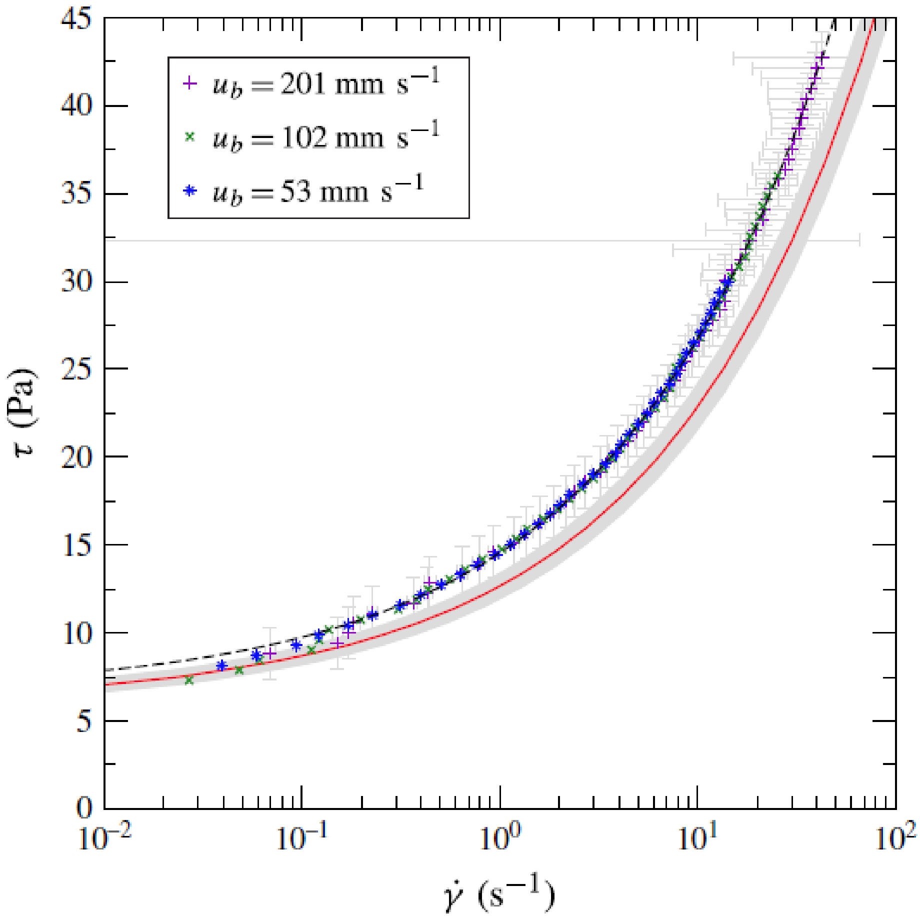

$$\tau = \rho g\, h \sin\theta$$

$$\dot{\gamma} = \frac{du}{dy}$$

➢ Need for a systematic correction of Carbopol rheological parameters:

- +10% on τ_c
- +20% on K

Rheological parameter correction

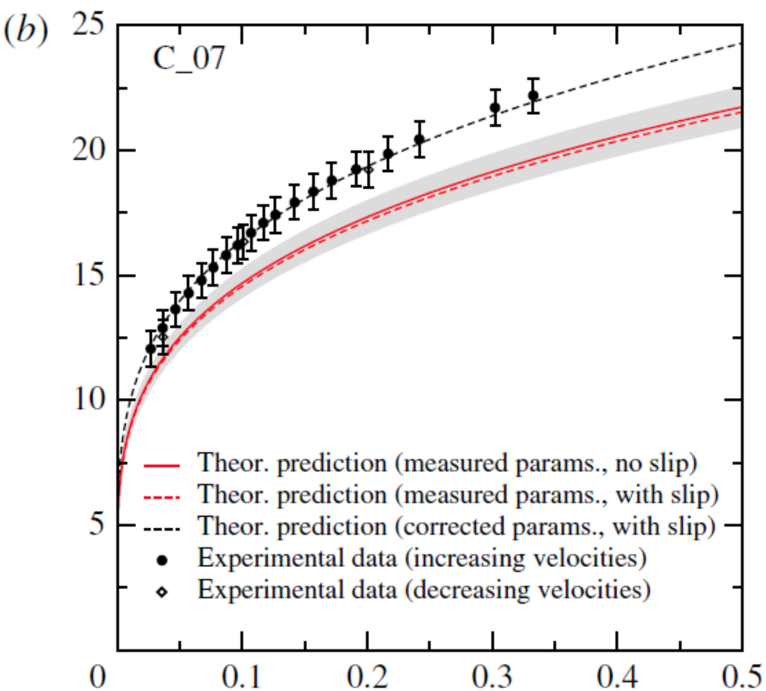

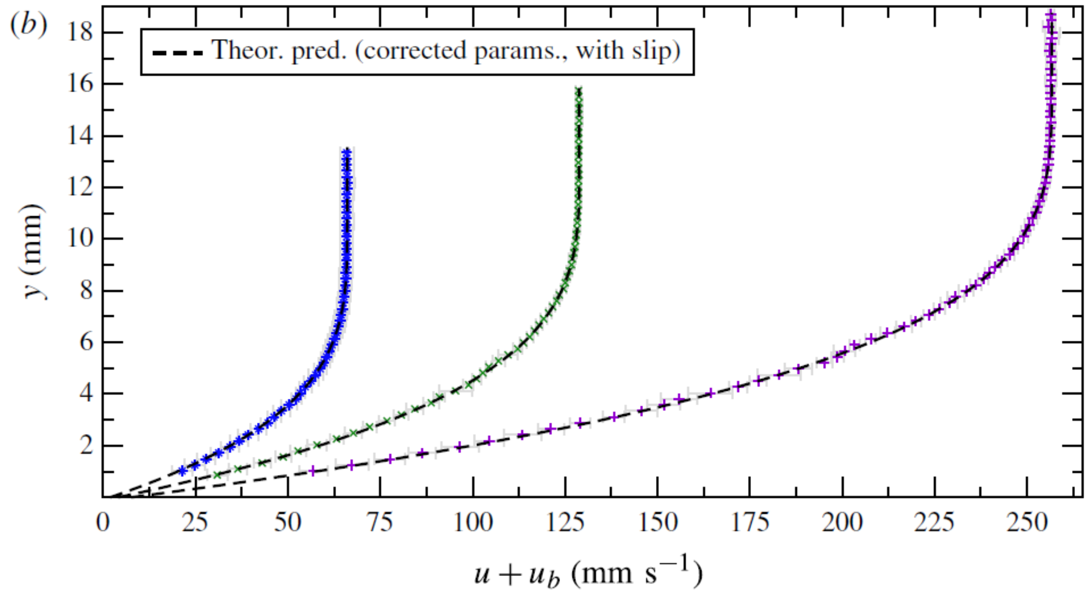

Origin of the correction: scale effects?

Conclusions

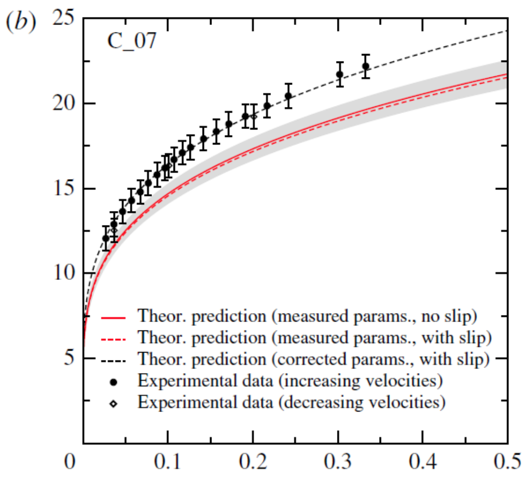

- Uncertainties on rheological measurements
  - ➢ significant influence on theoretical predictions (height, velocity, etc.)
- If possible, infer rheological parameters from the flow itself

Front internal dynamics

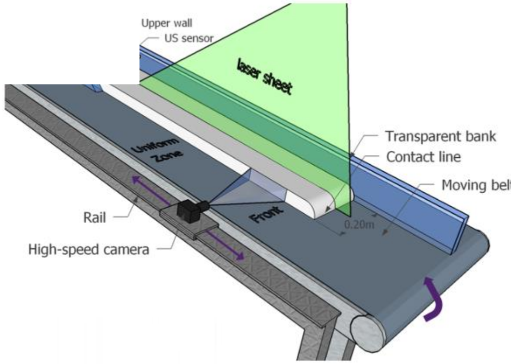

High-resolution space-time velocimetry (STV)

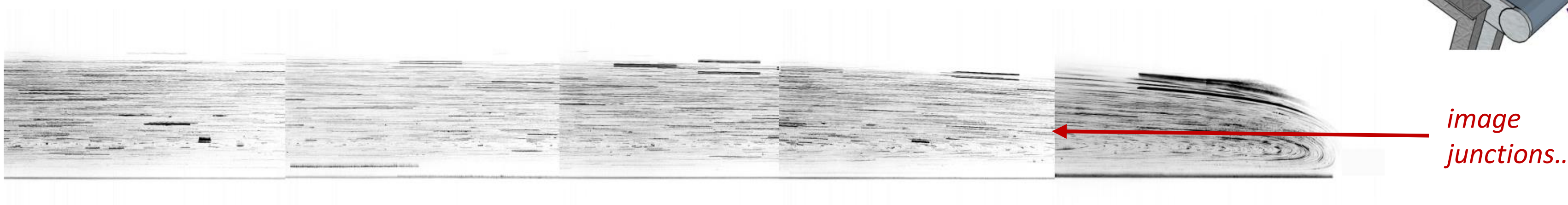

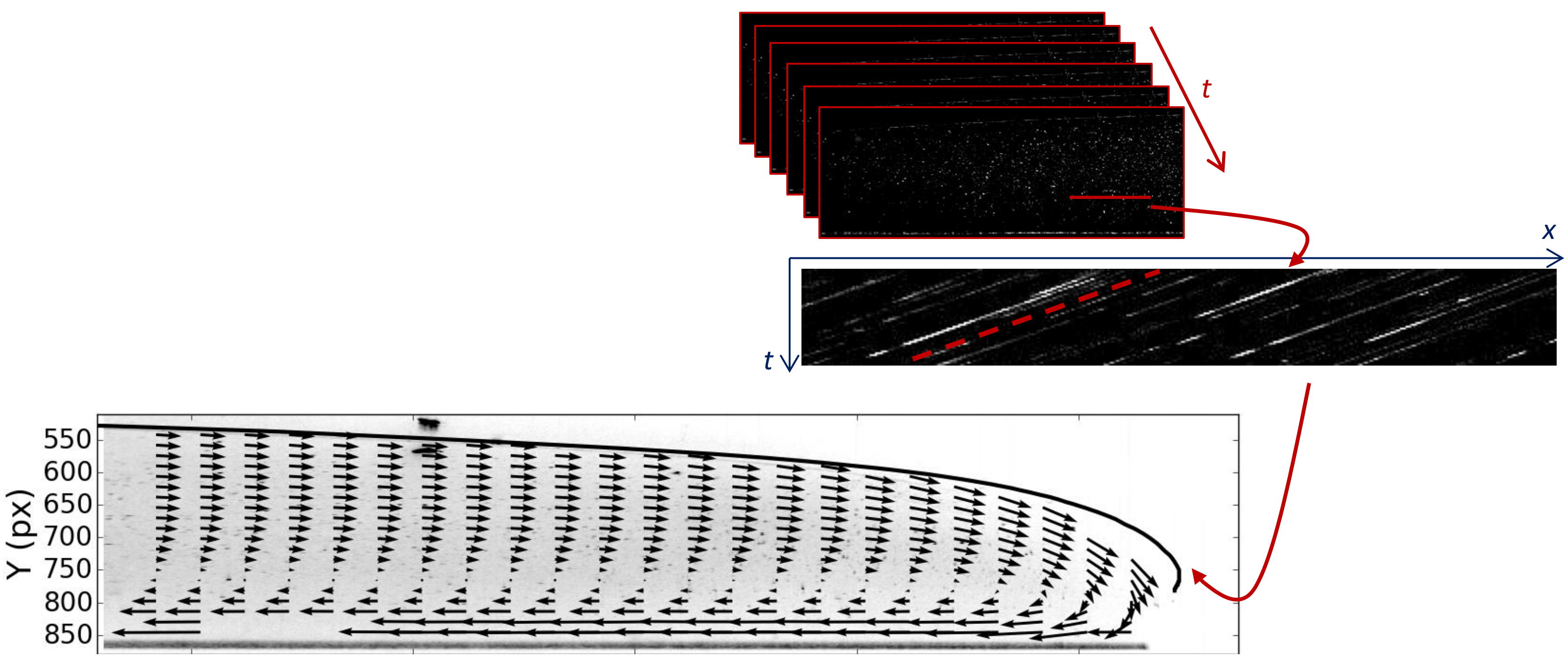

Freydier et al., JNNFM, 2018

Velocity fields

Longitudinal velocity

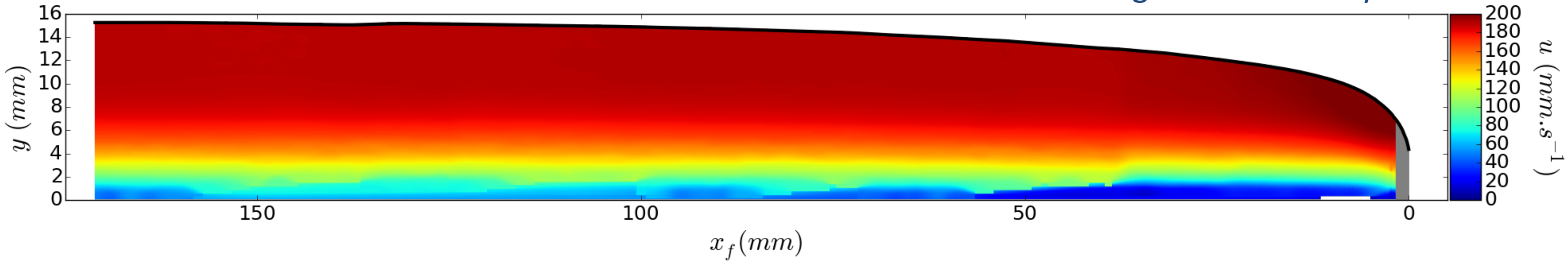

Vertical velocity

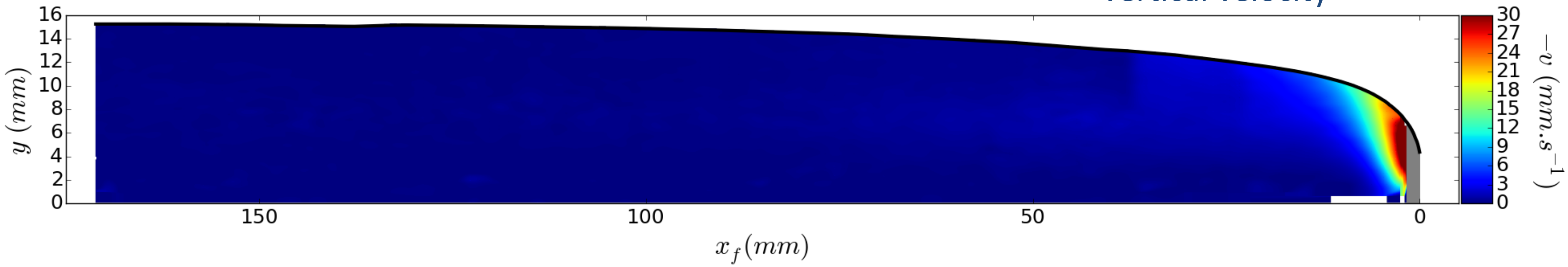

Velocity profiles

Longitudinal velocity

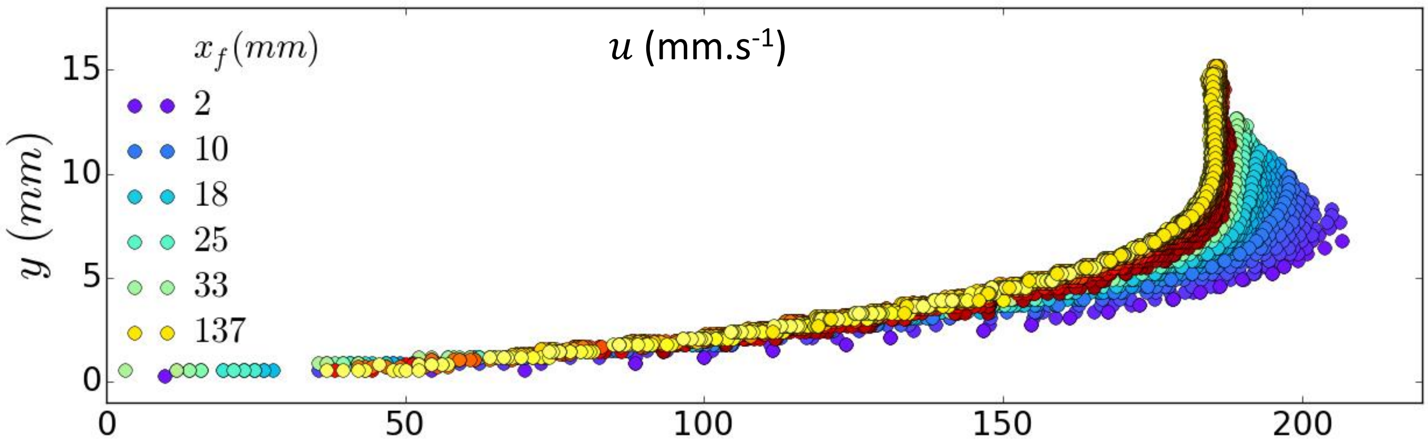

Vertical velocity

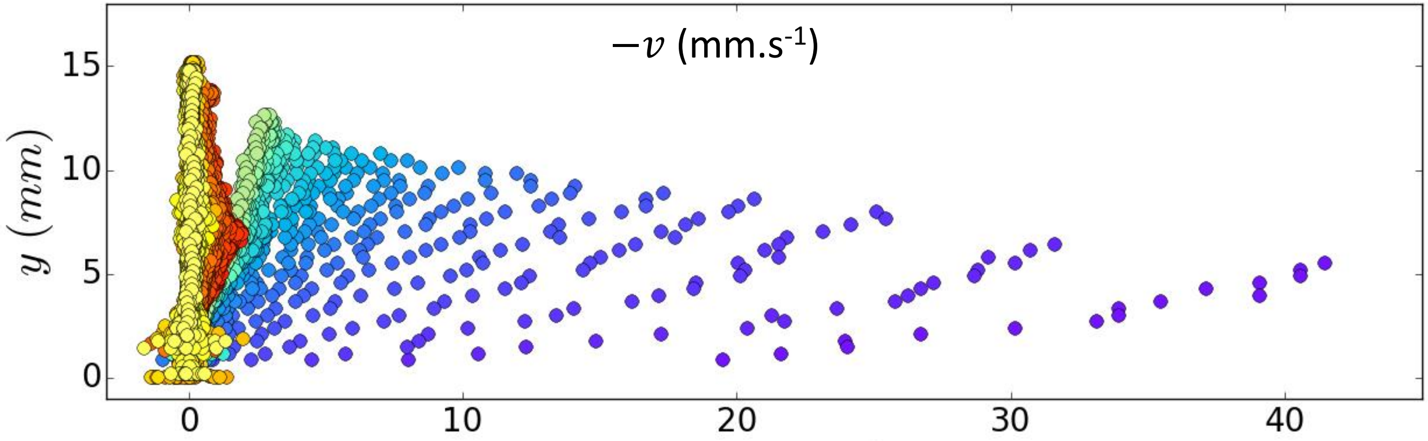

Evolution of the plug zone

Shear rate

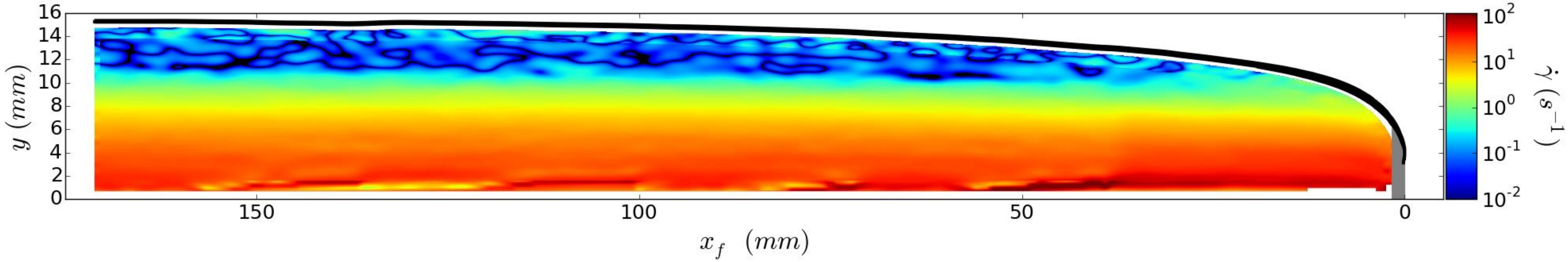

Apparent plug ($\dot{\gamma}$ threshold: 0.2 – 0.3 s^{-1})

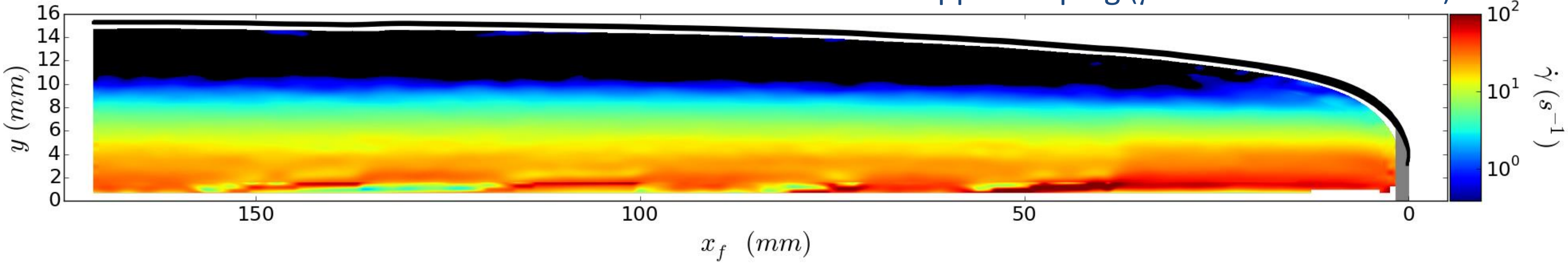

➢ Unsheared plug progressively thins, and disappears, in surge tip

Order-0 model (lubrication)

$$\frac{\partial u}{\partial x} + \frac{\partial v}{\partial y} = 0$$

$$\cancel{\epsilon Re \left(\frac{\partial u}{\partial t} + u \frac{\partial u}{\partial x} + v \frac{\partial u}{\partial y} \right)} = \overbrace{\frac{Re}{Fr^2} \tan\theta}^{\lambda} - \epsilon \frac{Re}{Fr^2} \frac{\partial p}{\partial x} + Bi \frac{\partial \sigma_{xy}}{\partial y} + \cancel{\epsilon Bi \frac{\partial \sigma_{xx}}{\partial x}}$$

$$\cancel{\epsilon^3 Re \left(\frac{\partial v}{\partial t} + u \frac{\partial v}{\partial x} + v \frac{\partial v}{\partial y} \right)} = -\epsilon \frac{Re}{Fr^2} - \epsilon \frac{Re}{Fr^2} \frac{\partial p}{\partial y} + \cancel{\epsilon^2 Bi \frac{\partial \sigma_{xy}}{\partial x}} + \cancel{\epsilon Bi \frac{\partial \sigma_{yy}}{\partial y}}$$

$$\begin{cases} u^{(0)} = u_p \left[1 - \left(1 - \frac{y}{h - h_p} \right)^{\frac{n+1}{n}} \right] & \text{for } y < h - h_p \\ u^{(0)} = u_p & \text{for } y \geq h - h_p \end{cases}$$

with $\quad u_p = \dfrac{n}{n+1} \Lambda^{1/n} (h - h_p)^{(n+1)/n}$

$$\boxed{h_p = \frac{Bi}{\Lambda} \qquad \Lambda = \lambda - \frac{\epsilon Re}{Fr^2} \partial_x h}$$

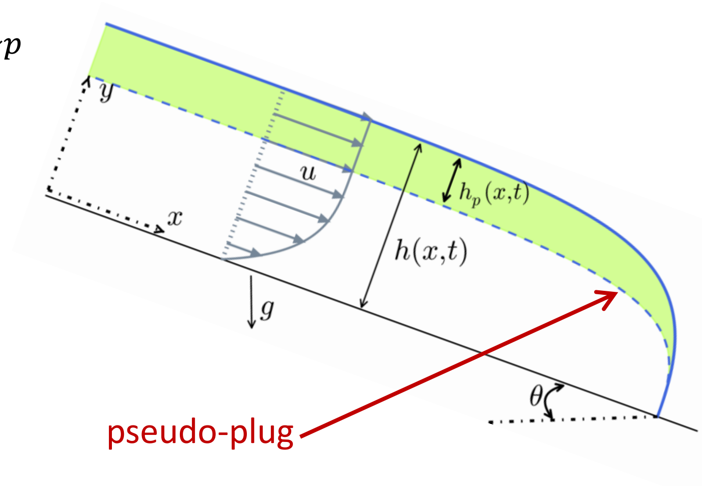

"Raw" comparison

Theoretical profiles based on computed free-surface shape (traveling wave solution)

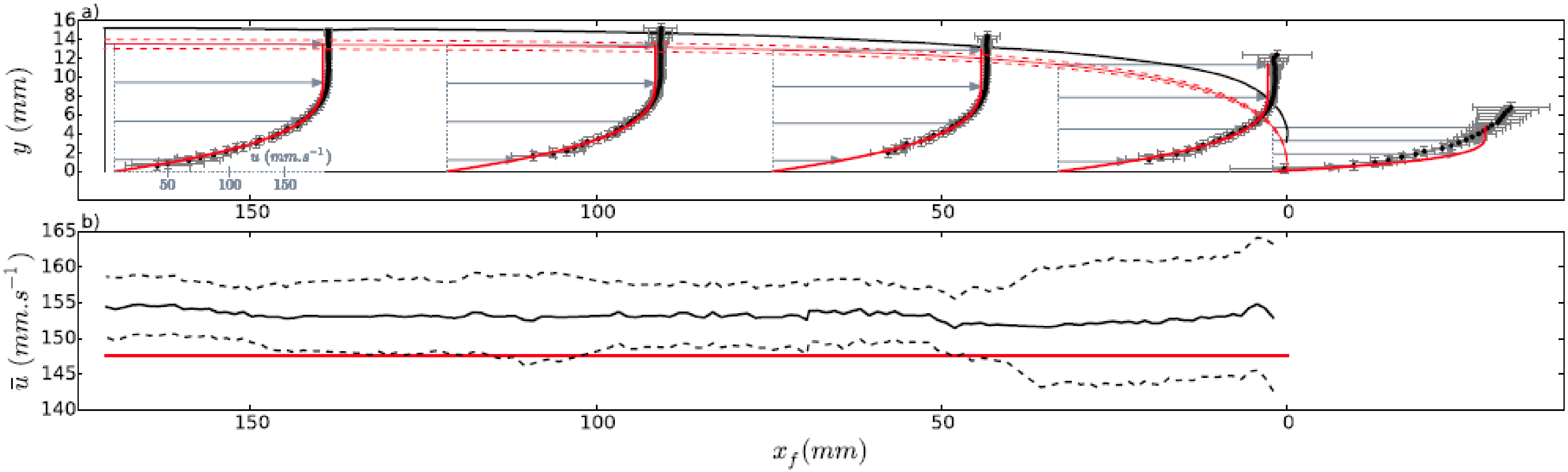

- Renormalization to account for experimental uncertainties on
  - rheological parameters: $h \rightarrow h/H_N$
  - average velocity (3D effects): $u \rightarrow u/\bar{u}$

Non-dimensionalized comparison

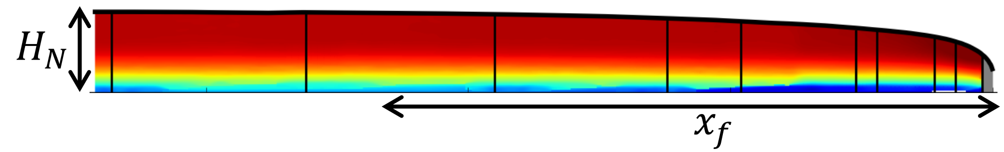

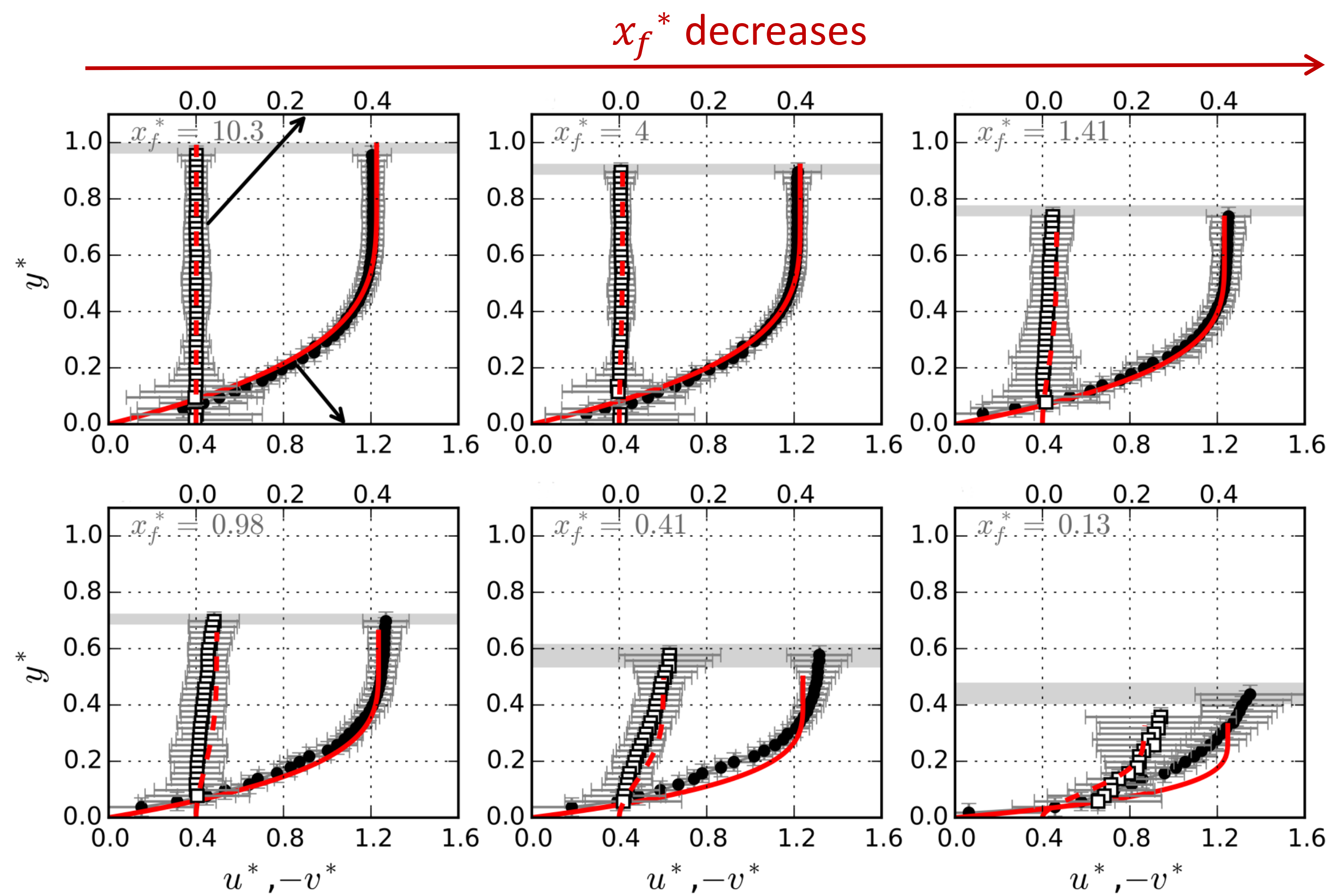

- Good agreement until $x_f \approx 1$

Surface velocity

$\theta = 15.3°; G = 0.35; Fr = 0.06$

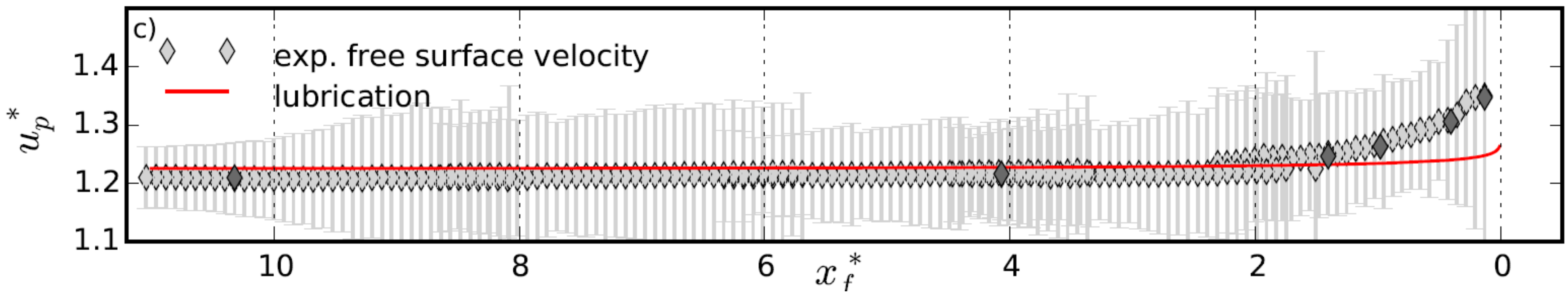

$\theta = 11.9°; G = 0.17; Fr = 0.38$

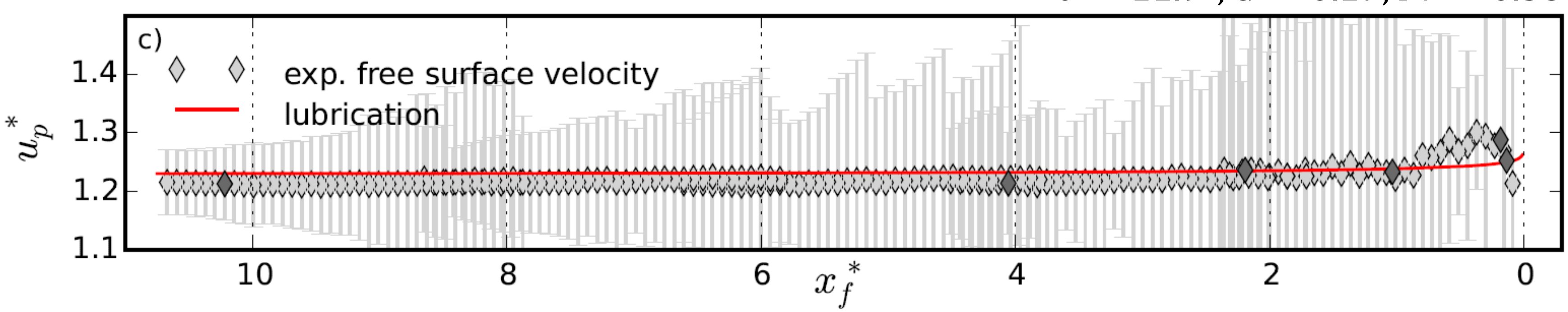

Order-1 model (ϵ^1)

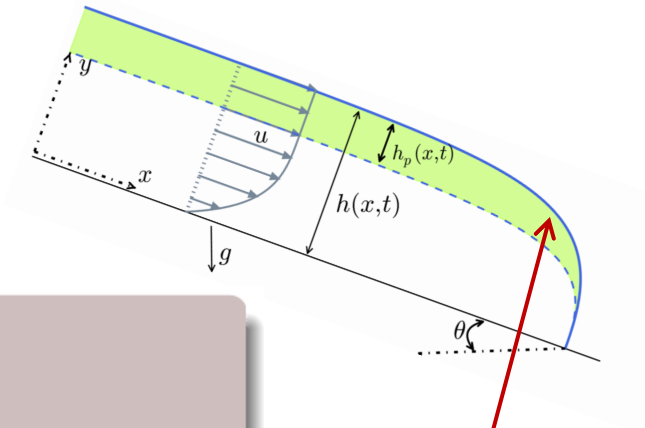

$$\frac{\partial u}{\partial x} + \frac{\partial v}{\partial y} = 0$$

$$\epsilon Re\left(\frac{\partial u}{\partial t} + u\frac{\partial u}{\partial x} + v\frac{\partial u}{\partial y}\right) = \frac{Re}{Fr^2}\tan\theta - \epsilon\frac{Re}{Fr^2}\frac{\partial p}{\partial x} + Bi\frac{\partial \sigma_{xy}}{\partial y} + \epsilon Bi\frac{\partial \sigma_{xx}}{\partial x}$$

$$\cancel{\epsilon^3 Re\left(\frac{\partial v}{\partial t} + u\frac{\partial v}{\partial x} + v\frac{\partial v}{\partial y}\right)} = -\epsilon\frac{Re}{Fr^2} - \epsilon\frac{Re}{Fr^2}\frac{\partial p}{\partial y} + \cancel{\epsilon^2 Bi\frac{\partial \sigma_{xy}}{\partial x}} + \epsilon Bi\frac{\partial \sigma_{yy}}{\partial y}$$

plastic normal stresses in the pseudo-plug

$$|\sigma| = Bi\sqrt{{\sigma_{xy}}^2 + {\boldsymbol{\sigma}_{\boldsymbol{xx}}}^2} = Bi + O(\epsilon)$$

Balmforth & Craster, JNNFM, 1999

$u = u^{(0)} + \epsilon u^{(1)}$ with:

$$\begin{cases} u^{(1)} = \overbrace{Re\,\mathcal{U}_I(x,y,t)}^{\text{correction due to inertia}} + Bi\,\mathcal{U}_N(x,y,t) & \text{for } y < h - h_p \\ u^{(1)} = Re\,\mathcal{U}_I(x,h-h_p,t) + Bi\,\underbrace{[\mathcal{U}_N(x,h-h_p,t) + \mathcal{U}_{np}(x,y,t)]}_{\text{corrections due to normal stresses}} & \text{for } y \geq h - h_p \end{cases}$$

Expressions of the corrective terms

Inertia:

$$\mathcal{U}_I = \Lambda^{(3-n)/n}(h-h_p)^{(2n+3)/n} p_{\mathcal{U}1}\left(\frac{y}{h-h_p}\right) \partial_x h$$

$$+ \Lambda^{(3-2n)/n}(h-h_p)^{(3n+3)/n} p_{\mathcal{U}2}\left(\frac{y}{h-h_p}\right) \partial_x \Lambda$$

$$- \Lambda^{(2-2n)/n}(h-h_p)^{(2n+2)/n} p_{\mathcal{U}1}\left(\frac{y}{h-h_p}\right) \partial_t \Lambda$$

Normal stresses:

$$\mathcal{U}_N = -\frac{\pi}{2}\Lambda^{(1-2n)/n} h_p (h-h_p)^{1/n}\left(1-\left(1-\frac{y}{h-h_p}\right)^{\frac{1}{n}}\right)\operatorname{sgn}(\partial_x u_p)\,\partial_x\Lambda$$

$$\mathcal{U}_{np} = 2\Lambda^{(1-n)/n}(h-h_p)^{1/n}\sqrt{1-\left(\frac{h-y}{h_p}\right)^2}\left[\partial_x h + \frac{1}{n+1}(h+nh_p)\frac{\partial_x\Lambda}{\Lambda}\right]\operatorname{sgn}(\partial_x u_p)$$

Model comparison

Longitudinal velocity profiles

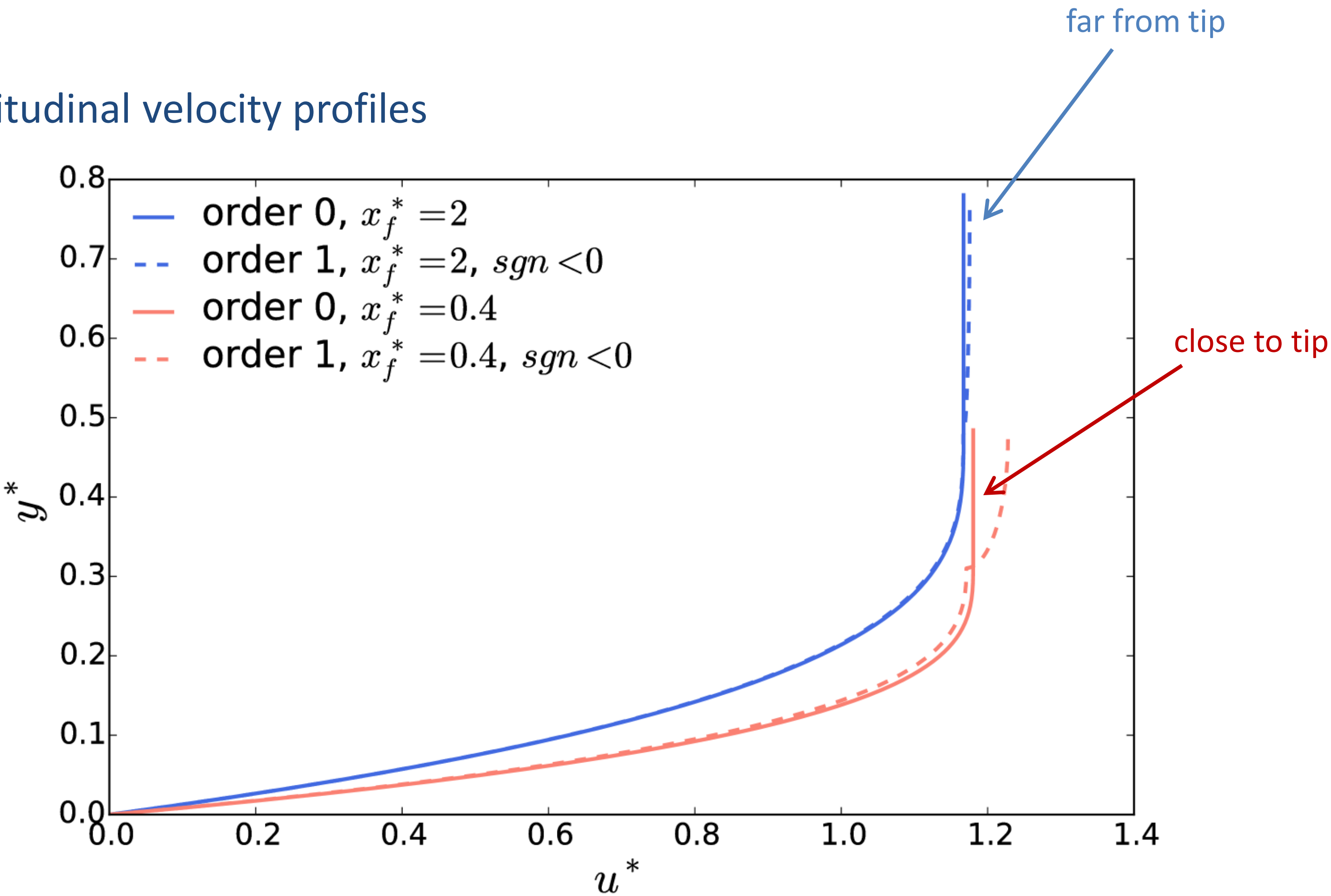

- Close to tip:
  - shear throughout the fluid layer
  - surface velocity is (generally) larger
- Non-differentiable matching at pseudo-plug interface…

<u>Surface velocity</u>

$\theta = 15.3°; G = 0.35; Fr = 0.06$

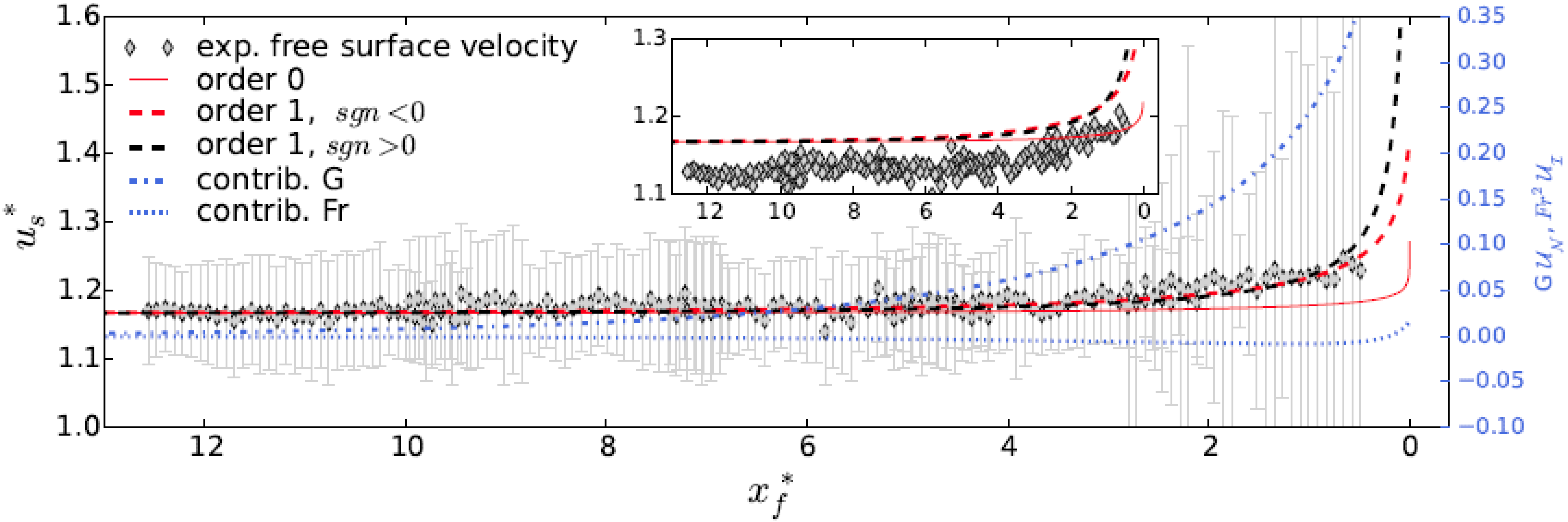

Surface velocity

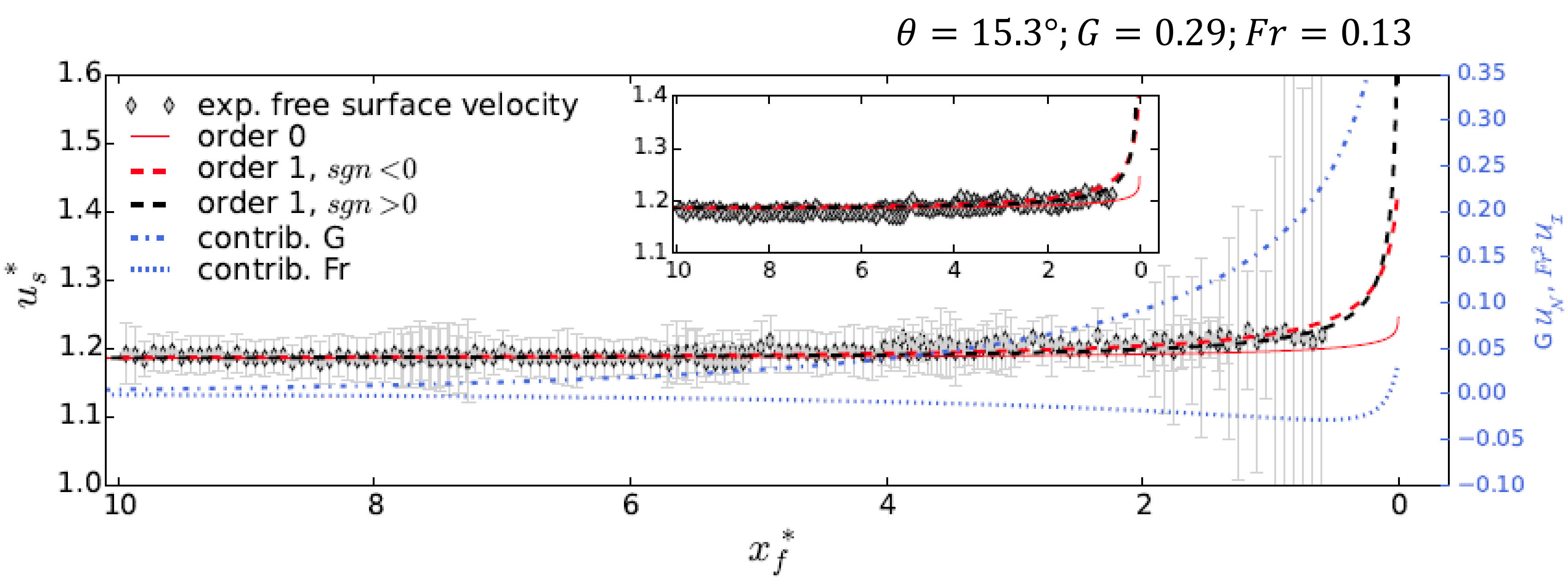

Surface velocity

$\theta = 15.3°; G = 0.24; Fr = 0.28$

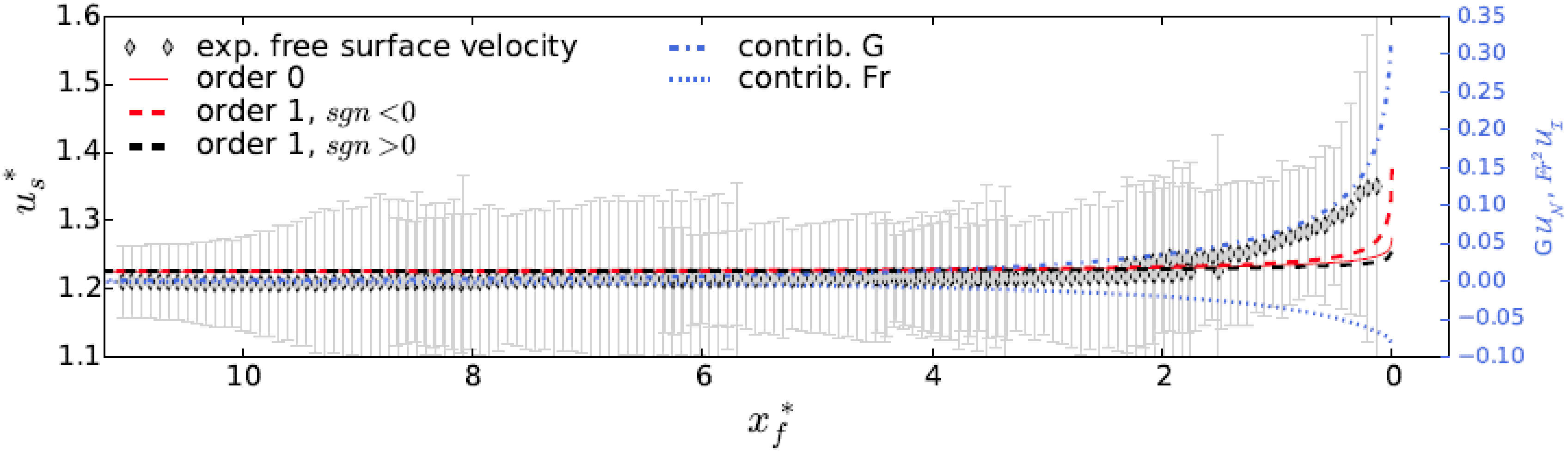

Global overview of all experiments

$$E = |u_{p,predicted} - u_{p,measured}|$$
at $x_f^* = 1$

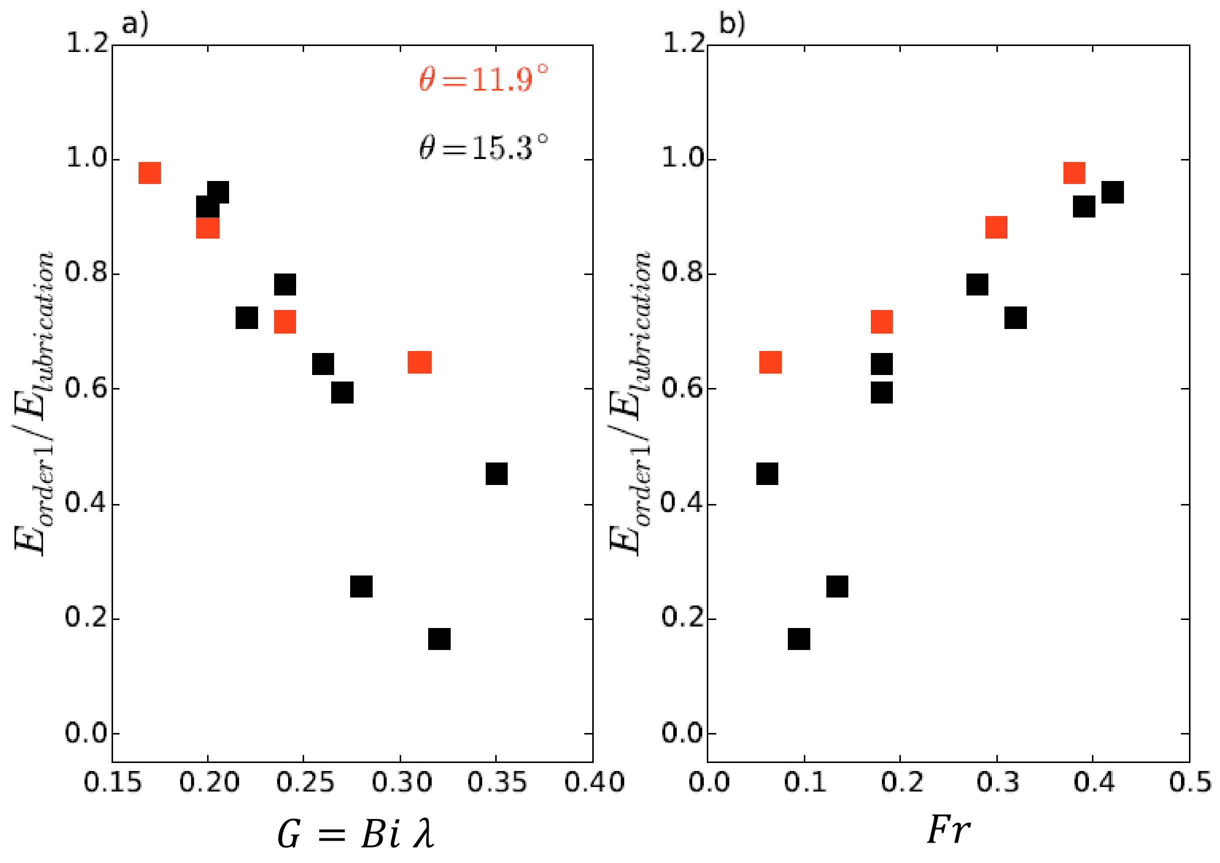

- ϵ^1 approximation improves quantitative agreement in the tip region
- Gain remains marginal for large values of Fr
  - *inertial correction terms need to be improved?*

Shear rate

Average shear rate in the pseudo-plug zone

$\theta = 15.3°; G = 0.31; Fr = 0.06$

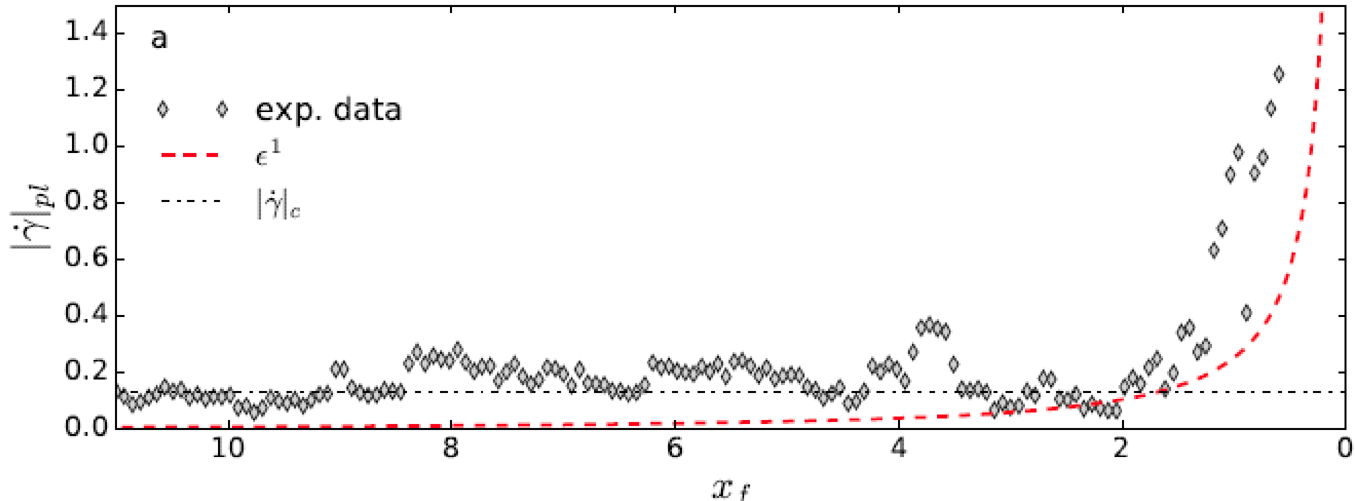

$\theta = 15.3°; G = 0.27; Fr = 0.18$

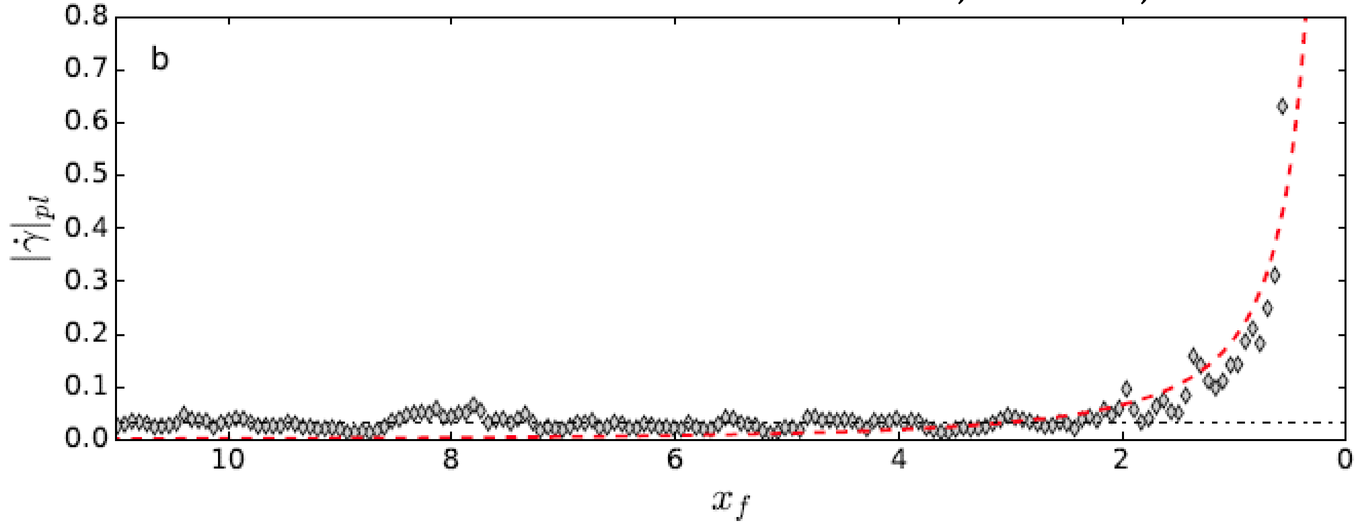

Apparent plug

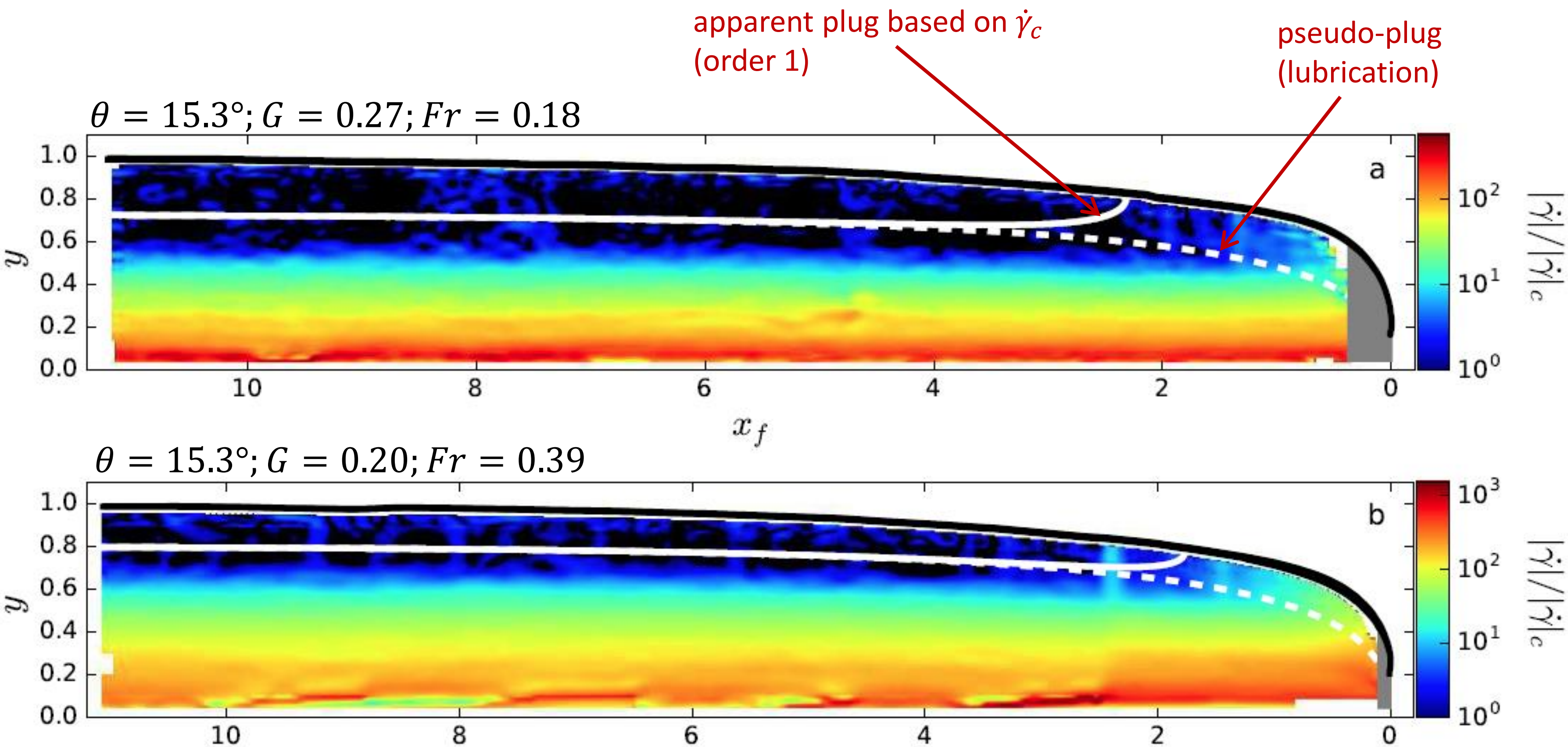

➢ Order-1 explains collapse of the unsheared region at the front

Conclusions

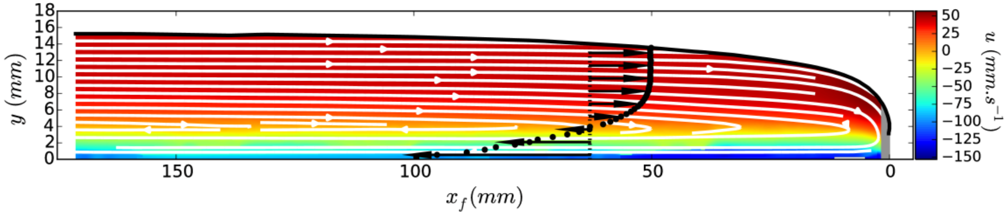

- Accounting for experimental uncertainties through proper non-dimensionalization of variables
- Experimental measurement of plug zones
- Quantitative comparisons of subtle features (e.g., pseudo-plug shear rate)
- Viscoplastic rheology enhances differences between ϵ^0 and ϵ^1 models!

Comparison with a Newtonian fluid

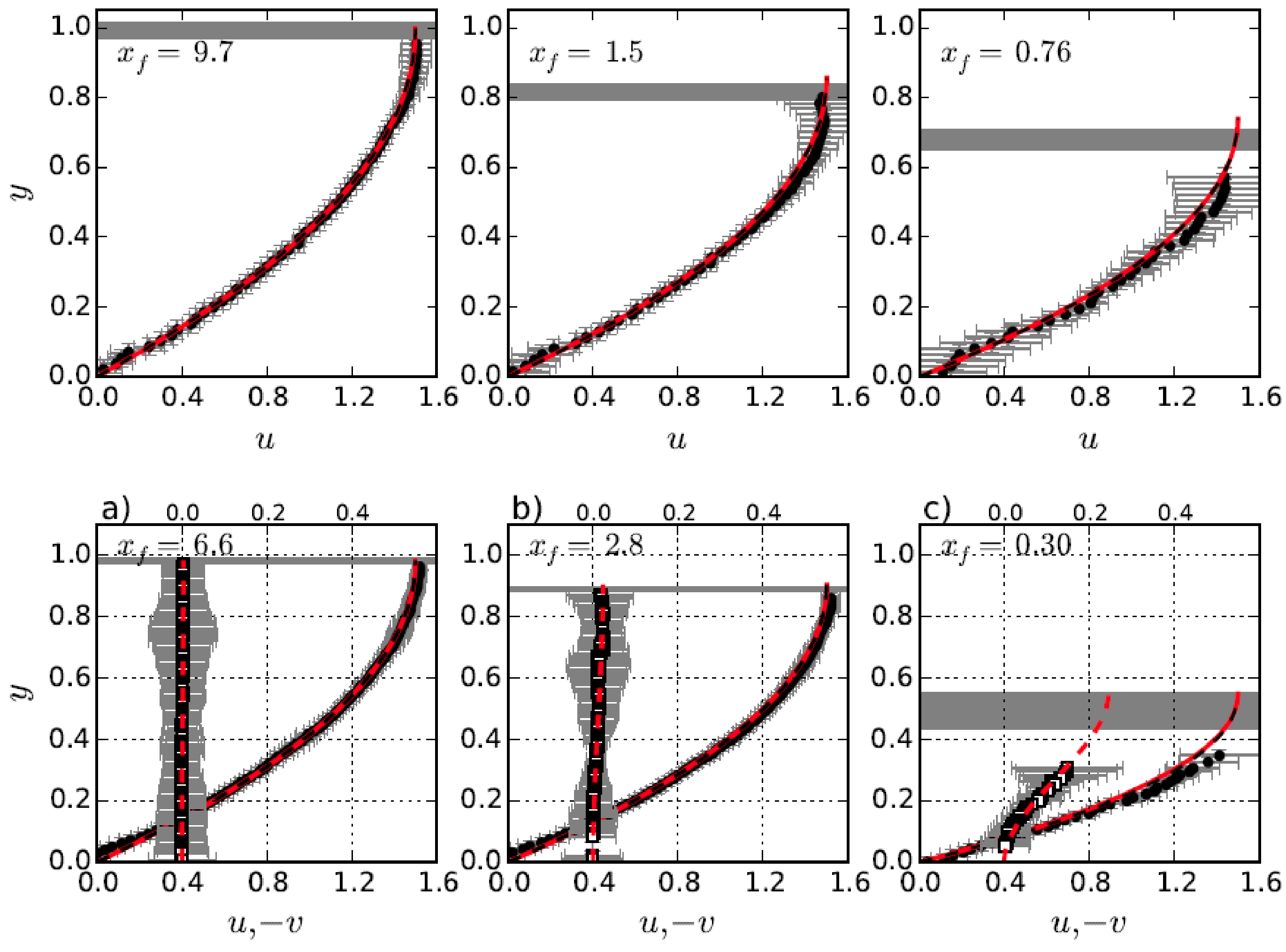

- Predictions of ϵ^0 and ϵ^1 models are virtually indistinguishable

Flow over a cavity

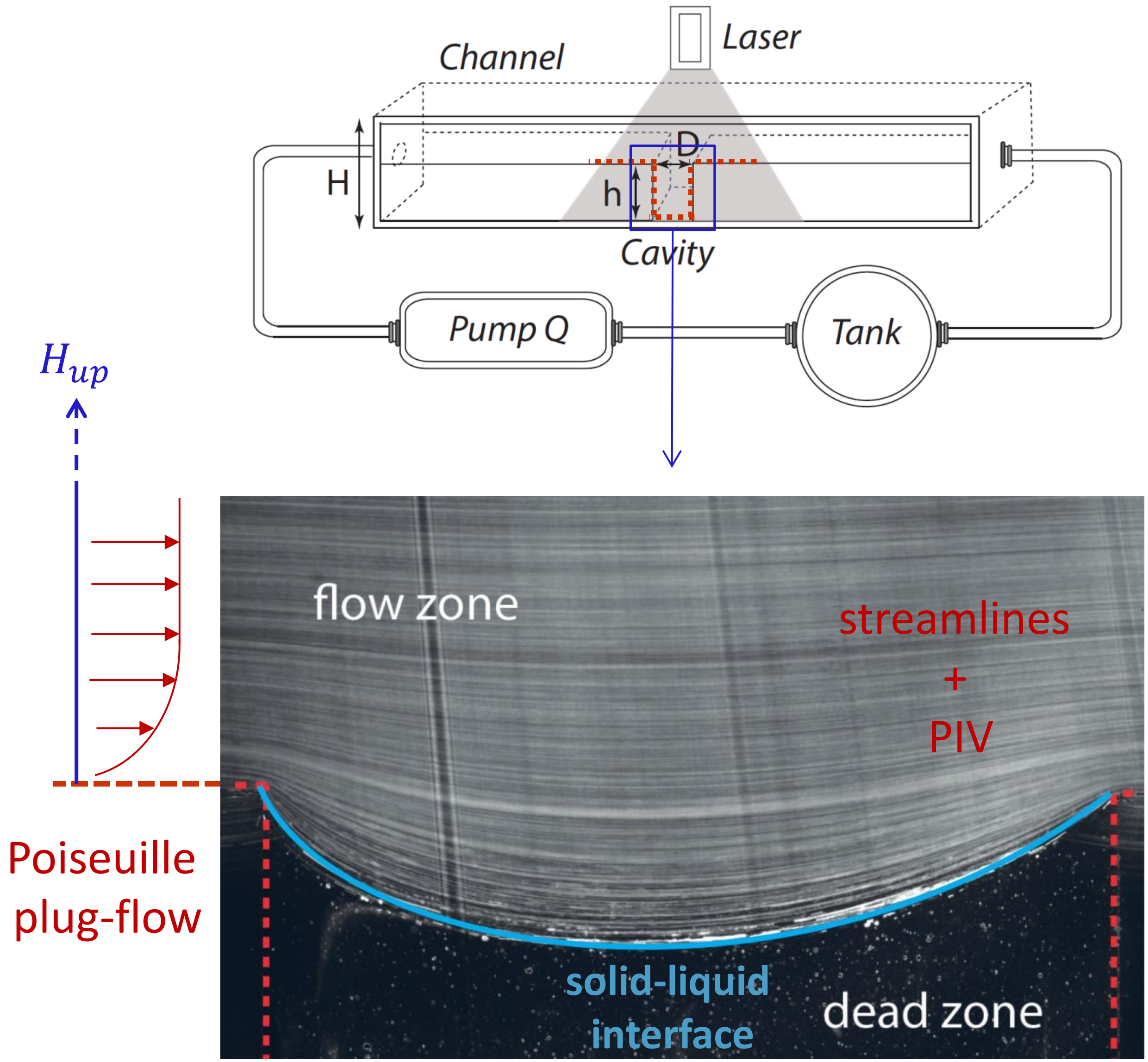

Chambon, Vigneaux, Marly, Luu, Philippe, JNNFM, subm, 2018

Viscoplastic boundary layer theory: large Bi

$$\partial_y \tau_{xy} + 2\,\partial_x \tau_{xx} = 0$$

viscous + plastic — plastic

$$Bi_\ell = \frac{\tau_c}{K}\frac{\ell}{U}$$

- *Oldroyd's (1947)* self-similar solution:

$$\delta \propto {Bi_\ell}^{-1/3}\ell$$

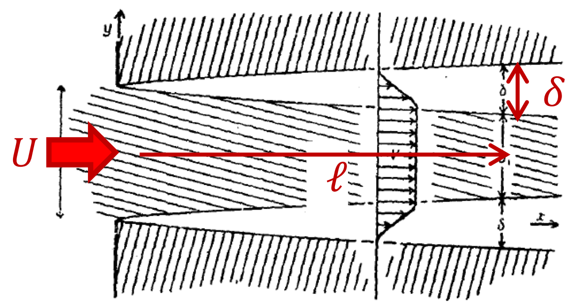

- *Piau (2002)*

- *Balmforth & Craster's (2017)* generalization (assume symmetric velocity profiles in the BL) :

$$y_E \propto {Bi_\ell}^{-1/3}\ell$$

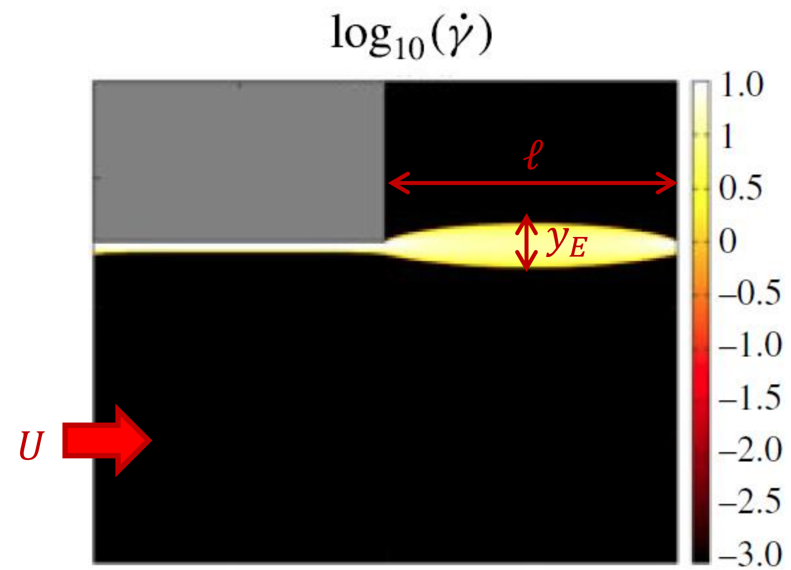

Yield surface position

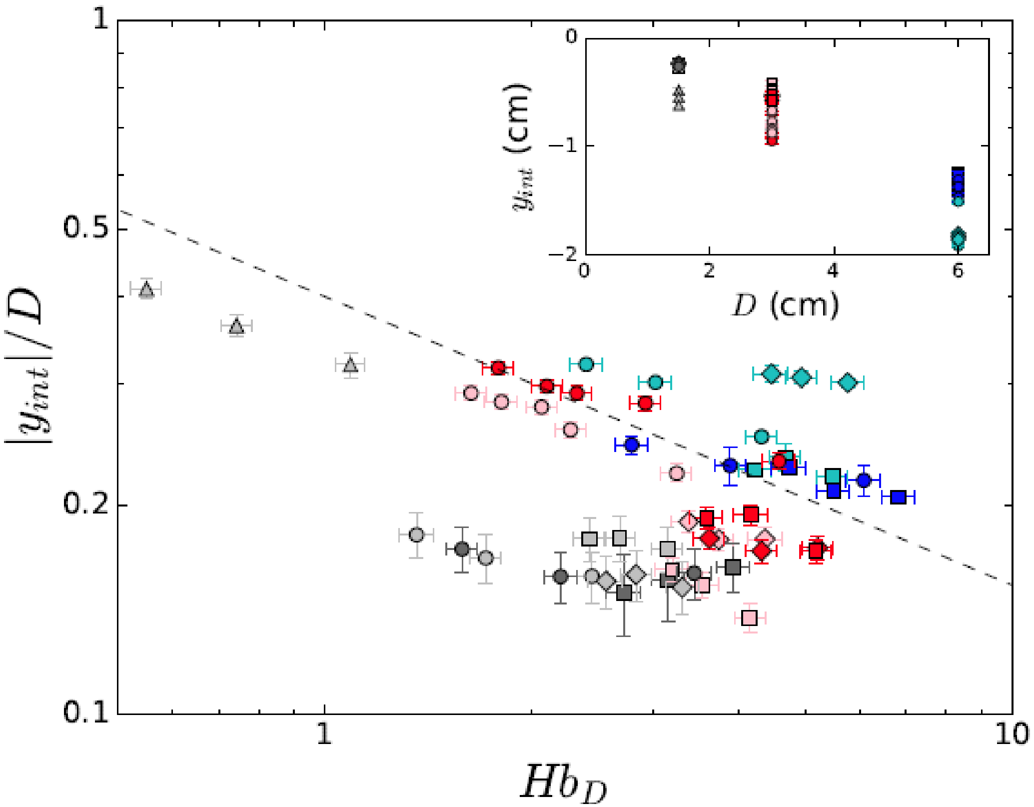

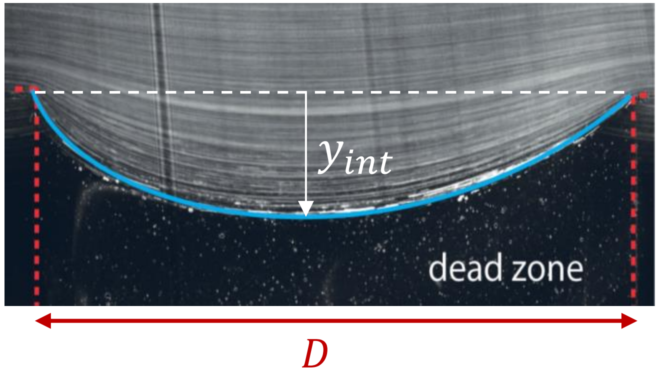

$$Hb_D = \frac{\tau_c}{K}\left(\frac{D}{U_{up}}\right)^n$$

➢ Control of y_{int}?

Direct numerical simulations

- Augmented Lagrangian
- Highly-accurate numerical scheme

Marly & Vigneaux, JNNFM 2017

- Bingham rheology $(n = 1)$ $\begin{cases} \dot{\gamma} = 0 & \text{si } \tau < \tau_c \\ \tau = \tau_c + \eta\dot{\gamma} & \text{si } \tau \geq \tau_c \end{cases}$

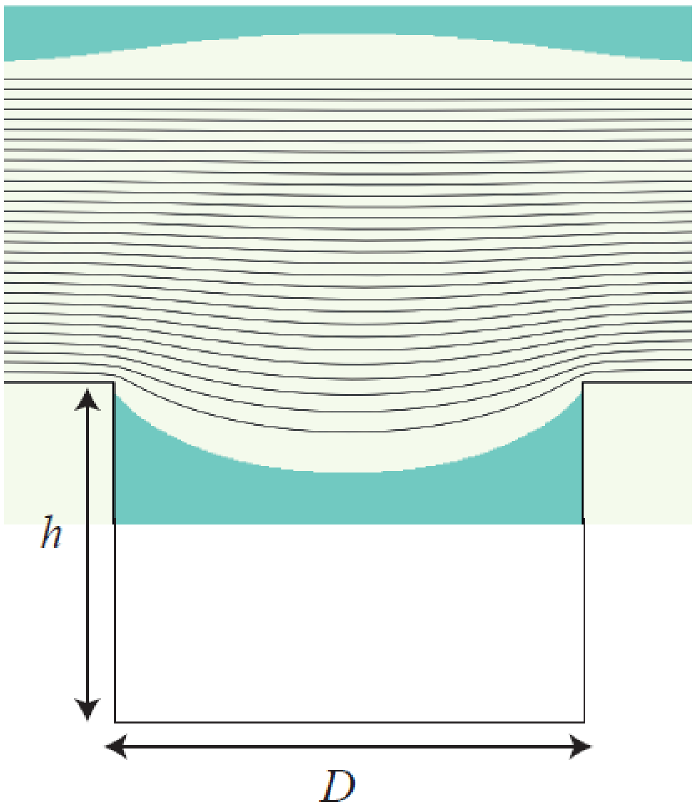

First qualitative comparison: stress fields

Numerical simulations

Experiments

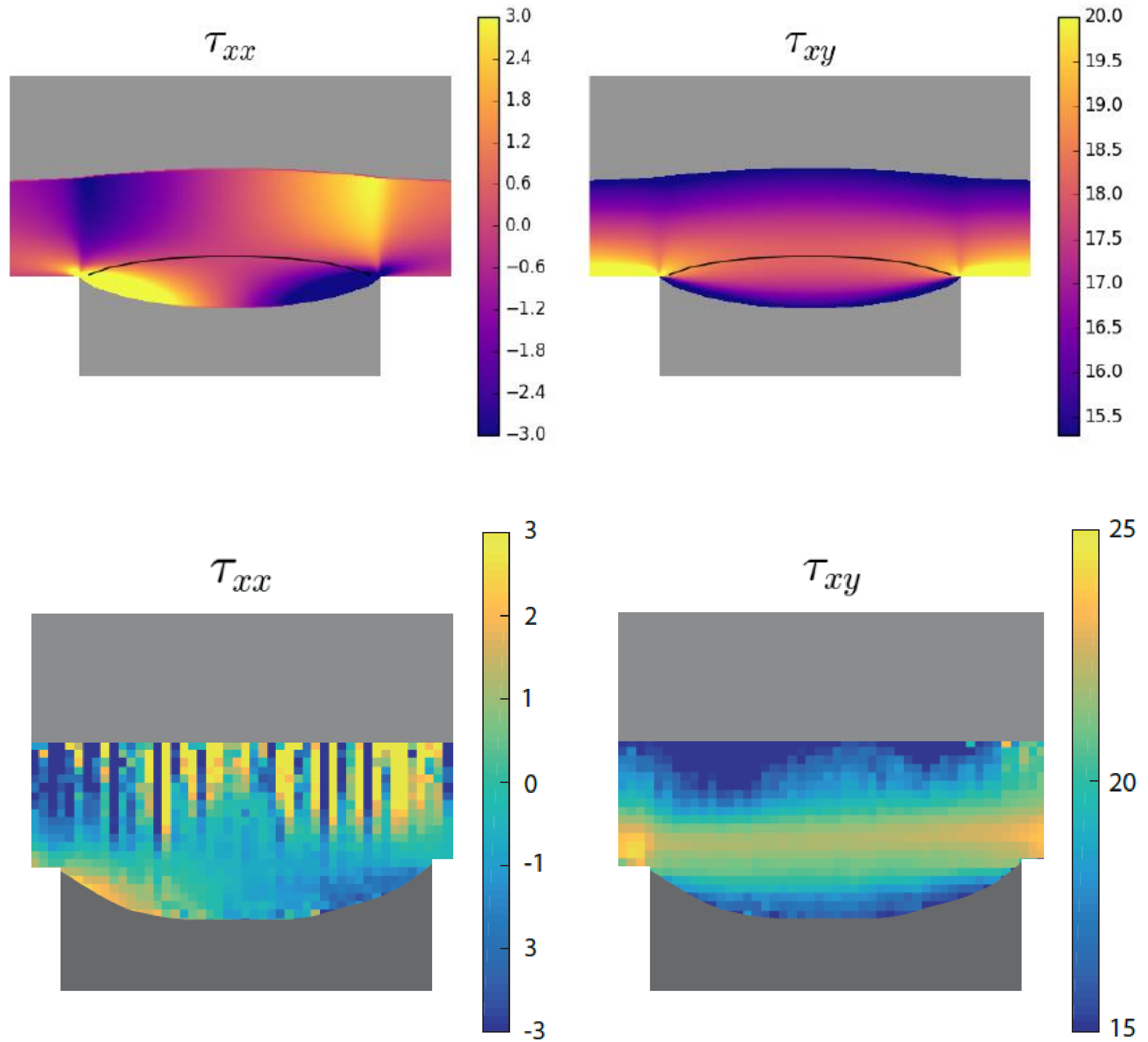

First qualitative comparison: interface shape

$$A_{tot} = \int_0^D |y_{int}(x_{1/2})| dx$$

Numerical simulations

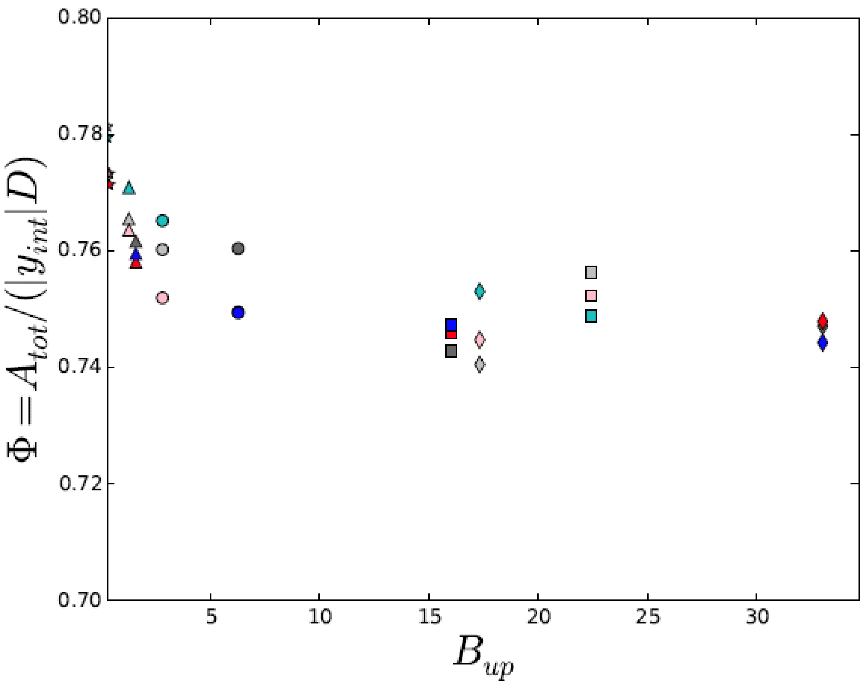

Experiments

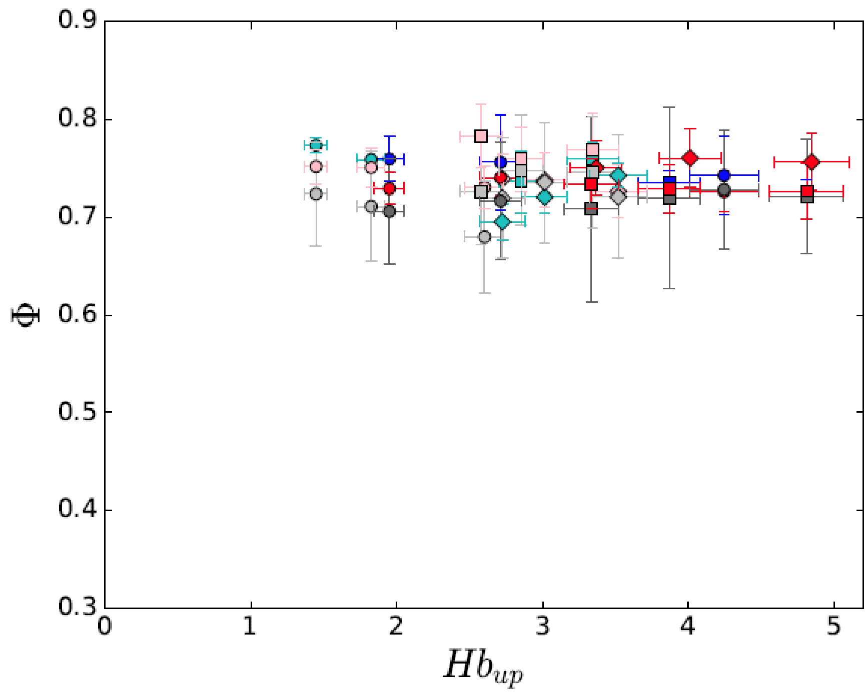

Yield surface position

Numerical simulations

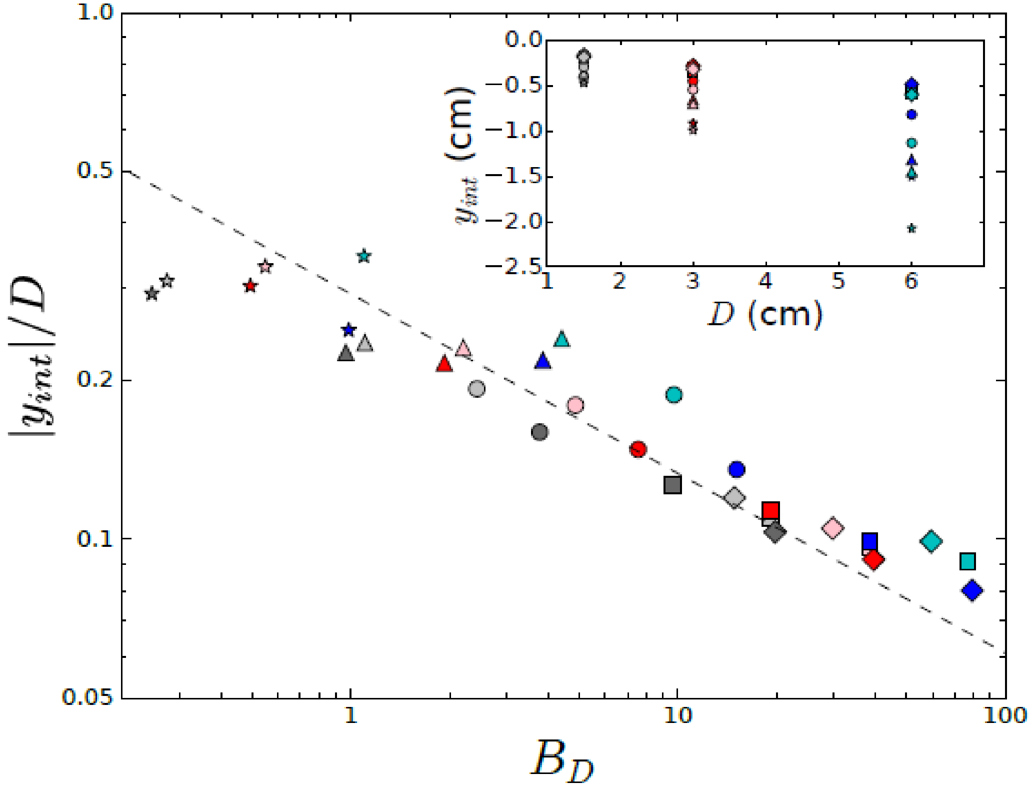

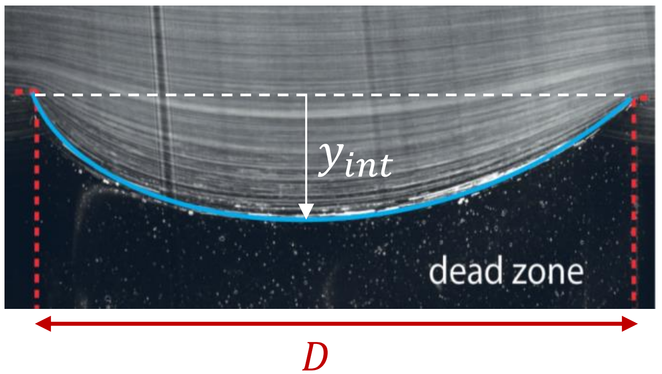

Experiments

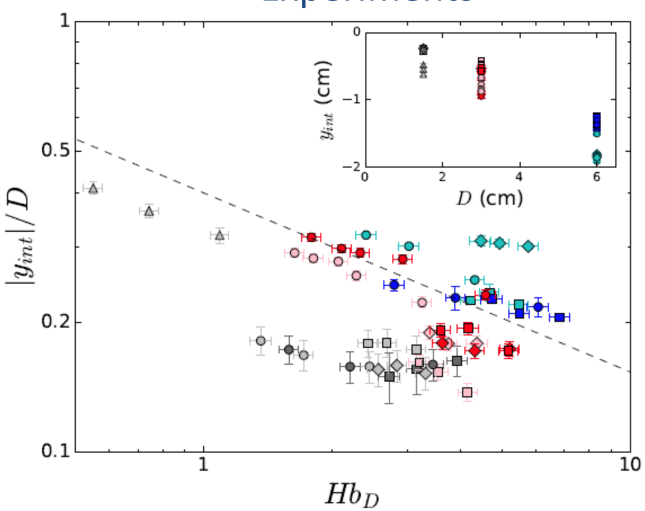

Velocity and strain-rate profiles

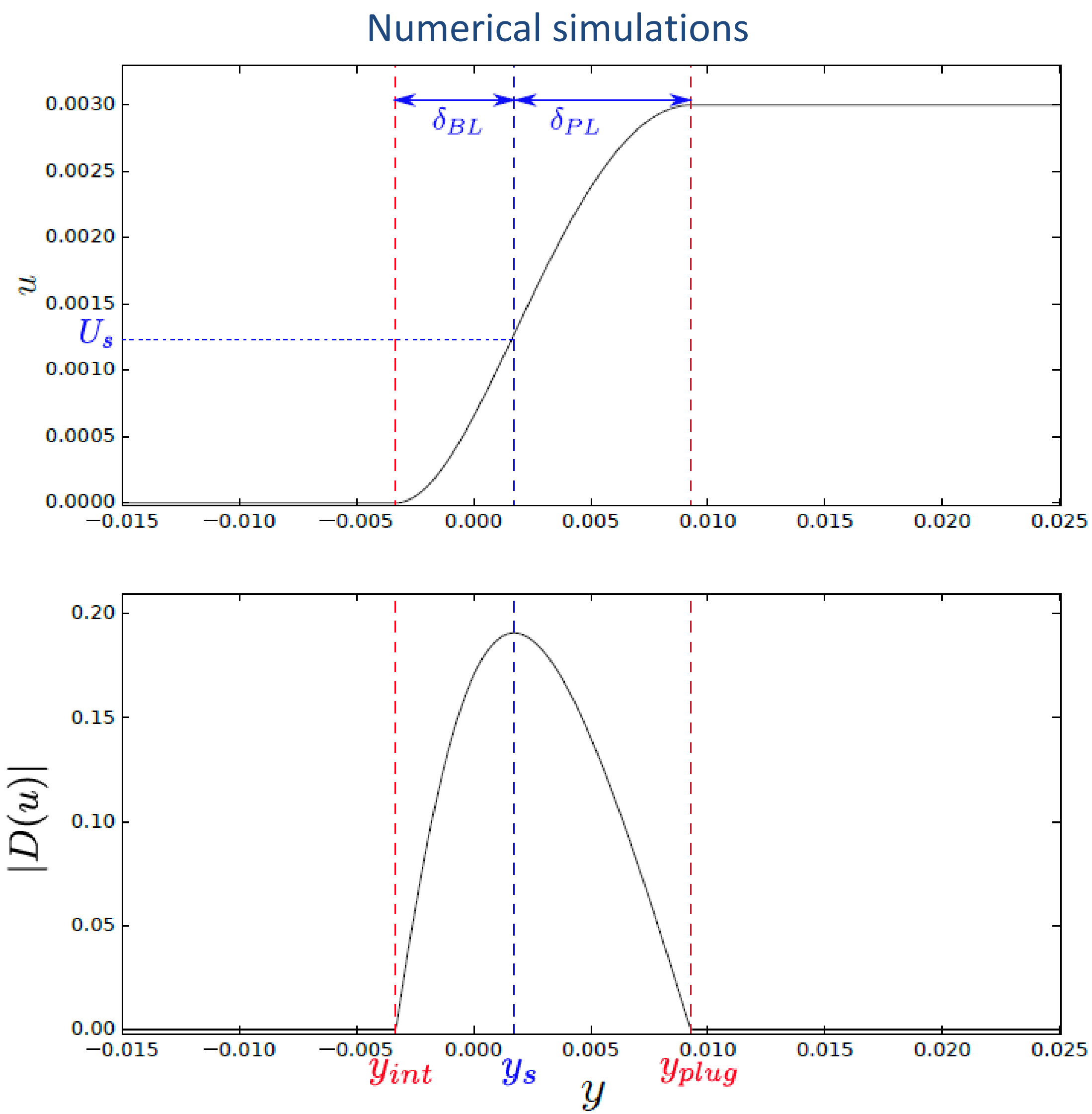

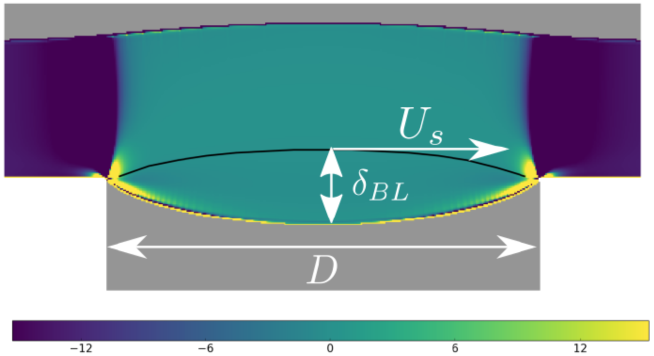

- Non-symmetric profiles
- 3 flow zones
  - *Upper plug*
  - *Poiseuille-like layer*
  - *Boundary layer*

Velocity and strain-rate profiles

Experiments

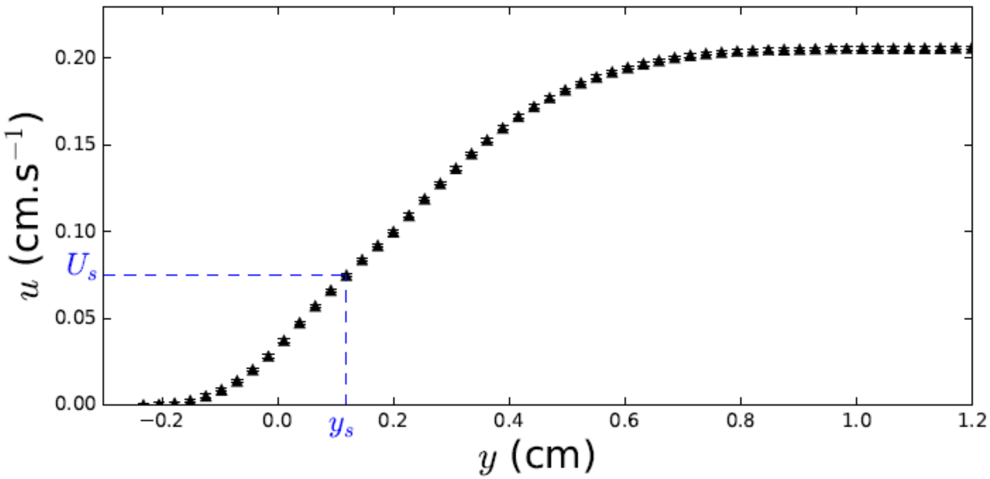

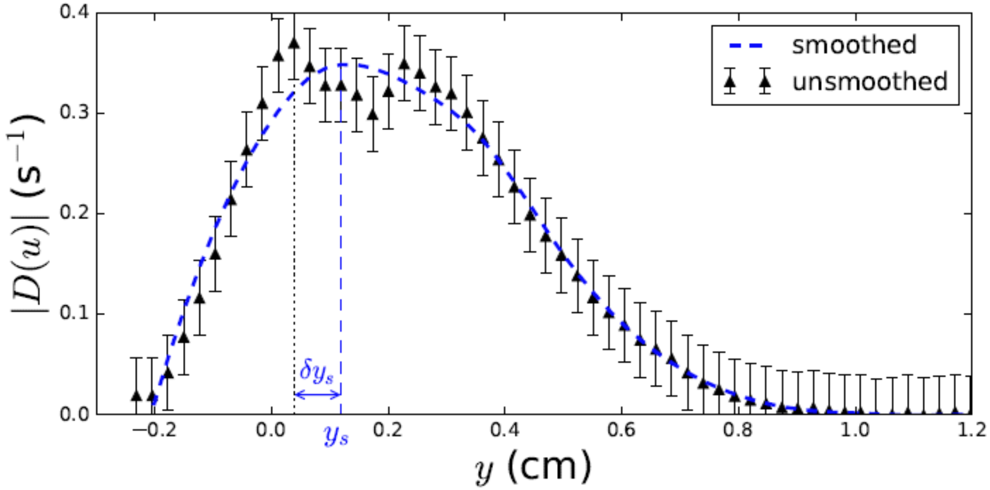

Shear stress: $\tau = \tau_c + K\,|D(u)|^n$

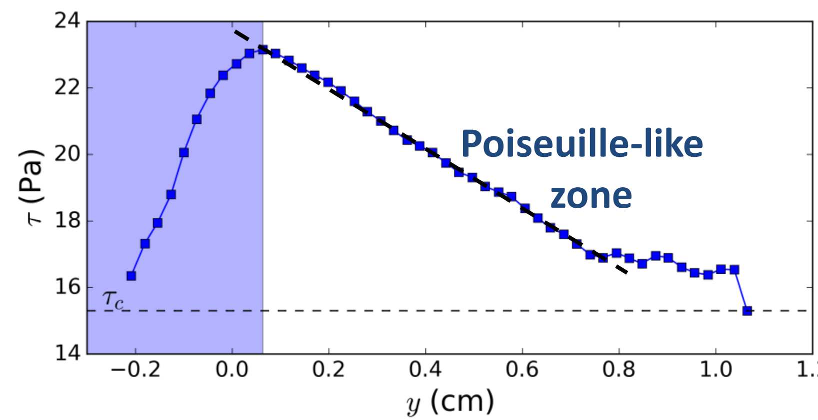

Oldroyd's boundary layer equation

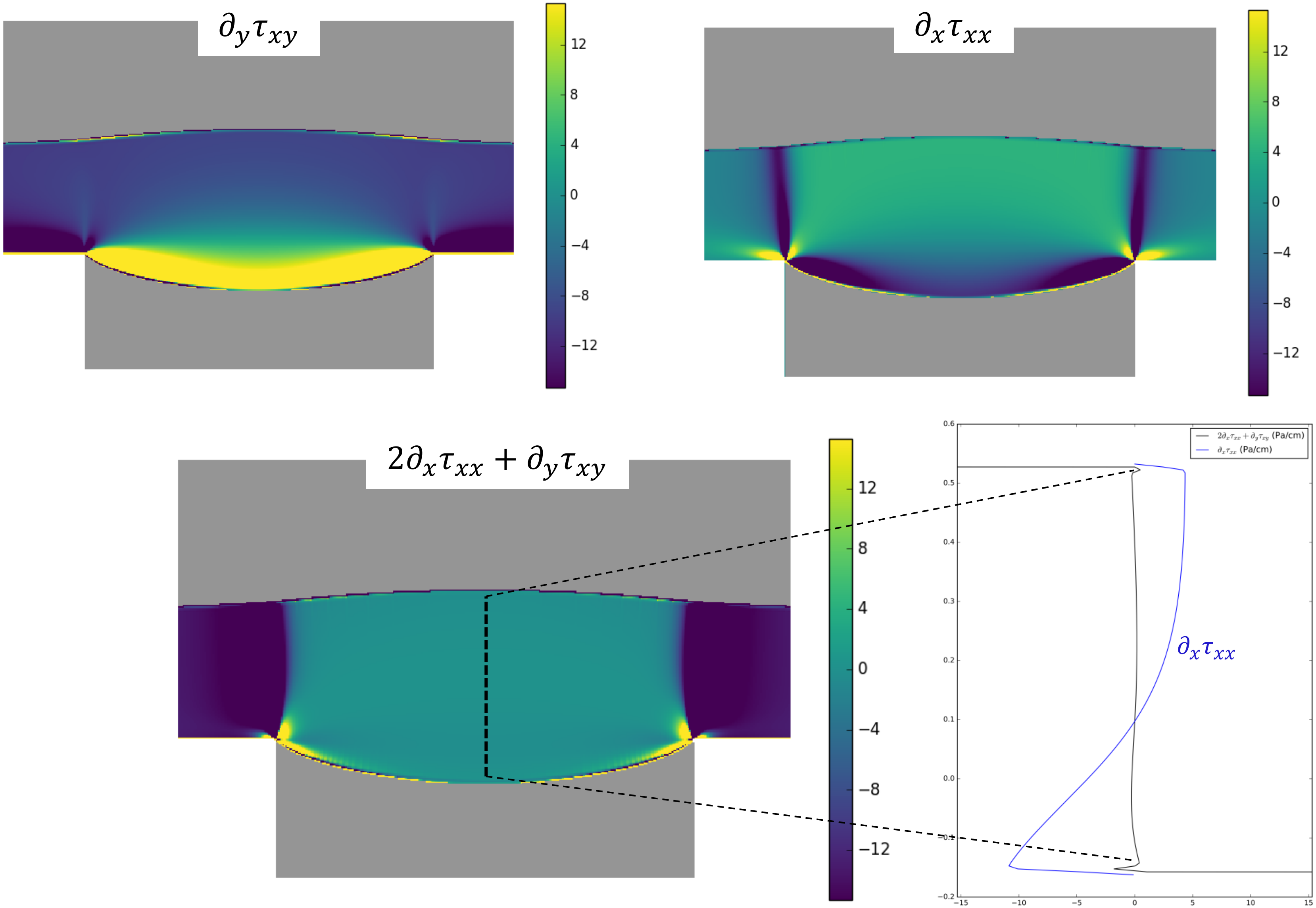

New scaling for BL thickness

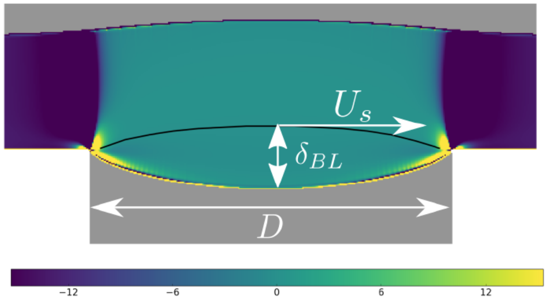

Numerical simulations

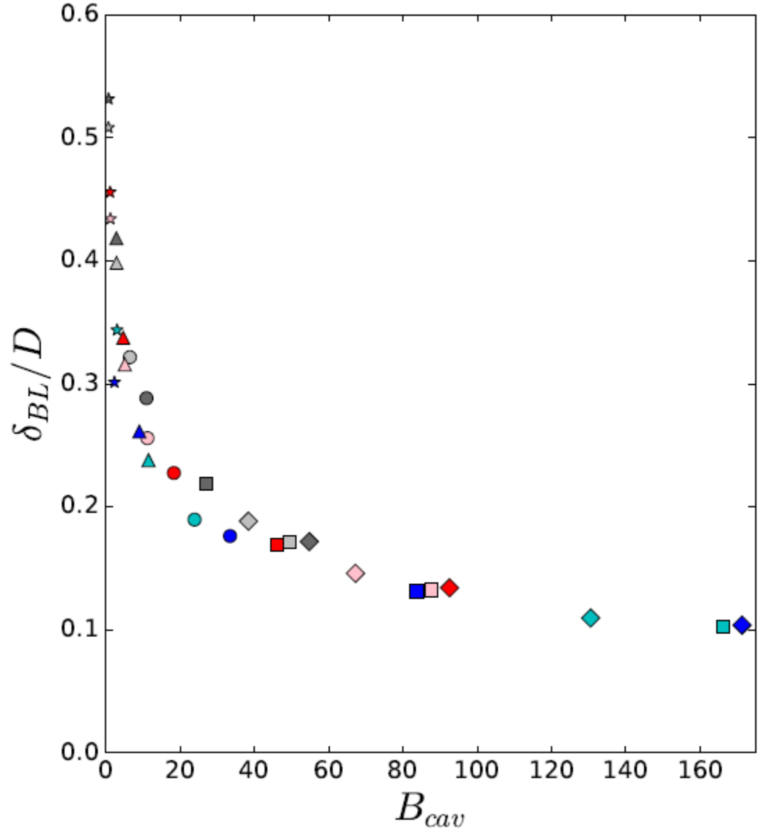

$$B_{cav} = \frac{\tau_c}{\eta}\frac{D}{U_s}$$

Experiments

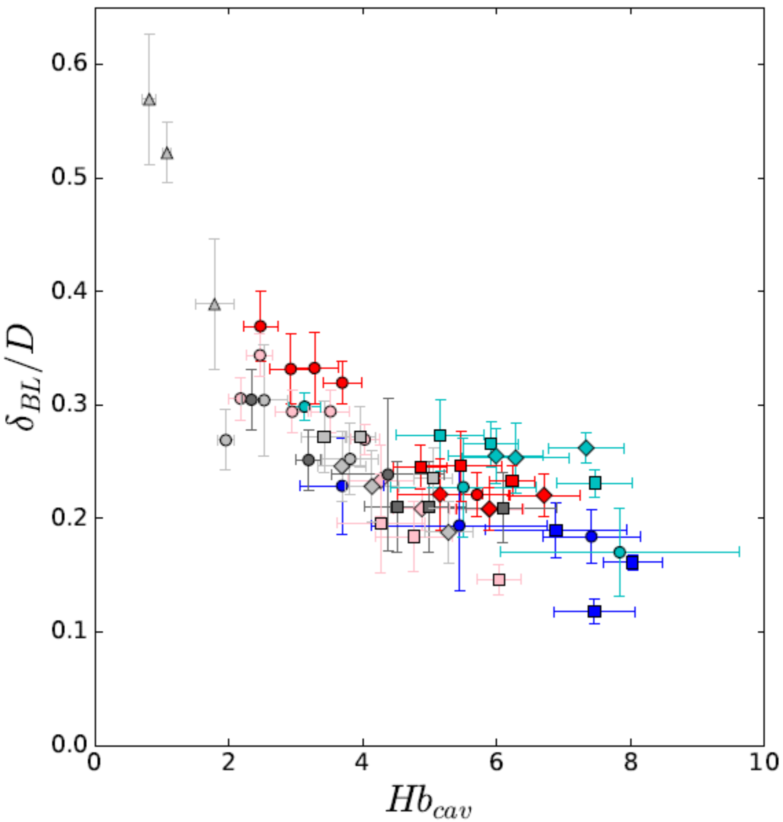

$$Hb_{cav} = \frac{\tau_c}{K}\left(\frac{D}{U_s}\right)^n$$

Generalized Oldroyd's scaling

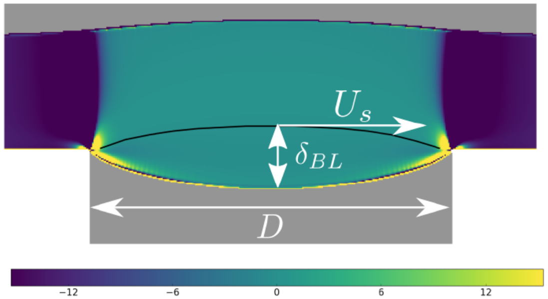

Numerical simulations

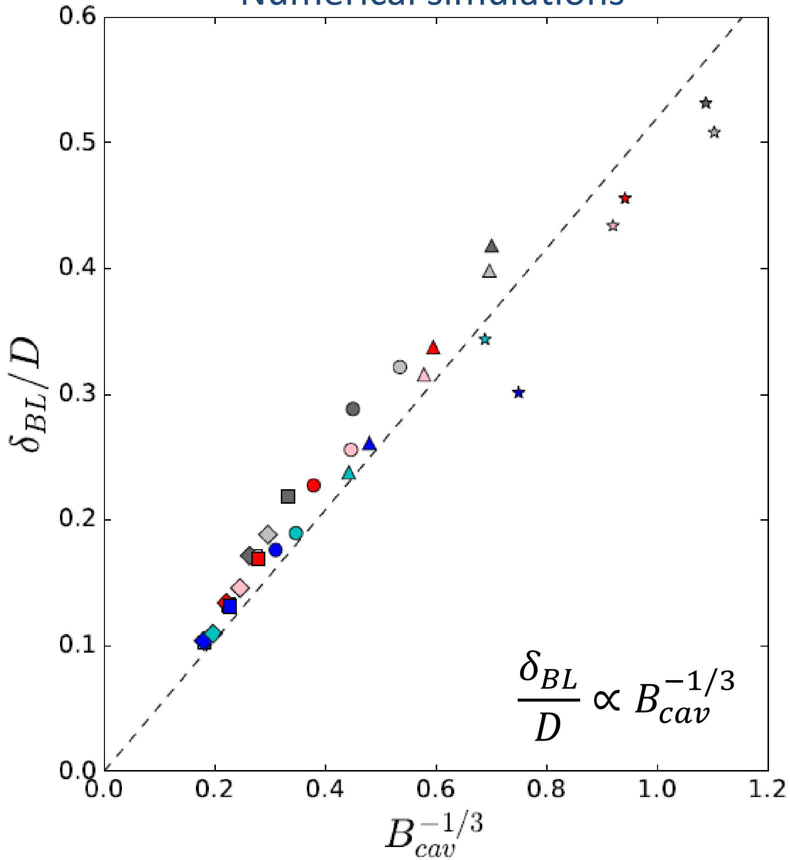

Experiments

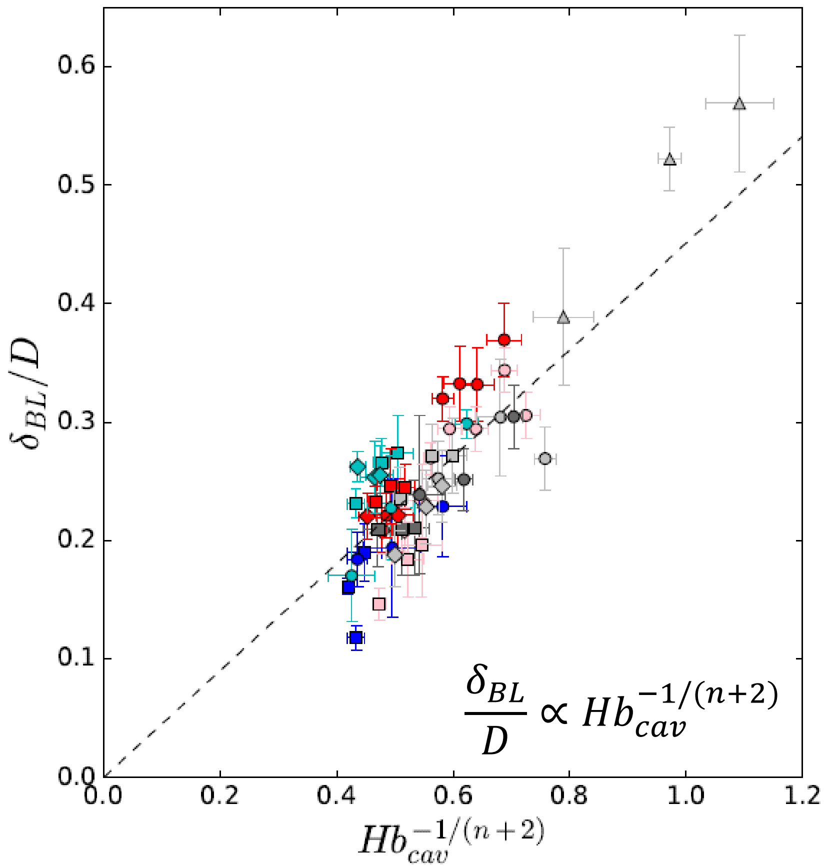

Boundary layer – PL zone interface

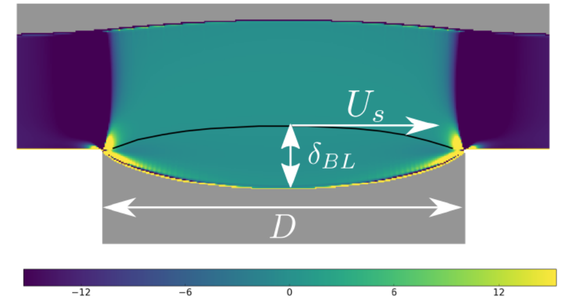

Slip velocity U_s

Numerical simulations

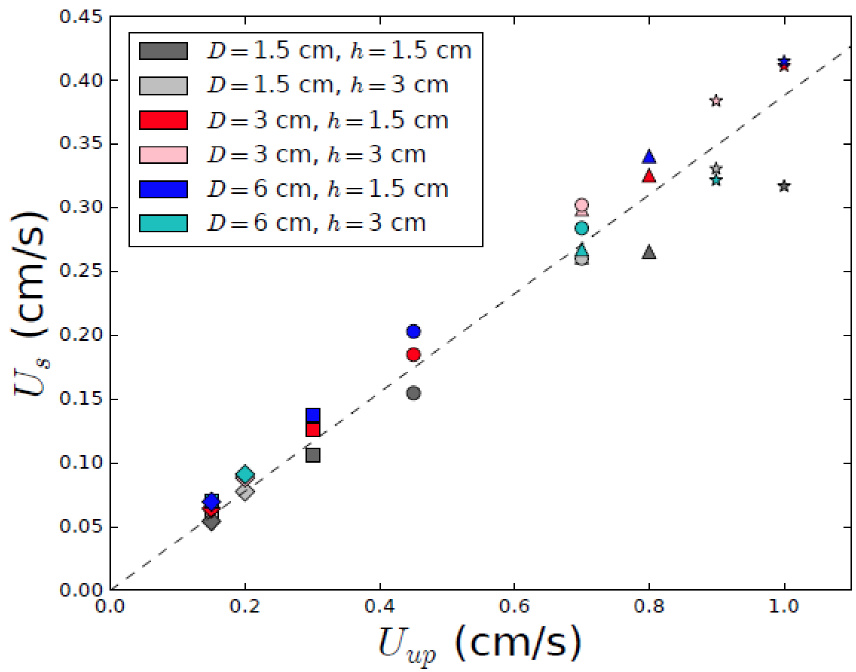

Experiments

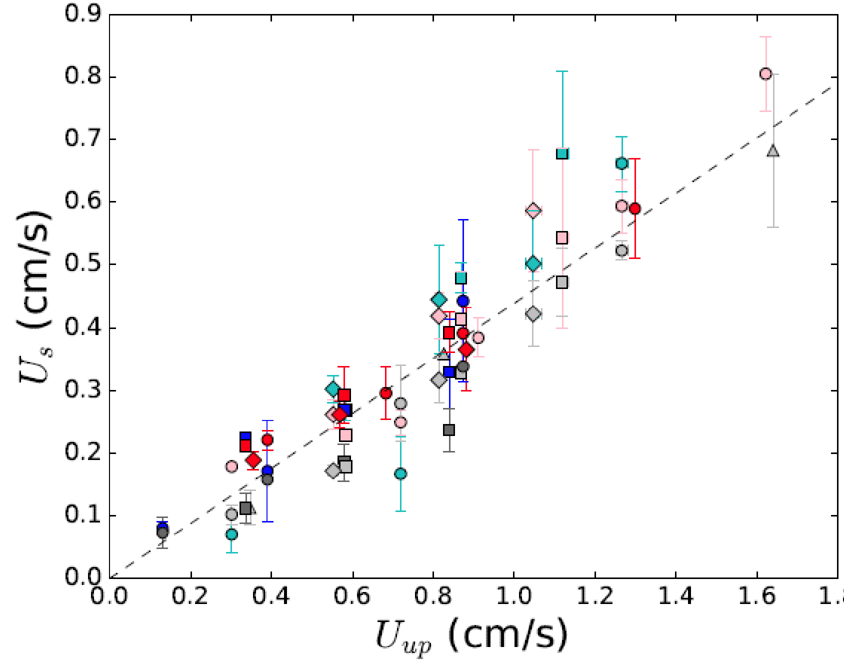

Boundary layer – PL zone interface

Maximum shear stress τ_m

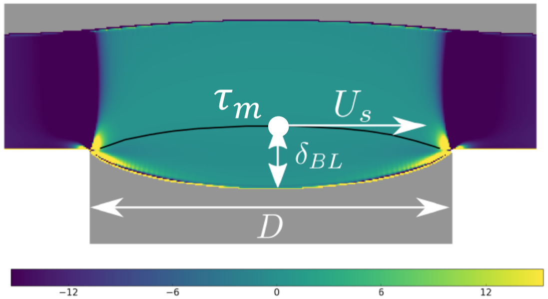

Numerical simulations

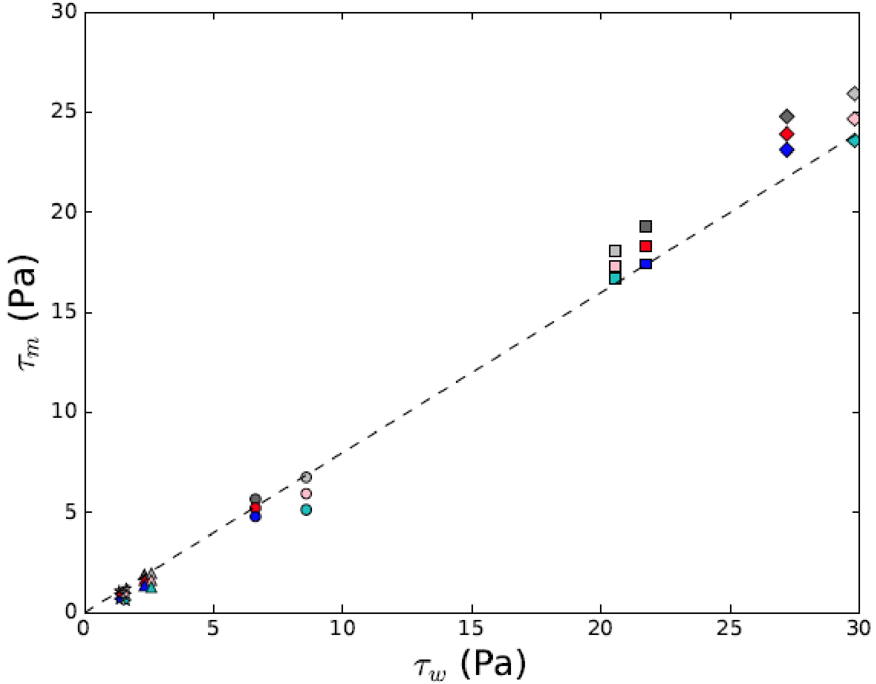

Experiments

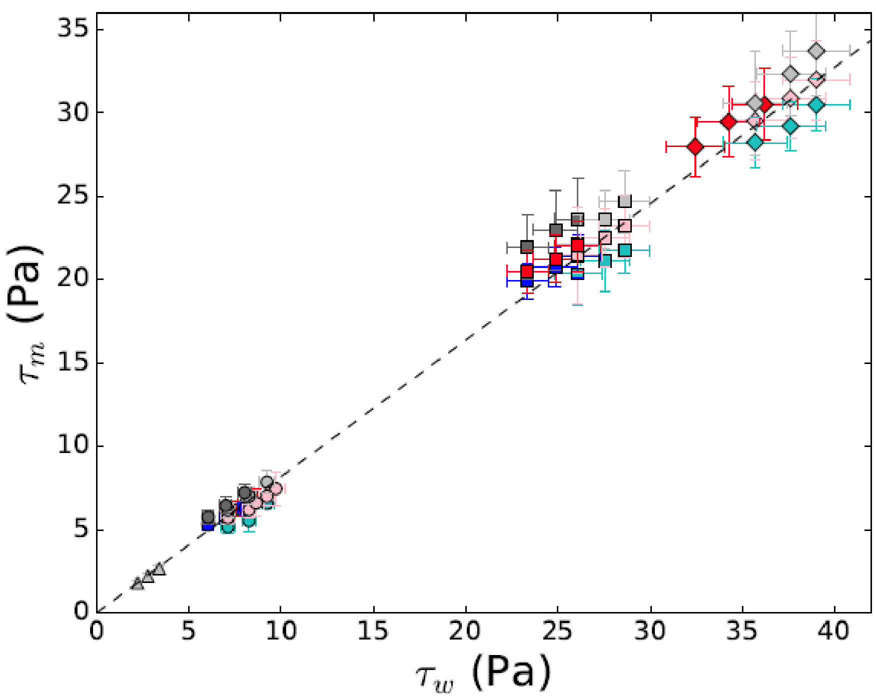

➢ Boundary condition of PL zone essentially controlled by upward flow

Boundary layer – PL zone interface

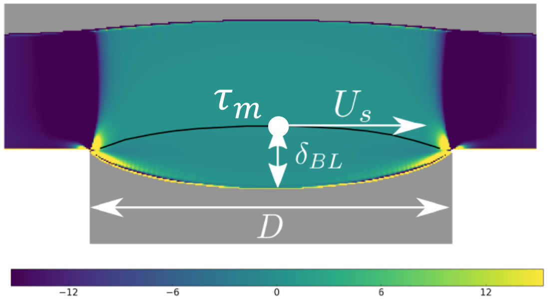

Stress ratio τ_m/τ_w

Numerical simulations

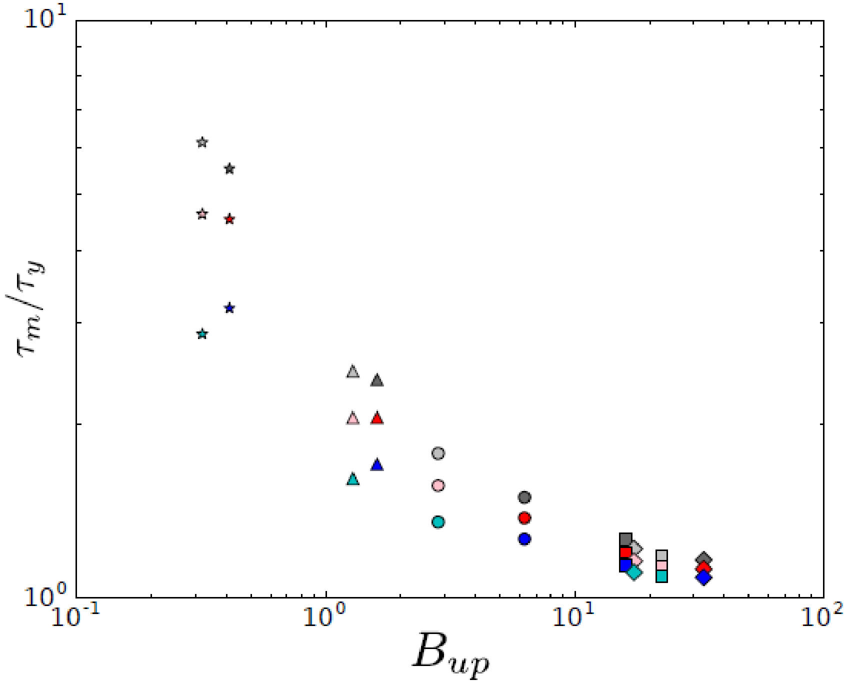

$$B_{up} = \frac{\tau_c}{\eta}\frac{H_{up}}{U_{up}}$$

Experiments

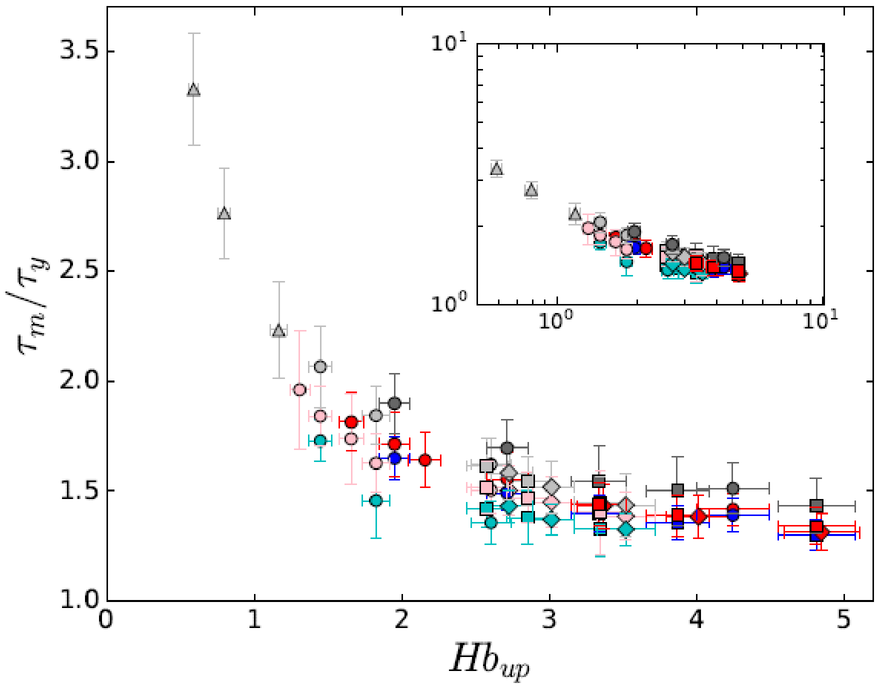

$$Hb_{up} = \frac{\tau_c}{K}\left(\frac{H_{up}}{U_{up}}\right)^n$$

PL zone thickness

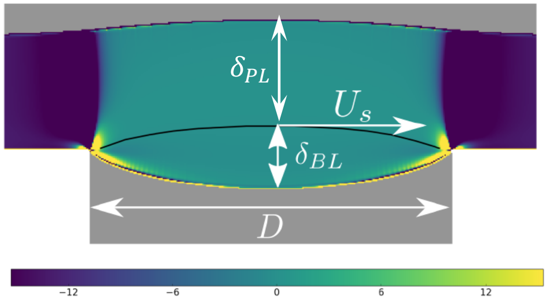

Numerical simulations

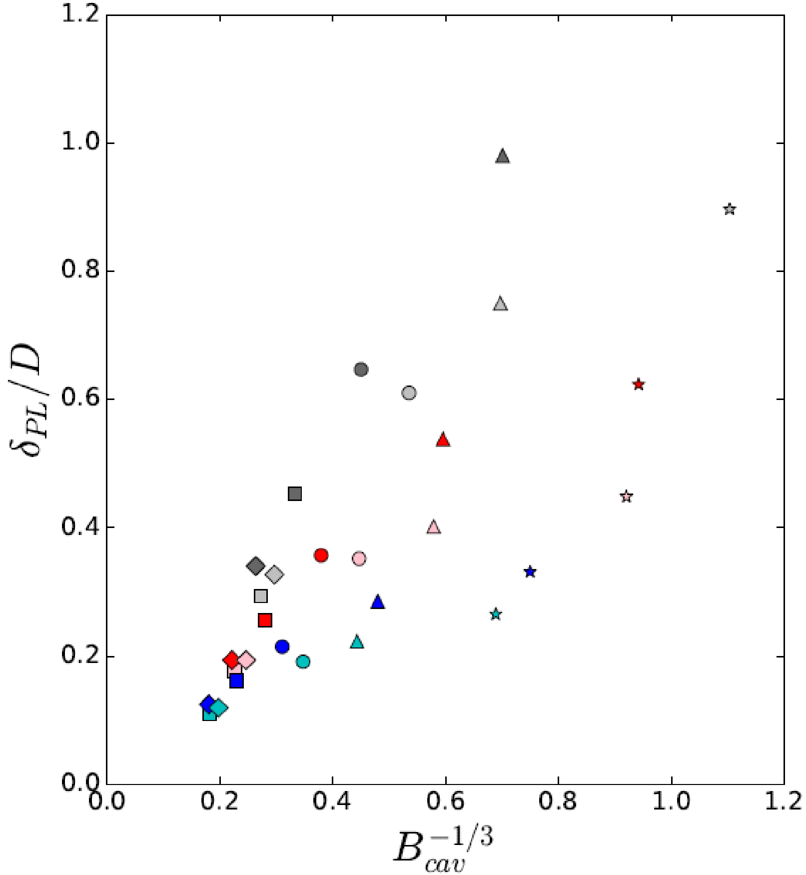

Experiments

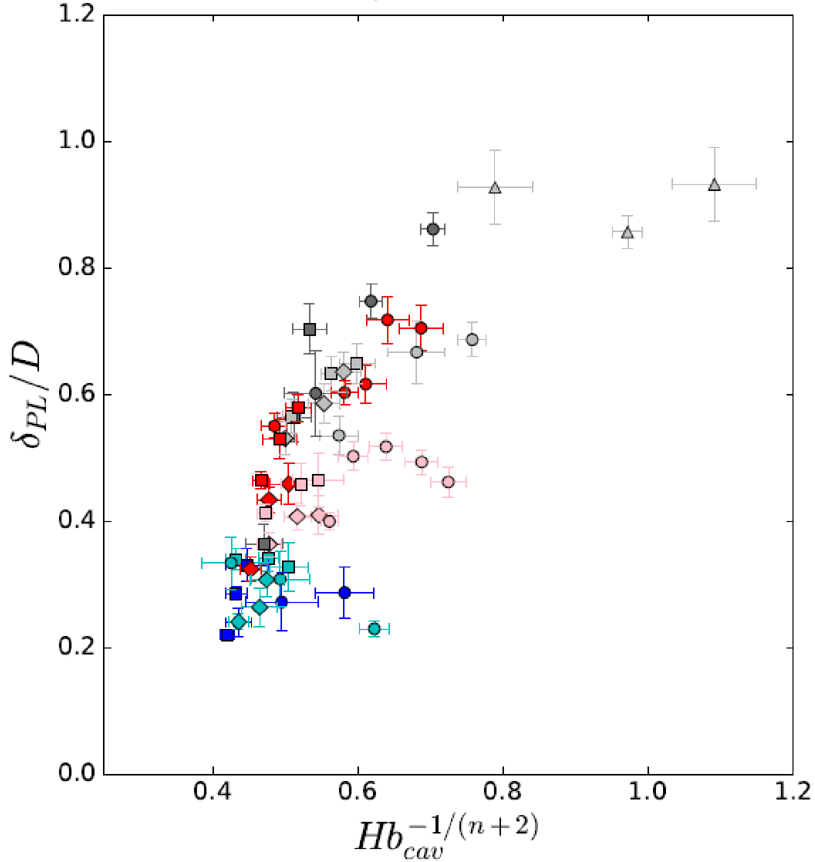

Conclusions

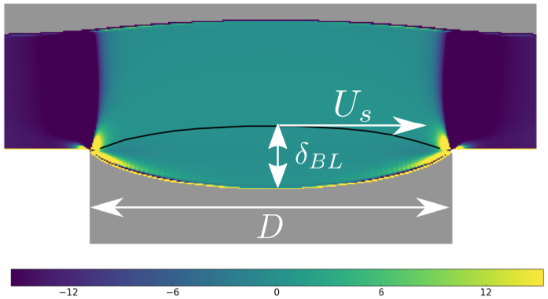

- Experiment / model comparison based mainly on qualitative trends and scaling laws
- Allows in-depth exploration of viscoplasticity-related features
- Opens interesting prospects for the extension of existing viscoplastic boundary layer theories